UNIVERSITY OF CALIFORNIA,
IRVINE

Elucidating the Role of IFN-λ in Alpha Herpesvirus Neuroinvasion

DISSERTATION

submitted in partial satisfaction of the requirements
for the degree of

DOCTOR OF PHILOSOPHY

in

Biomedical Sciences

by

Stephanie Salazar

Dissertation Committee:
Dr. Orkide O. Koyuncu
Dr. Thomas Burke
Dr. Nir Drayman
Dr. Matthew D. Marsden
Dr. Roberto Tinoco

2026

DEDICATION

To my loving family for all their support

&

To my life partner, Alex, who has been a cornerstone in my growth as a scientist and as a person.

TABLE OF CONTENTS

LIST OF FIGURES

LIST OF TABLES

ACKNOWLEDGMENTS

I want to start by expressing my deepest gratitude to my parents. Their unwavering love, constant support, and belief in my potential have been the foundation of my strength throughout this long journey. I am especially thankful for my mom, whose remarkable resilience, constant encouragement, and steady presence have shaped both the person I have become and the scientist I aspire to be. Her faith in me has carried me through every moment of doubt, and her pride in my work has reminded me why this path matters. I want to thank my partner, Alex, for being an amazing shoulder to cry on when experiments didn't go my way and for supporting all my weekends in the lab. To my friends, thank you for celebrating my milestones, boosting my spirits during difficult times, and reminding me to laugh, rest, and keep going. I am particularly grateful to my closest friends, Jessica Dang, Dr. Hemant Kadiamada-Ibarra, and Dr. Niveda Rao. Their kindness, support, and friendship have brought warmth, joy, and balance into my life, and I could not have completed this journey without them.

My introduction to research would not have been possible without the Minority Science Program (MSP). I am truly grateful to Dr. Marlene de la Cruz for opening the door to science and creating an environment where I could grow with confidence and enthusiasm. I also sincerely thank Dr. Amélie Garenaux, who mentored me during my first summer of research at MSP and helped me develop the skills and curiosity that would guide my future work. I also want to thank Dr. Lbachir BenMohamed, my first principal investigator, who introduced me to the exciting field of immunology. His mentorship, encouragement, and belief in my abilities laid the foundation for my scientific journey, which eventually led me to virology and the work presented in this dissertation.

During my summer internship at King's College London, I gained research experience that greatly influenced my scientific growth. Under the supervision of Dr. Rachel Moore and the guidance of Dr. Corinne Houart, Vice Dean for Research and Professor of Developmental Neurobiology at the Institute of Psychiatry, Psychology and Neuroscience, I learned new techniques, expanded my understanding of developmental neurobiology, and experienced the excitement of collaborative international research firsthand. Their support and mentorship made that summer one of the most formative moments in my academic training, and I am deeply grateful for their generosity and encouragement.

I also want to extend my heartfelt thanks to my dissertation committee members, Dr. Thomas Burke, Dr. Nir Drayman, Dr. Matthew D. Marsden, and Dr. Roberto Tinoco. Their thoughtful feedback, insightful questions, and steady support throughout the years have been invaluable in shaping the direction and rigor of my work. I am especially grateful to Dr. Nir Drayman for collaborating with me on our 2025 manuscript and for his significant contributions to this project. His involvement, guidance, and intellectual generosity have meant a lot to me, both professionally and personally.

Most importantly, I am deeply grateful to my principal investigator, Dr. Orkide O. Koyuncu. Her mentorship, patience, and unwavering dedication to my growth have transformed me both as a scientist and as a person. I will never forget accidentally burning my first semi-dry transfer blot and filling the lab with the unmistakable smell of miso soup. While I was panicked and embarrassed, she simply laughed and turned the moment into a gentle lesson. That experience perfectly captures who she is as a mentor: someone who turns mistakes into opportunities to learn and who treats setbacks as natural parts of becoming a better researcher. Her dedication to building the lab from scratch, her steady belief in my abilities, and her

willingness to invest her time and trust in my training have profoundly shaped my scientific identity.

I also want to sincerely thank my labmates, whose support helped me through the most challenging and rewarding moments of this journey. I am especially grateful to Taulima Nua, who started with me as our lab manager and grew alongside me during those early, chaotic, and formative days of building the lab from the ground up. Their resilience, humor, and steady presence made even the hardest weeks manageable. I am equally thankful to the Shi lab for their constant willingness to help, troubleshoot, and share ideas.

I want to thank Liang Liu for always being there to lend expertise; Marielle Valdez, whose friendship has been a pillar of strength; Jose Moran, my friend since the very day we interviewed at UCI, whose friendship has remained a steady and meaningful part of my graduate experience; and Megan Holmes, who was always there to troubleshoot experiment ideas over a coffee and some much needed companionship. Finally, I am grateful to my cohort and the broader Microbiology and Molecular Genetics department for creating an environment of collaboration, mutual support, and shared perseverance that enriched my time at UCI in countless ways.

To all the friends, mentors, and advisors who have offered support, shared wisdom, opened doors, and believed in me, I am sincerely grateful. This dissertation is not only the result of scientific work but also the product of the community that lifted me up every step of the way. Without each of you, this achievement would not have been possible. Thank you.

VITA

Stephanie Salazar

2020 B.S. in Biological Sciences, University of California, Irvine

2024 M.S. in Biomedical Sciences, University of California, Irvine

2026 Ph.D. in Microbiology and Molecular Genetics, University of California, Irvine

FIELD OF STUDY

Microbiology and Molecular Genetics

PUBLICATIONS

Salazar, S., Luong, K. T. Y., Nua, T., & Koyuncu, O. O. (2023). Interferon-λ Activates a Differential Response in Peripheral Neurons That Is Effective against Alpha Herpesvirus Infections. Pathogens (Basel, Switzerland), 12(9), 1142. https://doi.org/10.3390/pathogens12091142

Salazar, S., Luong, K.T.Y., Koyuncu, O.O. (2023). Cell Intrinsic Determinants of Alpha Herpesvirus Latency and Pathogenesis in the Nervous System. Viruses, 15, 2284. https://doi.org/10.3390/v15122284

Coulon, P.-G., Roy, S., Prakash, S., Srivastava, R., Dhanushkodi, N., **Salazar, S.,** Amezquita, C., Nguyen, L., Vahed, H., Nguyen, A. M., Warsi, W. R., Ye, C., Carlos-Cruz, E. A., Mai, U. T., & BenMohamed, L. (2020). Upregulation of Multiple CD8+ T Cell Exhaustion Pathways Is Associated with Recurrent Ocular Herpes Simplex Virus Type 1 Infection. The Journal of Immunology, 205(2), 454–468. https://doi.org/10.4049/jimmunol.2000131

Dhanushkodi, N. R., Srivastava, R., Prakash, S., Roy, S., Coulon, P.-G. A., Vahed, H., Nguyen, A. M., **Salazar, S.,** Nguyen, L., Amezquita, C., Ye, C., Nguyen, V., & BenMohamed, L. (2020). High Frequency of Gamma Interferon-Producing PLZFloRORγtlo Invariant Natural Killer 1 Cells Infiltrating Herpes Simplex Virus 1-Infected Corneas Is Associated with Asymptomatic Ocular Herpesvirus Infection. Journal of Virology, 94(9). https://doi.org/10.1128/JVI.00140-20

Roy, S., Coulon, P.-G., Prakash, S., Srivastava, R., Geertsema, R., Dhanushkodi, N., Lam, C., Nguyen, V., Gorospe, E., Nguyen, A. M., **Salazar, S.,** Alomari, N. I., Warsi, W. R., & BenMohamed, L. (2019). Blockade of PD-1 and LAG-3 Immune Checkpoints Combined with Vaccination Restores the Function of Antiviral Tissue-Resident CD8+ TRM Cells and Reduces Ocular Herpes Simplex Infection and Disease in HLA Transgenic Rabbits. Journal of Virology, 93(18). https://doi.org/10.1128/JVI.00827-19

PRESENTATIONS AND POSTERS

Salazar, S. & O. O. Koyuncu. 2022. *Investigating the effect of interferon responses on alpha herpesvirus invasion and spread in the nervous system*. Queer, Trans, and Allies in Biological Sciences (QTABS). Irvine, CA. (Poster)

Salazar, S. & O. O. Koyuncu. 2022. *Investigating the effect of interferon responses on alpha herpesvirus invasion and spread in the nervous system*. Center for Virus Research (CVR). Irvine, CA. (Oral presentation)

Salazar, S. & O. O. Koyuncu. 2023. *Investigating the effect of interferon responses on alpha herpesvirus invasion and spread in the nervous system*. Irvine, CA. (Oral presentation)

Salazar, S., K. T. Y. Luong, T. Nua, & O. O. Koyuncu. 2023. *Investigating the effect of interferon responses on alpha herpesvirus invasion and spread in the nervous system*. American Society for Virology (ASV). Athens, GA. (Poster)

Salazar, S., K. T. Y. Luong, T. Nua, & O. O. Koyuncu. 2024. *Interferon-λ Activates a Differential Response in Peripheral Neurons That Is Effective against Alpha Herpesvirus Infections*. MDPI: Viruses 2024 (Barcelona, Spain). (Oral presentation)

Salazar, S., A. D. Loaiza, K. T. Y. Luong, D. Cheng, Drayman, N., & O. O. Koyuncu. 2025. Investigating the Role of Interferon-Lambda Against Alpha Herpesvirus Neuroinvasion: HSV-1 vs. PR. International Herpes Workshop (IHW). Berlin, Germany. (Poster Presentation)

POSITIONS

Co-president and Founder of Queer, Trans, and Allies in Biological Sciences (QTABS), September 2021-2024

Bio 199 Undergraduate Student Mentor, September 2021-2025

LGBTQ+ Mentor, September 2021-2023

Minority Science Program (MSP) Instructor, Summer 2020-2021

FELLOWSHIPS AND RESEARCH GRANTS

NIH/NIAID T32 training grant "Virus-host interactions: a multi-scale training program," September 2023- August 2025

NIH- Minority Health and Health Disparities International Research Training (MHIRT), July 2022-September 2022

NIH- Initiative for Maximizing Student Development (IMSD) for Graduate Students, October 2021-June 2022
NIH- Initiative for Maximizing Student Development (IMSD) for Undergraduate Students, April 2018- August 2018

NIH-Minority Access to Research Careers (MARC), August 2018-June 2020

HONORS AND AWARDS

Inclusive Excellence Leadership Award from the UCI School of Biological Sciences Office of DEI, 2022-present

Award was provided to the QTABS program founded to provide a safe environment for graduate student that identify within the LGBTQ+

Faculty Mentor Program (FMP) Fellowship Honorable Mention Award, June 2023

Award was provided in the form of a stipend

MARC Scholar, August 2018-June 2020

Highest Scholarship program funded by National Institute of Health.
Seeks to increase the number of underrepresented minority (URM) researchers in biomedical research careers, by supporting junior and senior URM students in their preparation for graduate training in the biomedical/behavioral sciences.

ABSTRACT OF THE DISSERTATION

Elucidating the Role of IFN-λ in Alpha Herpesvirus Neuroinvasion
by
Stephanie Salazar
Doctor of Philosophy in Microbiology and Molecular Genetics
University of California, Irvine, 2025
Professor Dr. Orkide O. Koyuncu

Alpha herpesviruses (αHVs), including human pathogens, herpes simplex virus types 1 and 2 (HSV-1, HSV-2), varicella-zoster virus (VZV), as well as the animal pathogen, pseudorabies virus (PRV), initially infect mucosal epithelial cells. Subsequently, they invade peripheral neurons, establishing lifelong latent infections in the peripheral nervous system (PNS). While mucosal epithelia antiviral defenses are well characterized, the mechanisms governing neuronal antiviral responses remain poorly understood. Due to their postmitotic status and cellular polarity, neurons depend on antiviral responses that do not provoke inflammatory damage. Despite this constraint, neurons are exposed to a complex cytokine milieu produced by infected mucosal epithelia. Type III interferons (e.g IFN lambda; IFN-λ) are among the most abundant cytokines secreted by infected mucosa. This dissertation research elucidates mechanisms of how neurons respond to IFN-λ signaling, identifies key neuronal antiviral effectors, and reveals how αHVs, specifically HSV-1, evade these IFN-λ-mediated defenses during infection.

We first characterized IFN-λ signaling in PNS neurons and found that, unlike canonical IFN signaling, IFN-λ treatment specifically activated phosphorylation of STAT1 (but not STAT2) in neurons. Transcriptomic profiling revealed biphasic kinetics: an early phase associated with neuronal remodeling and a later phase characterized by the upregulation of interferon-stimulated genes (ISGs). RSAD2 (i.e. viperin) emerged as the most strongly upregulated effector during late-stage IFN-λ treatment, localizing to perinuclear ER membranes

in a neuron-specific manner. Other canonical ISGs of interest included *Mx1*, a GTPase that inhibits viral replication, and *Usp18*, an enzyme that de-conjugates ISG15 to fine-tune and negatively regulate IFN signaling- demonstrating that neurons mount antiviral responses to IFN-λ while exhibiting unique temporal and spatial characteristics tailored to their post-mitotic nature.

Functional studies demonstrated that IFN-λ pre-treatment restricts pseudorabies virus (PRV) replication in both fibroblasts and primary neurons, with pre-treatment prior to infection. In contrast, post-infection treatment yielded only modest inhibition, indicating that once immediate-early and early viral proteins accumulate, IFN-λ signaling becomes more restricted. Notably, antiviral restriction was retained even at higher MOIs, suggesting that neurons can sustain an antiviral program sufficiently strong to control viral replication even under high inoculum pressure. These findings reveal that IFN-λ produced at mucosal surfaces can establish a preemptive antiviral state in innervating sensory neurons, creating a barrier that limits or delays neuroinvasion.

Strikingly, while PRV was highly sensitive to IFN-λ restriction, HSV-1, exhibited resistance. This resistance is conferred by the neurovirulence factor ICP34.5, a gene uniquely encoded by the simplexvirus genus (HSV-1 and HSV-2) but absent in the varicelloviruses (VZV and PRV). Using ICP34.5-deficient HSV-1 mutants, we demonstrated that ICP34.5 counteracts the neuronal IFN-λ- RSAD2-mediated response through two mechanisms: (1) reversing eIF2α phosphorylation via PP1α recruitment, and (2) disrupting RSAD2 localization at the perinuclear membrane.

In separate studies on the characterization of RSAD2, we uncover a mucosal-PNS antiviral axis involving IFN-λ-driven responses and RSAD2-dependent restriction of αHV

(varicellovirus) neuroinvasion, which simplexviruses expressing ICP34.5 can bypass. These results highlight the divergent neuronal adaptation of two different αHV genera displaying different immune evasion strategies and identifies RSAD2 as a neuron-specific antiviral target with therapeutic implications for preventing neuroinvasion.

These discoveries led to the investigation of spatially distinct IFN-λ-mediated antiviral defenses in neuronal axons. Local axonal STAT1 activation was observed, which reduced retrograde αHV transport in axons, establishing an early immune checkpoint prior to viral genome delivery to the nucleus. Priming axons with IFN-λ decreases virion movement towards the cell body and delays PRV infection at later stages of infection in neuronal cell bodies. These findings position the axonal compartment as a promising therapeutic target and suggest that strategies that deliver IFN-λ to peripheral nerve termini or recruit activated STAT1 in axons during early infection could prevent viral neuroinvasion and may affect the establishment of latency in the PNS. Although further studies are required to elucidate the mechanism of this non-canonical IFN-STAT signaling in axons, these findings fundamentally advance our understanding of neuronal immune responses and axonal responses against neuroinvasion.

INTRODUCTION

Virus infections originating in peripheral tissues are usually contained by several biological barriers. The mucosal epithelium serves as a primary barrier, acting as both physical and immunological defense. When viruses infect these epithelial cells, they trigger various innate immune responses, including cytokine production, immune cell recruitment, and paracrine signaling warning and preparing nearby epithelial cells [1-3]. These responses generally lead to apoptosis or immune-mediated killing of infected cells limiting viral replication and spread of infection to other tissues. The nervous system (NS) is particularly well protected, and most virus infections do not spread to the NS. Some virus infections including emerging viruses (e.g. coronaviruses, influenza viruses) or zoonotic pathogens (e.g. West Nile virus, Zika virus) enter the nervous system by accident, and if they do, the infection is accompanied by severe pathology [1, 4].

Only a few virus families have evolved the ability to efficiently infect the nervous system by accessing sensory or autonomic nerve termini after infecting the mucosal epithelium. The alpha herpesviruses (αHVs), herpes simplex virus (HSV-1 and HSV-2), varicella-zoster virus (VZV), and closely related pseudorabies virus (PRV), represent successful neurotropic viruses. [2, 5-7]. Following entry at axon termini, αHVs are transported by the axonal transport machinery to distant sites, along microtubules. Unlike other neurotropic viruses (such as rabies viruses), which cause acute, destructive pathologies through a transient, lytic infection, the αHVs have adapted to the nervous system as an ecological niche, establishing lifelong persistence [8]. Upon reaching the neuronal nucleus, the viral genome enters a latent state, becoming transcriptionally silenced, maintained as an episome, and producing no infectious progeny. Evolutionarily, latency provides advantages for long-term virus survival, since the quiescent

virus infection purposefully evades immune system detection while preserving the ability to reactivate.

During latency, the αHV genome is packaged as a facultative heterochromatin, marked by repressive histone modifications that silence lytic genes [9]. The major transcript expressed during latency is the latency-associated transcript (LAT), which promotes neuronal survival and viral persistence by suppressing lytic gene expression and inhibiting apoptosis. [10]. However, during stress conditions (e.g., physical trauma, sunburn, or fever), this chromatin repression can be reversed [11]. Upon reactivation, the latent viral heterochromatin is remodeled to a transcriptionally permissive state, and lytic gene expression resumes. Subsequently, newly replicated virions are transported anterogradely, along axons towards epithelial cells, leading to the development of symptoms such as herpetic lesions to occur once more [10, 12, 13]. Remarkably, the ability of αHVs to alternate between latency and productive replication allows them to achieve lifelong persistence by spreading throughout host neuronal networks and among the population.

Neurons are highly specialized post-mitotic cells with exceptionally long lifespans, often persisting throughout an organism's life. They are characterized by their distinct structural regions, including the axon and soma, which are specialized to serve different functions [14]. Because neurons cannot be replaced once they die, the nervous system has evolved mechanisms to protect these cells from damage caused by infectious agents and inflammation. In many tissues, the immune system responds to viral infections through destructive processes such as apoptosis (programmed cell death) [15]. However, such responses would be highly damaging if they occurred within neural tissue, where cell loss and inflammation could impair vital functions.

The nervous system is often considered "immune-privileged," meaning it employs tightly regulated and less aggressive antiviral responses to prevent immunopathology, damage caused by the immune system itself. Despite this immune-privileged status, neurons are not completely inert immunologically. Neurons can detect viral infections by sensing viral molecules and activating intracellular antiviral pathways [16-18]. They also respond to immune signaling molecules such as interferons (IFNs), which are crucial cytokines in antiviral defense. This duality allows neurons to maintain a delicate balance: protecting themselves from infections while avoiding self-destructive immune-mediated damage.

IFNs are secreted signaling cytokines that are crucial components of the immune system's defense mechanism against viral infections. They are produced and released by host cells in response to the presence of pathogenic molecules and serve to alert neighboring cells to activate their antiviral defenses. Through autocrine signaling, secreted IFNs bind to receptors on the same cell that produced them, activating the JAK-STAT pathway to induce interferon-stimulated genes (ISGs) and enhance innate antiviral defenses. In paracrine signaling, IFNs diffuse to nearby cells, bind to their receptors, and initiate a similar ISG response, creating a protective antiviral shield that limits viral spread beyond the initial infection site [19, 20].

There are three main categories of interferons: type I, type II, and type III, each with distinct roles, receptors, and distributions [21]. Type I interferons, which include IFN-α and IFN-β, are produced by many cell types and are primarily involved in the innate immune response. They bind to specific receptors present on most cell types, leading to the activation of antiviral genes. Type II interferon, also known as IFN-γ, is mainly produced by natural killer cells and T lymphocytes, and it plays a key role in regulating both innate and adaptive immune responses, particularly in activating macrophages and promoting antigen presentation. Type III interferons,

known as interferon lambda (IFN-λ), have a similar antiviral function to type I IFNs but signal through a different receptor complex. The receptors for type I IFNs are expressed on most cells, enabling a broad antiviral response, whereas the IFN-λ receptor expression is more restricted, mainly found on epithelial cells at mucosal barriers and some immune (e.g., dendritic cells, neutrophils, B cells, and plasmacytoid dendritic cells) and structural cells (e.g., keratinocytes and hepatocytes) [21-26]. This restricted expression pattern suggests specialized roles for IFN-λ at barrier surfaces.

Prior studies have established that IFN-λ activation at mucosal epithelial barriers inhibits viral replication, maintains epithelial integrity, and limits immunopathology [27, 28]. However, it is unclear whether peripheral neurons could respond to IFN-λ. This work demonstrates that neurons express functional IFN-λ receptors and can activate downstream antiviral pathways. Recent studies, including results of this thesis, demonstrated that peripheral neurons not only express functional IFN-λ receptors but also mount robust antiviral responses, including induction of interferon-stimulated genes (ISGs) [18, 29]. This discovery reveals a previously underappreciated connection between immune responses in mucosal tissues and the peripheral nervous system, suggesting that epithelial IFN-λ production may directly protect innervating sensory neurons.

This work demonstrates that IFN-λ signaling in peripheral neurons induced a unique transcriptional response that restricts PRV replication. Unlike canonical IFN signaling, which induce phosphorylation of both STAT1 and STAT2, IFN-λ signaling in neurons leading to strong STAT1 phosphorylation without activating STAT2. This predominantly STAT1-biased signaling produces a delayed yet sustained antiviral state through selective ISG induction. This pattern

suggests that neurons have evolved mechanisms to mount effective antiviral defenses while avoiding rapid, inflammatory responses that could be neurotoxic.

To identify functionally relevant antiviral effectors, I examined the expression of ISGs in peripheral neurons after IFN-λ stimulation. RNA-seq analysis revealed distinct temporal patterns: early transcriptional response (3 h post-treatment) primarily involved neuronal signaling and growth-related pathways, whereas the late responses (24 h post-treatment) were associated with innate immunity and antiviral defenses. Among the most highly upregulated antiviral genes was RSAD2 (viperin), a broad-spectrum antiviral enzyme.

In neurons, RSAD2 is localized to distinct punctate structures surrounding the nucleus, consistent with endoplasmic reticulum (ER)-derived membrane domains. Previous studies have confirmed that RSAD2 localizes to the cytosolic surface of the ER via its N-terminal amphipathic α-helix [30]. Mechanistically, RSAD2 produces a nucleotide analog, 3′-Deoxy-3′,4′-didehydro-cytidine triphosphate (ddhCTP), which inhibits viral genome synthesis by acting as a chain-terminating substrate during replication of RNA viruses, including Zika, dengue, West Nile, and hepatitis C virus [31, 32]. Despite its evident antiviral effects against multiple RNA viruses, its activity against DNA viruses such as αHV remains poorly understood.

Comparative analysis of IFN-λ restriction on different αHVs revealed a striking disparity: while IFN-λ pre-treated primary neurons restricted PRV replication, HSV-1 was notably resistant to this antiviral activity. This work revealed that HSV-1's resistance to IFN-λ-mediated restriction is liaised by ICP34.5, a gene present in simplexviruses (HSV-1 and HSV-2) but absent from varicelloviruses (PRV and VZV). ICP34.5 is essential for counteracting the host's antiviral response during neuronal infection. It redirects the phosphatase activity of protein phosphatase 1 alpha (PP1α) to dephosphorylate eIF2α, thereby reversing the host's translational shutdown.

HSV-1 restores cellular conditions favorable for viral translation and replication by displacing phosphorylated eIF2α and redistributing RSAD2 from the perinuclear region. Through these coordinated actions, HSV-1 effectively counteracts the IFN-λ-induced antiviral state in neurons.

This discovery clarifies how HSV-1 has specifically evolved to overcome neuronal innate immunity and reveals key differences in evasion strategies among αHVs. While all αHVs must contend with host antiviral defenses, simplexviruses (HSV-1, HSV-2) uniquely encode ICP34.5, enabling them to counteract both the IFN signaling and the neuron-specific RSAD2 restriction mechanisms. In contrast, veterinary αHVs, such as PRV, and the human pathogen VZV lack this neurovirulence factor and consequently exhibit greater sensitivity to IFN-λ-mediated restriction in neurons. This divergence highlights how simplexviruses have evolved specialized neurovirulence tactics optimized for their primary reservoir (the PNS), where IFN-λ and RSAD2 serve as critical barriers to viral persistence.

This work also uncovered a spatially distinct antiviral mechanism operating in neuronal axons. Live cell imaging and functional assays revealed that IFN-λ exposure, when applied either globally or locally to axons, significantly reduced retrograde transport of incoming αHV particles, indicating that distal neurites can initiate antiviral signaling prior to viral genome delivery to the soma. Immunofluorescence detection of axonal p-STAT1 following IFN-λ exposure confirmed that neurons can activate STAT1-dependent antiviral pathways locally, independent of nuclear signaling. This establishes early regulation of immune response against αHV infection, in which fewer virions can successfully reach neuronal cell bodies. Axonal priming with IFN-λ decreased the number of PRV particle movement and delayed productive infection, suggesting that early IFN-λ exposure at mucosal nerve terminals could reduce neuroinvasive efficiency.

This dissertation reveals a previously unrecognized mucosal epithelia-PNS axis in which IFN-λ protects the peripheral neurons from αHV neuroinvasion through spatially compartmentalized defense mechanisms. Axonal STAT1 signaling restricts retrograde viral transport at the earliest stage of infection. Next, nuclear transcriptional response to IFN-λ, including RSAD2 upregulation and ER localization, blocks viral replication in the neuronal cell body. Together, these mechanisms create layered barriers that protect neuronal integrity while avoiding the inflammatory responses that would cause damage.

CHAPTER 1: Basics of Alpha Herpesvirus Infections

1.1 Alpha Herpesviruses

Alphaherpesvirinae is a subfamily of the Herpesviridae family that infects a broad range of hosts [33]. The human αHVs include herpes simplex virus 1 and 2 (HSV-1 and HSV-2), and varicella zoster virus (VZV) [34]. Well-studied veterinary αHVs include pseudorabies virus (PRV), bovine herpesvirus 1 (BHV-1), and equine herpesviruses 1 and 4 (EHV-1 and EHV-4) [33]. PRV has been extensively used to study the kinetics of αHV spread in neuronal cultures and animal models. αHVs are characterized by the large size of their double-stranded DNA (dsDNA) genomes and complex virion architecture (Figure 1.1A). The Alphaherpesvirinae subfamily is divided into two genera: simplexviruses (including HSV-1 and HSV-2) and Varicelloviruses (including VZV, EHV-1, EHV-4, PRV, FHV-2). αHV are characterized by the large size of their double-stranded DNA (dsDNA) genomes packaged within an icosahedral capsid, surrounded by a complex tegument layer, a protein-rich matrix that lies between the capsid and the outermost membranous envelope. The viral envelope is surrounded by 11 membrane glycoproteins that mediate viral entry and cell-to-cell spread.

Although simplexviruses and varicelloviruses share numerous homologous genes, each possesses a unique set of genes that is not present in the other species (Figure 1.1B). For example, ORF-O and ORF-P are only found in HSV-1, whereas ORF1 is found only in VZV [35, 36]. Most of the genes share their similar function and complement each other *in vitro*. Another distinct difference in genomic organization is the number of origins of replication: HSV-1 and PRV contain three origins of replication, whereas VZV contains only two [35, 37]. While numerous genes are conserved across all αHVs due to shared fundamental functions (e.g., capsid structure, DNA replication), the overall nucleotide and amino acid sequences show

significant divergence between genera (Figure 1.1C). This divergence reflects ancient separation and co-evolution within their respective hosts (e.g., pigs for PRV and primates for simplexviruses) [37-39].

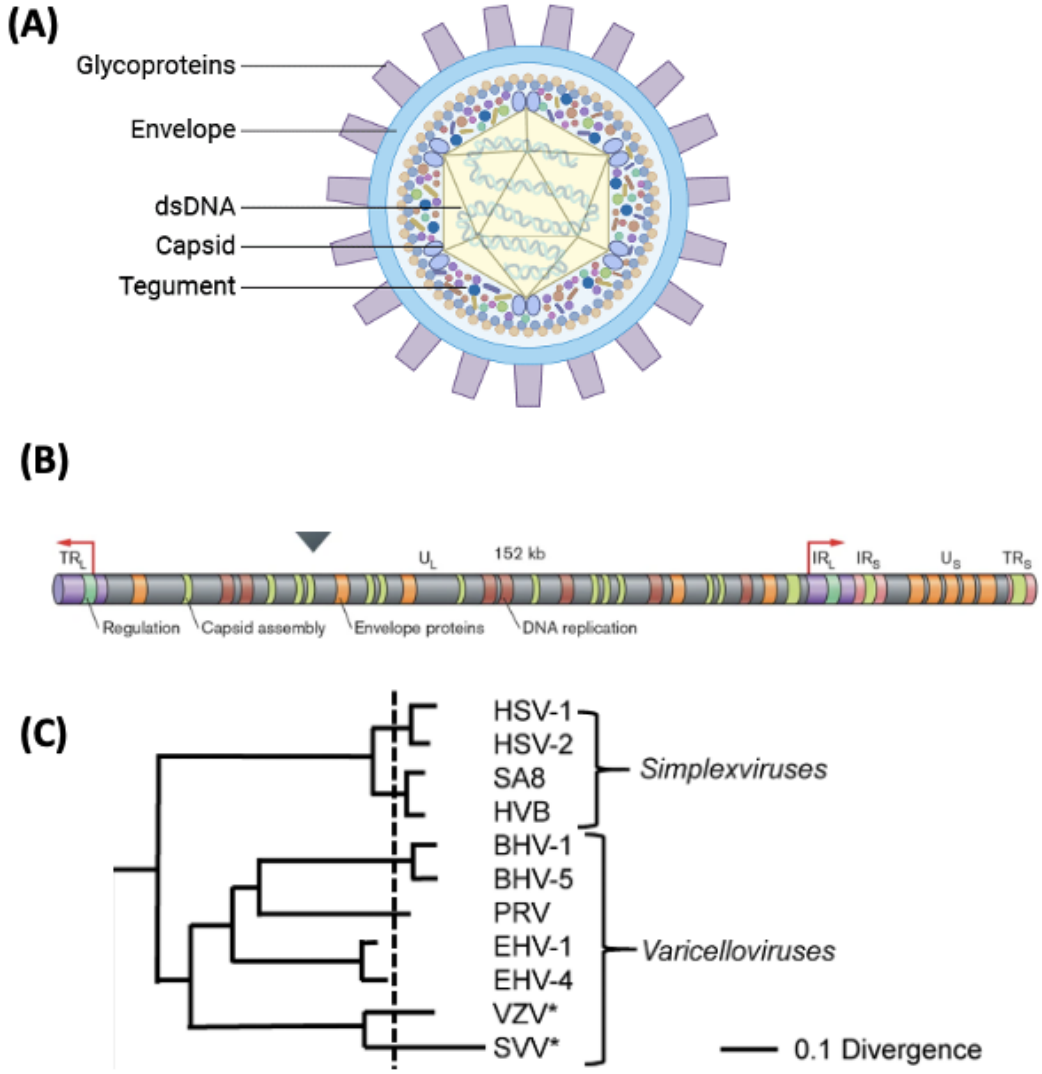

Figure 1.1. Structure and genomic organization of α-herpesviruses. A) The α-herpesvirus virion consists of a linear double-stranded DNA genome enclosed in an icosahedral nucleocapsid, surrounded by a tegument layer that delivers regulatory proteins and modulates host processes including mRNA degradation. The outer lipid envelope contains ~11 viral glycoproteins required for entry and immune evasion. **B)** The ~150-kbp dsDNA genome encodes more than 80 genes, providing the capacity for efficient replication, immune modulation, and lifelong persistence in peripheral neurons. (**C**) Phylogenetic tree representing the αHVs evolved into the simplexviruses (HSV-1, HSV-1, herpesvirus B (HVB), and simian agent 8 (SA8)), and varicelloviruses (VZV, EHV-1, EHV-4, PRV, FHV-2). Adapted from Gray, W.L. 2022 [40].

1.2 HSV-1 entry and establishment of productive infection

Most αHV infections begin in the periphery at the mucosal epithelium, such as the oral, genital, nasal, or oropharyngeal mucosa [41]. αHV infections within the mucosal epithelia result in productive replication, yielding hundreds to thousands of progeny per infected cell [42]. Some of these newly made virus particles spread the infection to neighboring epithelial cells, fibroblasts, or nerve endings. Despite recent discoveries, there is a large knowledge gap between the connection of the mucosal epithelia and the PNS junction. Importantly, the virus-host interactions during the αHV spread from epithelial cells to latency establishment in the peripheral ganglia remain to be elucidated.

HSV-1 entry into epithelial cells is achieved by receptor-mediated fusion of the viral envelope with the plasma membrane, requiring the concerted action of viral glycoproteins; gC, gB, gD, gH, and gL [9]. Cellular receptors nectin-1, a member of the tumor necrosis factor receptor family, and herpesvirus entry mediator (HVEM) serve as HSV-1 entry receptors [43-45]. The role of these receptors differs depending on the cell type and the route of infection. Nectin-1 is the major entry receptor for neuronal infection and is shown to be accumulated at cell–cell junctions [46, 47]. gD on the viral membrane can bind to nectin-1, HVEM, or 3-O-sulfated heparan sulfate. Of those receptors, nectin-1 is the main entry receptor for neuronal and epithelial cells [48]. HVEM and nectin-1 as gD receptors and paired immunoglobulin-like type 2 receptor α (PILRA), myelin-associated glycoprotein (MAG), and myosin heavy chain 9 (MYH9) as gB receptors are also present in the adult human brain with increased expression in the hippocampus, which suggests underlying susceptibility of this brain region to HSV infection [49] (Figure 1.2).

When bound to its receptor, gD undergoes conformational changes and activates the gH/gL heterodimer, which, in turn, activates gB, the principal fusogen that mediates the fusion of viral envelope and host cell membrane [50]. Upon entry, the viral nucleocapsid is transported to the nucleus via molecular motors. Only the inner tegument proteins (e.g., US3, UL37, and UL36) stay associated with the incoming nucleocapsids [51, 52]. Outer of outer tegument proteins with nucleocapsids have rarely been observed during PRV and HSV post-entry transport [73]. Once the viral capsid and tegument proteins enter the cytoplasm, the tegument protein VP16, along with the host cell factors HCF-1 and Oct-1, travel to the nucleus independently, while the inner tegument proteins: UL36, UL37, and US3, remain attached to the capsid to facilitate transport on microtubules toward the cell nucleus [52, 53]. Viral DNA is ejected into the nucleus, and viral genes are transcribed by host RNA polymerase II [54].

Productive αHV infection follows a temporal cascade of protein synthesis, starting with immediate-early (IE) and early (E) gene expression, and followed by DNA replication and subsequent late (L) protein synthesis [55] (Figure 1.2). The relatively large genomes of αHVs are not assembled into nucleosomes in the virions, but upon translocation into the nucleus, host histones are rapidly recruited onto viral genomes [56]. Through interactions with HCF-1 and Oct-1, incoming VP16 initiates the transcription of IE genes, including infected cell proteins (ICPs): ICP0, ICP4, ICP22, ICP27, and ICP47 [56-58]. The IE proteins then participate in the transcription of early and late genes. Early proteins such as ICP8 and thymidine kinase (TK) carry out functions involved in viral DNA replication [9, 46].

Once DNA replication occurs, late genes are expressed, followed by virus assembly [59]. Late genes can be subdivided into two classes: “leaky-late” or “true-late” genes. “Leaky-late” gene expression is amplified upon viral DNA replication, while “strict-late” genes are expressed

only upon viral DNA replication [59, 60]. Viral DNA replication, capsid assembly, and DNA packaging occur in the nucleus [61]. Mature capsids bud from the nuclear membrane, acquire tegument proteins, and undergo secondary envelopment through the trans-Golgi network (TGN) [62]. Inner tegument proteins associate with the capsid first, while outer tegument proteins do so later. The virions can egress from the infected cells to infect distant cells by using the canonical fusion machinery [50]. Alternatively, they can infect neighboring cells through cell–cell junctions using gE/gI heterodimers [63].

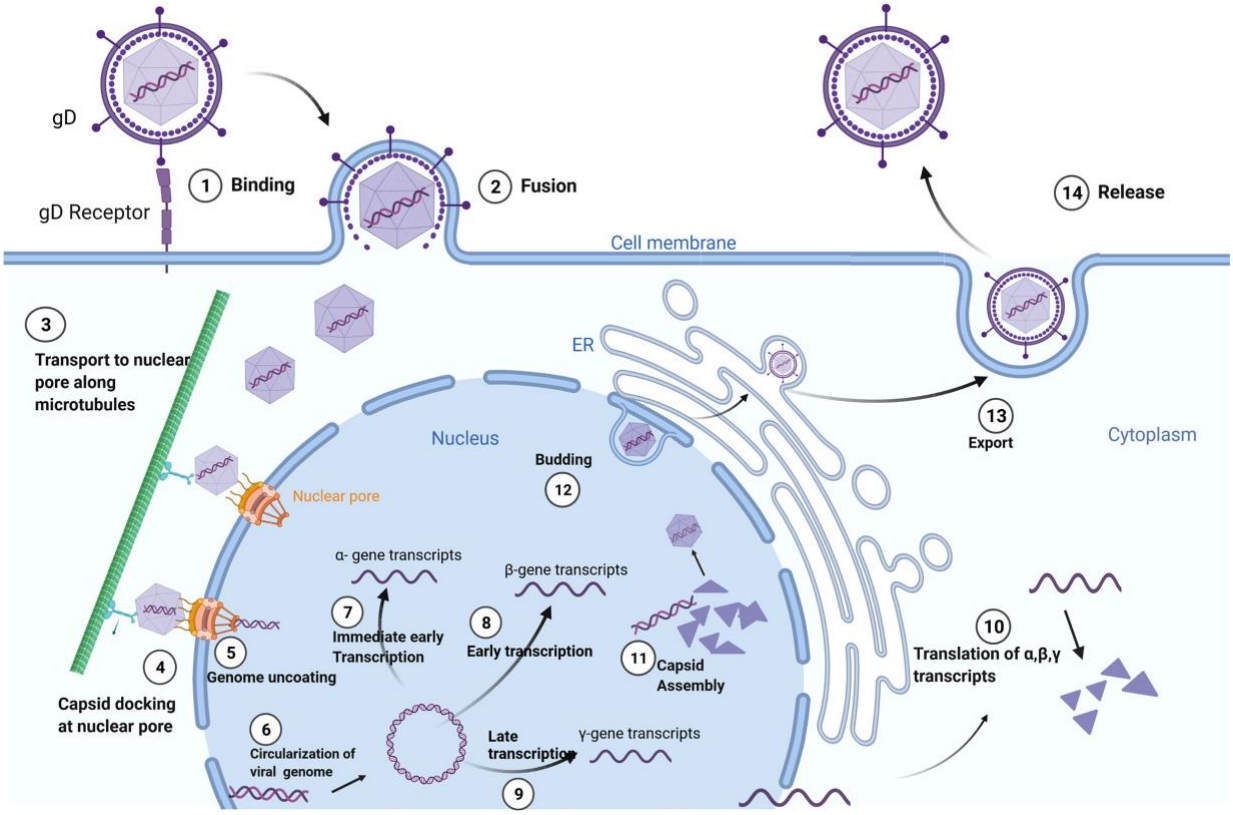

Figure 1.2. Schematic representation of the productive phase of HSV-1 infection. Figure taken from Scanlan, H. et al. (2022) [64]. Infection begins when viral glycoprotein D (gD) engages cell-specific gD receptors, facilitating adsorption and membrane fusion (**1**). Fusion between the viral envelope and host membrane allows capsid entry into the cytoplasm and release of tegument proteins (**2**). The naked capsid then traffics toward the nucleus (**3**) and docks at nuclear pore complexes (**4**), where the viral genome is released and transported into the nucleus (**5**). Once inside, the linear DNA circularizes (**6**) and undergoes three sequential waves of transcription: immediate-early (α) genes (**7**), early (β) genes (**8**), and late (γ) genes (**9**). Translation of late structural proteins occurs only after viral DNA replication has been initiated by β-gene products. Viral transcripts exit the nucleus for translation in the cytoplasm or on ER-associated ribosomes (**10**). Newly synthesized genomes are packaged into icosahedral capsids assembled in the nucleus (**11**). Capsids acquire a primary envelope by budding through the inner nuclear membrane (**12**), then transit through the ER and mature within the Golgi. Fully assembled virions are finally released by exocytosis (**13**), enabling spread to neighboring cells.

1.3 Interferon response: Type I versus Type III IFN

During αHV infection in mucosal epithelia, infection at these sites triggers an antiviral response with two key components: intrinsic immunity, a cell-autonomous defense, and innate immunity, mediated by paracrine cytokine signaling to nearby uninfected cells. Host intrinsic and innate responses play a vital role in protection against the spread of viral progeny and in inducing a systemic antiviral response against invading αHV virions [65]. Both intrinsic and innate immune responses synergize to reduce or delay acute replication, albeit dependent on the cell type [66]. The host's defenses usually contain the primary infection effectively; however, some viral progenies enter axon terminals that innervate the infected tissue.

Intrinsic immunity provides an immediate and direct antiviral response to pathogen invasion, mediated by physical barriers and restriction factors. However, it lacks cell-to-cell communication and response amplification [67, 68]. This intrinsic antiviral immunity is conferred by constitutively expressed host cell restriction factors that are encoded by almost all cell types [69]. To counteract viral invasion, these restriction factors directly and immediately subvert viral gene expression by inhibiting stages of the productive replication cycle, often leading to self-degeneration. Central to innate antiviral immunity are cytokines, which induce the expression of numerous antiviral factors by activating interferon-stimulated genes (ISGs) [70]. ISGs include proteins such as transcription factors that are essential for the initial amplification of the antiviral response. To counteract viral invasion, these restriction factors directly and immediately subvert viral gene expression by inhibiting stages of the productive replication cycle, often leading to self-degeneration. Some key examples of better-characterized ISGs essential for the antiviral response include Mx1 and OAS, proteins that inhibit viral replication at different stages of the viral life cycle. Mx1 degrades incoming viral nucleocapsids, directing

capsids for degradation through GTPase activity, while OAS works to activate latent RNase L, degrading viral and cellular RNA, halting viral replication [71, 72]. Intrinsic and innate responses are linked: IFN can induce the expression of a range of proteins in the intrinsic antiviral response, and the natural immune response can induce the expression of IFN and other cytokines. However, the magnitude and efficacy of this response may vary considerably across cell types, with neurons exhibiting distinct interferon-mediated responses that influence outcomes of αHV infection [20, 73].

Neurons can sense and respond to immunostimulatory molecules and express type I IFNs themselves; albeit less than in mitotic cells [74, 75]. The differential response to infection between different neuron types can influence the heterogeneity of HSV-1 latency, as IFN-induced responses to HSV-1 in murine dorsal root ganglion (DRG)-derived neurons seem to be reduced [75]. Interestingly, type I IFN treatment of neurons prior to infection with HSV-1 limited productive replication, promoted latency establishment, and even restricted reactivation of viral genomes in individual neurons [17, 76]. *In vitro* cultures of TG have also demonstrated decreased viral replication upon dose-dependent type I IFN treatment prior to infection [14, 77]. In the NS, type I IFNs have been shown to play a role in early control of HSV-1 replication within the trigeminal ganglia (TG), where they are sensed via axons [14, 78].

Type I and type III interferons engage the JAK-STAT signaling cascade, beginning with IFN receptor ligation, activation of JAK1 and TYK2, and downstream phosphorylation of STAT transcription factors (Figure 1.3) [19]. This signaling axis is central to antiviral immunity, as phosphorylated STAT1 and STAT2 regulate the transcriptional program that activates interferon-stimulated genes.

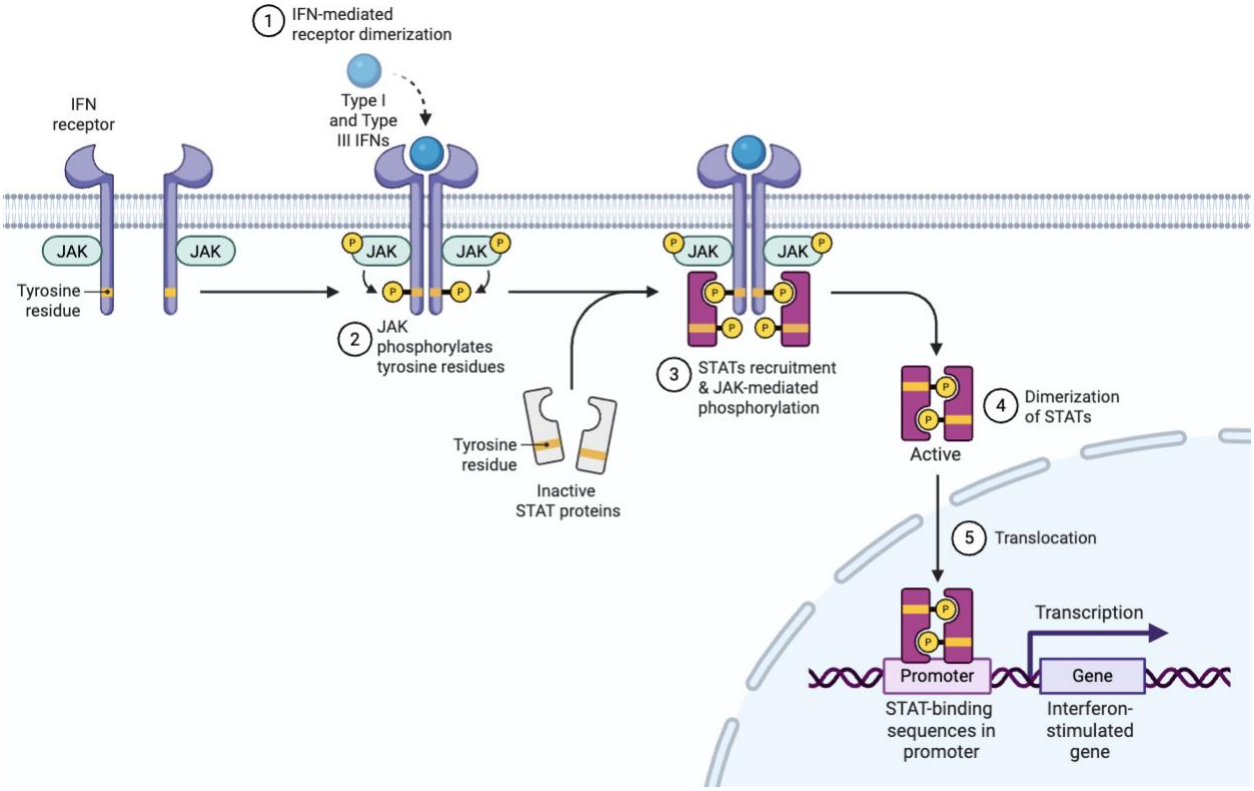

Figure 1.3. Activation of the JAK–STAT signaling pathway by Type I and Type III interferons. Upon IFN binding, interferon receptors undergo ligand-mediated dimerization (**1**), enabling the associated JAK kinases to phosphorylate intracellular tyrosine residues on the receptor tails **(2**). Phosphorylated receptors then recruit STAT proteins, which are subsequently phosphorylated by JAKs (**3**). Activated STATs dimerize (**4**) and translocate into the nucleus (**5**), where they translocate and bind ISRE/GAS elements within promoter regions to initiate transcription of interferon-stimulated genes (ISGs), establishing an antiviral state. Created on Biorender.com.

It is possible that during the early stages of infection, while the virus replication is controlled by the intrinsic and innate defenses at the mucosal surface, exposure of nerve termini to type I and III IFNs stimulate local responses in axons, independent of the distant cell bodies, which limit the entry and/or transport of αHV particles [79]. A previous study, using compartmentalized primary superior cervical neurons (SCGs) in tri-chambers showed that, when axons are exposed to IFN-β, STAT1 is phosphorylated, retained in axons, and initiates a non-canonical antiviral action [79]. The presence of phosphorylated STAT1 (pSTAT1) in axons interrupted retrograde HSV-1 and PRV capsid transport. The mechanism by which pSTAT1 in axons restricts the transport of herpes viral capsids is not clear. Accumulation of STATs in axons may trigger responses such as autophagy that would limit the number of capsids reaching the connected cell body. The number of virus particles reaching the neuronal nuclei significantly affects the mode of infection, as shown by a productive infection threshold (in the number of infecting viral particles), particularly when the infection is acquired through axons [80, 81]. If the infection dose is below this threshold, viral genomes are immediately silenced in the neuronal nuclei before the lytic gene transcription is initiated, and latency is established. This hypothesis was also supported by multiple other studies that have inferred that axonal pre-exposure to exogenous type I IFNs have an increased antiviral response against αHV infection, essentially by priming the neuron for the upcoming viral invasion [18, 79].

The potent antiviral role of type III IFNs, particularly in mucosal epithelial cells, has been expanded in recent years highlighting the tissue-protective potent antiviral action of these cytokines at the barrier surfaces. Because of these features, type III IFNs have been investigated for their potential to protect the nervous system against αHV invasion. In this thesis, I investigated the neuronal versus non-neuronal cell response to type III IFNs within the mucosa-

NS junction using primary SCG neurons and fibroblasts. Interestingly, while type III IFN treatment led to STAT1 phosphorylation in both cell types, only fibroblasts showed STAT2 phosphorylation upon treatment [29]. This led to a differential ISG response in neurons characterized by the induction of a subset of SCGs at a lower magnitude. Type III IFN pretreatment reduced PRV virus yield in both SCGs and Rat2s. However, whether type III IFNs can efficiently restrict HSV-1 latency establishment or reactivation remains to be elucidated. Danastas, et al. have recently shown that pretreatment of isolated axons of DRG neurons grown in microfluidic chambers with IFN-λ impairs HSV-1 egress from axons [18]. These studies demonstrate the importance of the mucosal epithelial-neuronal cell junction, as paracrine cytokine signaling can ultimately affect productive infection and subsequent neuroinvasion.

1.4 Autophagy

Autophagy is a highly conserved catabolic pathway critical for cell survival and homeostasis. This process eliminates harmful protein aggregates, damaged organelles, and intracellular pathogens via lysosomal degradation [82]. Importantly, autophagy primarily functions as a cellular survival mechanism rather than a cell death program, allowing cells to recycle cellular components and maintain integrity under stress conditions [83]. The postmitotic nature of neurons renders them highly dependent on autophagy to preserve their integrity and long-term viability. Autophagy plays a role in development, cell differentiation, apoptosis, pathogen infection, and starvation, and its impairment can contribute to neuronal death. Defects in the autophagy pathway are implicated in various neurodegenerative disorders (e.g., Alzheimer's disease (AD)) [82]. Neurons exhibit atypical autophagy responses compared to mitotic cells: neuronal autophagy is highly compartmentalized, insensitive to standard modulation methods (e.g., starvation and rapamycin), and forms unusual autophagosome clusters

under conditions of viral infection and IFN treatment [75, 84, 85]. In postmitotic neurons, xenophagy (a specialized form of selective autophagy) provides critical pathogen clearance by engulfing and degrading viable virions without triggering the inflammatory or cytotoxic responses that would cause irreversible damage in the brain [86].

Autophagy functions as a key effector mechanism of intrinsic immunity against HSV-1 infection, specifically in neurons [75]. In a study performed by Overdahl, et al., HSV-1 mutants lacking factors to antagonize or inhibit autophagy demonstrate significant attenuation in the nervous system [87]. Additionally, it was observed that HSV-1 retained a higher viral yield and exhibited greater virulence in mice lacking the autophagy machinery. HSV-1 has also developed strategies to counteract autophagy-mediated restriction. During early HSV-1 infection, ICP0 downregulates the expression of two autophagy adaptor proteins, sequestosome-1 (SQSTM1) and optineurin (OPTN), in a proteasome-dependent manner. The viral neurovirulence protein ICP34.5 directly binds to Beclin-1 and inhibits Beclin-1-dependent autophagy [87]. Beclin-1 is a well-established regulator of autophagy and membrane trafficking [88]. The Beclin-binding domain (BBD) of ICP34.5 is essential for HSV-1 to suppress autophagy in neurons. Deletion of the BBD results in decreased viral replication, increased cell death, and higher mortality in vivo [87]. The viral titer of the ICP34.5 mutant virus lacking BBD is significantly lower than that of the rescued virus in the cornea, trigeminal ganglia, periocular skin, and brain tissues [89]. In contrast, only a limited phenotype of the BBD mutant was observed in nonneuronal cell types *in vitro* [90].

In addition to ICP34.5, the US11 protein inhibits autophagy by disrupting the *tripartite motif* protein 23-TANK-binding kinase 1 (TRIM23-TBK1) complex by directly binding to the Auxin response factor (ARF) domain of TRIM23 [91]. US11 interacts with PKR to suppress

cellular autophagy and autophagosome formation in fibroblasts subjected to poly(I:C) treatment or starvation, without interacting with Beclin-1, unlike ICP34.5 [92].

1.5 Latency establishment in the PNS and periodic reactivations leading to pathologies

Understanding the αHV latency requires examining the initial entry of virions to neurons (i.e. neuroinvasion), the establishment of the latent state, the maintenance of that state, and stress-induced reactivation. A complex interplay between viral strategies and neuronal defenses shapes each stage. Following primary infection at mucosal surfaces, HSV-1 enters sensory nerve axons innervating these tissues through receptor-mediated endocytosis (e.g., nectin-1) and membrane fusion, gaining access to the axonal compartment. Following entry, viral capsids undergo retrograde transport along microtubules from axon termini to cell bodies, where HSV-1 establishes latency rather than lytic infections.

The unique biology and structure of PNS neurons directly influence latency. PNS neurons are highly polarized with single axons containing more than 99% of the cell's cytoplasm, necessitating finely tuned long-distance communication between axon termini in the periphery and cell bodies in the distant ganglia. However, neurons must balance responsiveness to signals from peripheral axons with resistance to apoptosis to ensure survival as post-mitotic, irreplaceable cells. HSV-1 exploits this balance, establishing latent infections that persist without triggering neuronal death pathways, while remaining capable of responding to reactivation signals transmitted from axon terminals during stress events.

Once established, latent αHV infections are characterized by profound transcriptional silencing of viral lytic genes through heterochromatin formation. Upon nuclear entry, viral DNA associates with histones, forming repressive heterochromatin marked by inhibitory modifications

including histone H3 lysine 9 trimethylation (H3K9me3) and histone H3 lysine 27 trimethylation (H3K27me3) [93]. This silencing is facilitated by the absence or deletion of critical viral tegument proteins during retrograde axonal transport. VP16, a viral tegument protein and key transactivator of IE genes, can be depleted or spatially separated during retrograde long-distance axonal transport. VP16 activates transcription of ICP0, which is essential to initiating lytic gene expression, and its absence reinforces a repressive chromatin state that favors latency [58]. ICP0 prevents heterochromatin assembly by degrading components of promyelocytic leukemia (PML) nuclear bodies and other repressive factors. In the absence of VP16, ICP0 expression is reduced, allowing rapid heterochromatin assembly and transcriptional silencing, thereby promoting latency [94].

Additionally, neuronal culture experiments demonstrated that axonal infections can be redirected toward lytic outcomes by delivering VP16 to cell bodies via helper viruses or by introducing stress-inducing compounds that mimic VP16 [95, 96]. Conversely, when tegument proteins are absent from the cell body during axonal infection, productive infection can still occur but requires slower alternative activation pathways involving protein kinase A (PKA) and c-Jun N-terminal kinase (JNK), rather than direct tegument-mediated promoter activation [97]. These findings underscore that availability of tegument proteins or activation of stress signaling kinases during the critical early phase of neuronal infection determines the lytic infection versus latency establishment.

Beyond viral factors, the intrinsic immunity of neurons plays a central role in controlling HSV-1 infection, guiding the genome into a latent state. Neurons are equipped with multiple cell-autonomous defense mechanisms that recognize and restrict viral infection, including

chromatin-mediated silencing of foreign DNA, autophagy, and interferon-stimulated gene (ISG) expression. The highly polarized and terminally differentiated nature of PNS neurons, along with their long-distance separation of infection sites from the cell nucleus, creates a unique environment where incoming viral genomes are particularly vulnerable to these intrinsic defenses. Another strategy of host cells to repress viral gene expression involves chromatin repressor complexes and epigenetic modification mechanisms such as the HDAC/CoREST/LSD1/REST repressor complex, which acts as a critical component in regulating latency and reactivation [55].

IFN signaling plays a complex, paradoxical, and significant role in the NS. Previous findings reveal that type I IFN/STAT1 signaling promotes the efficient silencing of HSV-1 and PRV through mechanisms that involve LAT modulation and PML (promyelocytic leukemia) nuclear body upregulation, while also supporting neuronal survival and facilitating re-establishment of latency during reactivation events [98-100]. However, *in vivo* experiments make the model more complex. Although latency can be established in the absence of STAT1, albeit with delayed kinetics, impaired IFN responses *in vivo* lead to uncontrolled lytic replication and severe CNS disease, including fatal herpes simplex encephalitis [17, 101]. Thus, IFN-mediated latency may reflect a coevolutionary Nash equilibrium: the host tolerates lifelong viral persistence and periodic reactivations that enable transmission, while avoiding the acute pathological consequences of productive infection. This perspective suggests that latency is not merely viral evasion but rather a mutually beneficial state, adding nuance to our understanding of αHV-host dynamics and the neuronal interferon response (Figure 1.4).

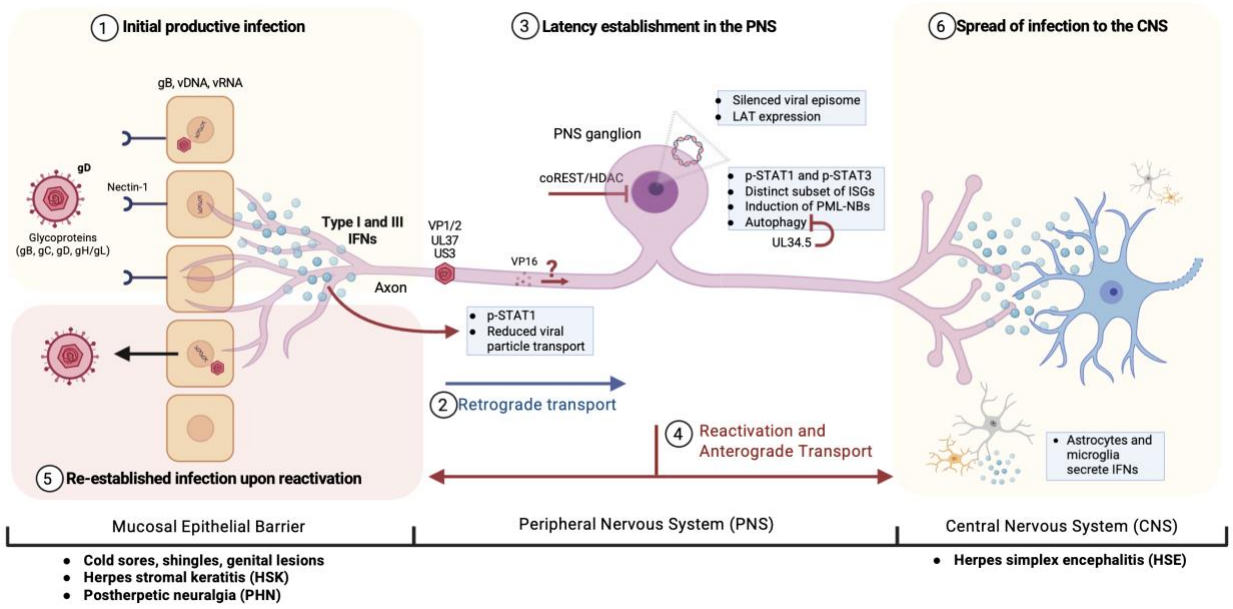

Figure 1.4. Model of HSV-1 infection and spread to the nervous system. (**1**) HSV-1 enters the mucosal epithelial cell and starts productive replication. Infection is detected by PRRs and receptor complexes, which induce the secretion of type I and III IFNs. Viral proteins such as ICP0, ICP27, ICP34.5, US3, and UL37 counteract antiviral sensing. (**2**) Once capsids enter axons of sensory neurons, outer tegument proteins are released in the cytoplasm while inner tegument proteins, such as UL36 (VP1/2), UL37, and US3, remain attached to the capsid. Within the axons, p-STAT1 is accumulated upon exposure to type I IFNs, limiting retrograde viral particle transport. (**3**) HSV-1 genomes are maintained as circular chromatinized episomes during latency (except the LAT region). Activation of STAT1 and STAT3 leads to the induction of a subset of ISGs in neurons. IFN exposure induces PML-NB formation in the neuronal nuclei. Autophagy restricts HSV-1 replication in neurons; however, ICP34.5 inhibits Beclin-1-dependent autophagy. HDAC/CoREST/LSD1/REST repressor complex regulates latency and reactivation of viral genomes. (**4**) Reactivation of HSV-1 is triggered by stress signaling pathways, which alter silencing histone modifications, initiating the transcription of viral genes to produce infectious progeny. The new progeny can be transported anterogradely from the cell body toward the initial site of entry (**5**), triggering re-establishment of infection that can lead to cold sores, genital lesions, or shingles. Severe cases may result in oral or genital ulcerations, keratitis, or blindness via HSK, or post-herpetic neuralgia (PHN). (**6**) Upon reactivation, new progeny can also be transported anterogradely to the CNS, which is one synapse away. Astrocytes and neurons mostly rely on TLR3 for IFN production, with microglia activating the cGAS-STING pathway. It is still unclear whether αHVs can establish latency in the CNS. Adapted from Salazar et al. (2023) [102]. Created on Biorender.com.

Reactivation differs fundamentally from initial lytic infection in that latent genomes contain extensive repressive histone modifications and lack any viral proteins. Environmental stress signals, including fever, UV exposure, or physical trauma, remodel chromatin, enabling a biphasic reactivation process that produces infectious progeny [11, 13, 60]. Notably, reactivation is inefficient: only a subset of latently infected neurons reactivate in response to a given stimulus, and within individual nuclei, only some viral genome copies restart transcription. This heterogeneity likely reflects multiple factors, including genome copy number, neuronal intrinsic properties, and tissue-specific signals. However, the complete host and viral factors involved in maintaining latency and triggering reactivation are not fully understood.

Clinically, αHV reactivation causes substantial morbidity worldwide, including recurrent oral lesions (HSV-1), genital ulcers (HSV-2), and shingles with asocial post-herpetic neuralgia (VZV). Ocular HSV-1 reactivation causes herpes stromal keratitis, leading to corneal blindness, while herpes simplex encephalitis (HSE), though rare, carries mortality exceeding 70% without treatment and frequently results in permanent neurological damage even with therapy (Figure 1.5) [69]. The capacity for lifelong persistence and repeated reactivation underscores the importance of understanding the molecular mechanisms that govern the latency-reactivation cycle and the intrinsic neuronal defenses that restrict it. Therefore, this thesis addresses a knowledge gap, particularly in the spread of viral infection from infected epithelia to the NS and the role of IFN signaling in neuroinvasion.

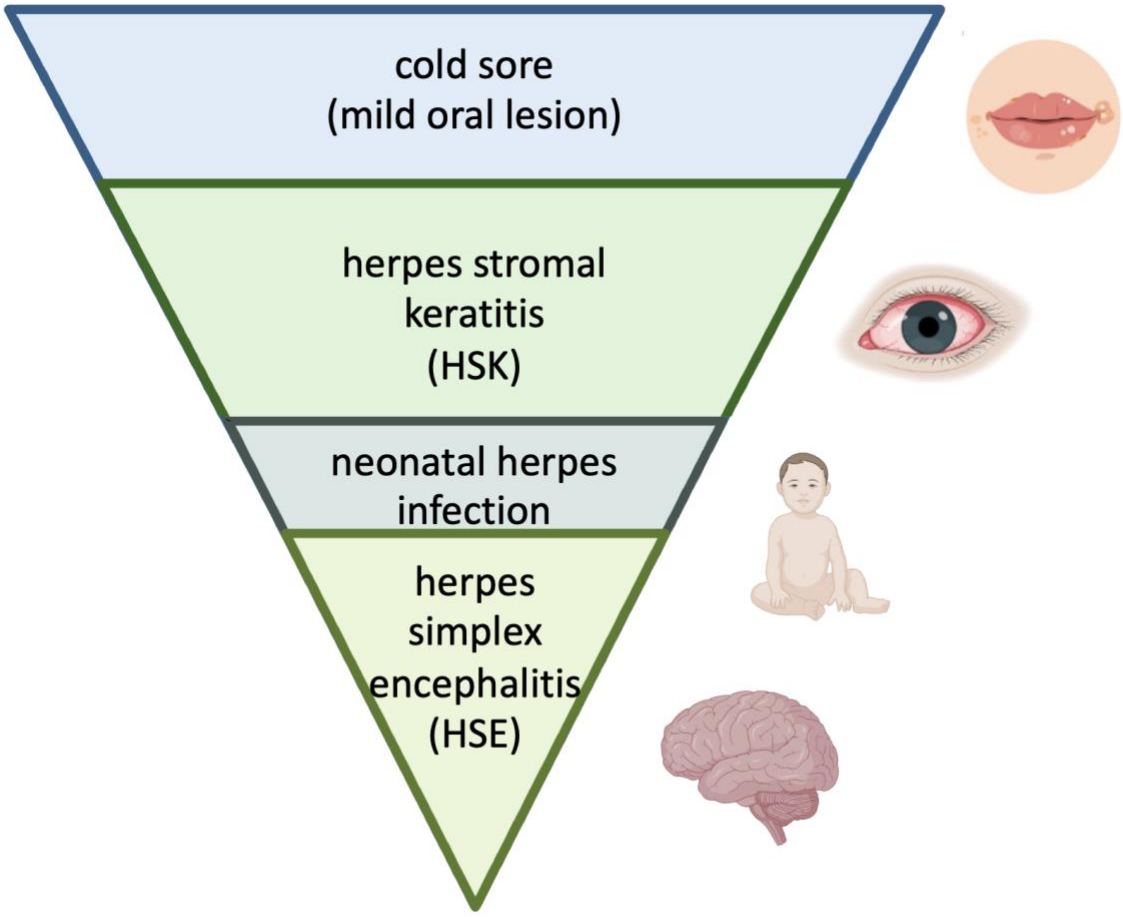

Figure 1.5. A schematic representation of diseases caused by HSV-1 infection. This figure is adapted using studies from Looker, et al. [103]. The figure displays diseases ordered from most common (top) to rarest (bottom). Created on Biorender.com.

1.6 Tri-chamber neuronal cultures for the study of αHV infection

While dissociated neuronal cultures have represented the standard approach for α-herpesvirus latency studies, these systems lack the spatial compartmentalization characteristic of sensory ganglia *in vivo*. To elucidate the establishment of productive infection and subsequent latency in neurons, researchers have developed an *in vitro* model system to recapitulate the polarization of PNS neurons called tri-chamber cultures [104]. Peripheral neurons are among the longest cells in the human body, with some extending over one meter from distal axon terminals in the toes to cell bodies located in dorsal root ganglia near the spinal cord. This anatomical organization positions neuronal cell bodies, which house the nucleus and genomic DNA, in protected ganglia deep within the body. At the same time, peripheral nerve terminals remain exposed to mucosal and epithelial surfaces. This extreme polarization, although difficult to recapitulate *in vitro*, is one of the key factors determining neuroinvasion and latency establishment be HVs.

Superior cervical ganglia (SCGs) are the largest sympathetic cervical ganglia in the neck providing autonomic innervation to the head and neck region. SCG neurons present several experimental advantages over alternative neuronal models such as dorsal root ganglia (DRG). First, SCGs yield a more homogenous population, whereas DRGs contain a heterogeneous population with distinct transcriptional profiles and differential susceptibility to viral infection [105, 106]. The homogeneity of SCGs reduced experimental variability and simplified the interpretation of population-level response to treatment and viral infection [104]. Additionally, SCGs extend long, robust axonal projections that can penetrate the barriers separating compartments in tri-chamber culture systems. Finally, SCGs are naturally permissive to αHV infection. Both HSV-1 and PRV infect sympathetic ganglia *in vivo*, making SCG neurons a physiologically relevant model. In our studies, SCGs were harvested from embryonic day 16-17

(E16-17) rat embryos. The E16-17 developmental time point balances neuronal maturity (capable of robust IFN-λ receptor expression and signaling) with *in vitro* viability.

Mimicking the physiological barriers of infection in humans, the tri-chamber system is made up of three sections: the soma (S) compartment, where the neuronal cell bodies are cultured; the methocel (M) compartment, where axons pass through the initial barrier; and the neurite (N) compartment, where axon termini emerge (Figure 1.6A). Compared to microfluidic devices, which offer superior axonal alignment through narrow microchannels, tri-chambers provide several critical advantages: a larger, open culture area that facilitates ease of adding reagents for biochemical analyses; imaging compatibility with fluorescent microscopy; and directional virus infections [107]. Measuring infection spread in tri-chambers by titering progeny virus has yielded valuable insights. These compartmented neuronal cultures allow infecting neuronal soma or axons and harvesting each compartment separately during a time course of infection for protein, nucleic acid or virus yield analysis. Recombinant viruses expressing fluorescent proteins, such as PRV-180, containing mRFP1-VP26 in a PRV-Becker background or OK14 (mRFP-VP26 in HSV-1 17 background), enable real-time assessment of infection and spread dynamics over multiple time points using live-cell microscopy (Figure 1.6B) [79, 108]. This integrated approach, combining anatomically relevant spatial compartmentalization with real-time fluorescence imaging, provides a physiologically pertinent platform for dissecting the spatiotemporal dynamics of αHV neuroinvasion.

The ability to selectively treat individual compartments (e.g., applying exogenous IFN-λ to the N-compartment to mimic mucosal cytokine secretion) while monitoring infection outcomes in the S-compartment enables mechanistic investigation of how neuronal antiviral responses restrict viral spread across distinct subcellular domains. Consequently, compartmented neuronal

cultures represent an optimal experimental system for investigating the compartmentalized intrinsic and innate immune responses that govern αHV neuroinvasion.

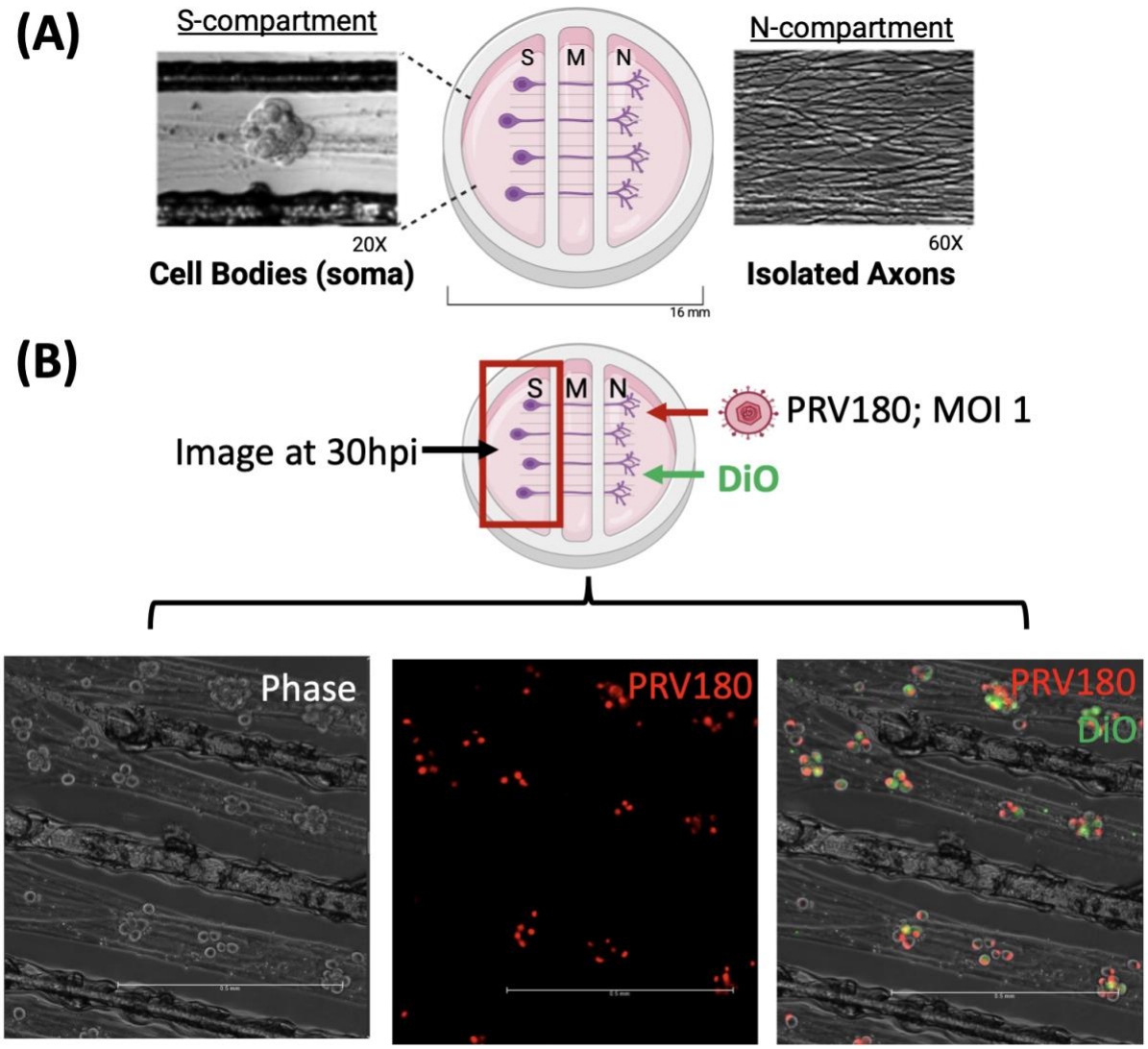

Figure 1.6. Tri-chamber neuron culture system. (**A**) The tri-chamber system features a teflon ring outlined with a thin layer of silicone grease, positioned inside a 35-mm tissue culture dish. The S- (soma) compartment houses neuron cell bodies, while the M- (methocel) and N- (neurite) compartments contain an extensive network of axons. (**B**) PRV180 (red) infection was performed in the N-compartment at MOI 1. DiO (green), a lypophilic dye, was added to the N compartment media 6 hpi to label cell bodies connected to the N-compartment. The S-compartment was imaged at 30 hpi. Images were taken at 20X and bars represent 50 μm.

CHAPTER 2: Cell-Specific Induction of ISGs in Response to Type III IFN Treatment

Abstract

Type III interferons (IFN-λ) serve as essential antiviral mediators at mucosal surfaces, yet their impact on peripheral nervous system (PNS) neurons remains largely unexplored. Because αHVs initiate infection at mucosal epithelia before accessing peripheral neurons, defining neuron-specific responses to IFN-λ is critical for understanding early viral restriction. In this chapter, we compared the effects of IFN-λ on rat primary superior cervical ganglion (SCG) neurons and fibroblasts to determine how cell identity shapes downstream signaling and interferon-stimulated gene (ISG) induction. We found that fibroblasts mounted a canonical IFN-λ response characterized by robust phosphorylation of STAT1 and STAT2, accompanied by high-magnitude induction of ISGs. In contrast, SCG neurons selectively phosphorylated STAT1 with minimal STAT2 activation, revealing a noncanonical, neuron-specific signaling state. This signaling divergence resulted in distinct ISG expression profiles: neurons displayed lower overall ISG induction but preferentially upregulated antiviral genes such as Ifit1, Stat3, and Tlr7, whereas fibroblasts strongly induced classical ISGF3 (Interferon-Stimulated Gene Factor 3) - dependent ISGs, including Oas1a and Irf9. RNA sequencing demonstrated that IFN-λ triggers a temporally biphasic transcriptional program in neurons. Early responses (3 h) upregulated genes involved in neuronal plasticity and homeostasis, while canonical antiviral ISGs dominated at 24 hours, with RSAD2 (viperin) emerging as the most strongly induced late-response ISG. Compared to IFN-β, IFN-λ elicited slower and more moderate ISG induction, further emphasizing pathway specificity. Overall, these findings reveal that peripheral neurons mount a uniquely tuned IFN-λ response optimized for long-term survival rather than rapid inflammatory

defense, providing key insight into how early neuronal antiviral environments shape α-herpesvirus neuroinvasion.

2.1 Introduction

The natural immune responses of mucosal epithelia serve as a critical barrier, preventing virions from reaching peripheral neurons during primary infection. Inducing host responses at these sites is facilitated by natural and intrinsic immunity. Among the various forms of natural immunity are restriction factors, which are constantly produced by host cells and directly block viral transcription and replication without alerting neighboring uninfected cells. In parallel, pattern recognition receptors (PRRs) detect pathogen-associated molecular patterns (PAMPs), triggering cytokine production. Cytokines respond to infections, and immune effector cells such as neutrophils, plasmacytoid dendritic cells, and natural killer cells become activated and recruited; these cells are also considered part of natural immunity.

Interferons (IFNs) are a group of cytokines classified into three types based on their receptors and biological functions. Type I IFNs (IFN-α/β) and type III IFNs (IFN-λ) mediate intrinsic and natural antiviral immunity, while IFN-γ (type II) is involved in adaptive immunity [21, 109]. In contrast to type I IFN receptors (IFNAR1/2), type III IFN (IFN-λ) receptors, composed of IFNLR1/IL-10RB heterodimer, are not ubiquitously expressed and are instead preferentially expressed on mucosal epithelial cells and immune cells, such as neutrophils, dendritic cells, and B cells [28, 110, 111]. Mucosal epithelial cells are a subset of epithelial cells that line the mucosal barriers of the genital, respiratory, and gastrointestinal systems. Interestingly, IFN-λ production increases as cells polarize, and the quality of the IFN response is determined by the differentiation state of mucosal epithelial cells [110].

In humans, type III IFNs consist of subsets IFN-λ 1-4, whereas mice express only IFN-λ2 and IFN-λ3 [112]. Despite signaling through distinct receptors, both type I and type III IFNs activate overlapping downstream pathways (e.g., JAK-STAT pathway) involving STAT phosphorylation and ISG induction. However, functional studies have demonstrated that type III IFN treatment of mucosal epithelia cells upon αHV infection had a higher protective response when compared to type I IFN treatment [28, 113, 114]. Importantly, intravaginal pretreatment of IFN-λ prior to HSV-2 infection in a murine model elicited a potent antiviral response [115]. These findings established IFN-λ as a key mediator of mucosal antiviral defense against αHVs.

Given that α-herpesvirus infection begins at the mucosal epithelium and that peripheral nerve endings are the first neuronal components exposed to this cytokine-rich microenvironment, we hypothesized that neurons might also respond to type III IFN signaling. Supporting this possibility, Li et al. previously demonstrated that IFN-λ pretreatment significantly reduced HSV-1 replication in cultured cortical neurons, indicating that at least some neuronal populations possess functional IFN-λ receptor expression and downstream antiviral signaling capacity [116]. However, cortical neurons represent the central nervous system (CNS) neuronal population that are not naturally exposed to mucosal type III IFN production during peripheral HSV-1 infection. Whether peripheral neurons, physiologically relevant targets of αHV neuroinvasion similarly express IFN-λ receptors and mount antiviral responses remained unknown.

This chapter demonstrates that peripheral neurons respond to IFN-λ through a noncanonical pathway distinct from the classical JAK-STAT pathway. Unlike fibroblasts, which activate both STAT1 and STAT2 upon IFN-λ treatment, neurons exhibit selective STAT1 phosphorylation without STAT2 activation. This STAT1-dominant signaling drives a temporally biphasic transcriptional response: early neuronal treatment (3 h) followed by delayed but robust

induction of antiviral ISGs (24 h), with RSAD2 (viperin) emerging as the most highly upregulated antiviral gene of interest. Compared with type I IFN, which elicits rapid, high-magnitude ISG induction, IFN-λ produces a delayed, more sustained response in neurons. These findings reveal a neuron-specific IFN-λ pathway that balances antiviral defense with cellular preservation.

2.2 Results

IFN-λ treatment activates a differential response in Rat2 cells versus primary neurons

To determine whether treatment of primary neurons with type III IFN elicits a similar response to non-neuronal cells, superior cervical ganglionic (SCGs) neurons were compared to Rat2 cells (fibroblast cell line). SCG is the largest cervical sympathetic ganglia that innervates head and neck and has been shown to be a site for αHV latency [117, 118]. Rat2 cells were chosen because of the positioning of fibroblasts within the connective tissue of the skin: they are found in two key areas known as the dermis (stratified squamous epithelia), which also hosts specialized immune cells, and the hypodermis (lamina propria), mostly consisting of adipocytes along with macrophages and axons of sensory neurons (Figure 2.1A). IFN-λ2 was utilized for the purpose of this study as it was shown to be conserved among humans, mice and rats, and to show higher antiviral activity in human and murine cells [112]. Rat2 cells were treated with either type I (IFN-β) or type III IFN (IFN-λ2) for 24 h prior to harvest and analysis (Figure 2.1B). STAT1 and STAT2 phosphorylation were monitored at different concentrations of IFN-λ2 and IFN-β treatment for comparative detection of phosphorylated STAT1 (p-STAT1) (Figure 1B). Based on this data, in the subsequent experiments, we used IFN-λ2 at 200 ng/mL and IFN-β at 100 U/mL concentration. Rat2 cells and neuronal cell bodies and axons within the S-compartment were

harvested after 24 h IFN treatments to determine the phosphorylation status of STAT1 and STAT2, key mediators of the JAK-STAT signaling pathway by using p-STAT1 and p-STAT2 specific antibodies. Both cell types demonstrated comparatively increased levels of p-STAT1 when they were treated with IFN-λ2 as opposed to their untreated counterparts (Figure 2.1C). However, IFN-λ2-treated Rat2 cells demonstrated a much higher STAT2 phosphorylation when compared to SCG neurons (Figure 2.1C). When we monitored STAT2 activation in neurons at earlier time points after IFN-λ2 treatment (1- and 3 h post-treatment), we did not detect any p-STAT2 accumulation (Figure 2.1D). Together, these results indicate that there is a cell-type specific induction of the signaling cascade upon exposure to type III IFNs.

Mounting evidence indicates that IFN-λ is a key player in the antimicrobial defense of mucosal epithelia, but its role in neurons has not been explored. Peripheral sensory neurons face infection damage, but they are long-lived, and the inflammatory response to viral infection could lead to irreversible neuronal damage. Neurons are therefore considered to be immunologically constrained to antiviral responses of a magnitude appropriate to control viral infection without causing the cytotoxic effects of these responses. Recent evidence contradicts the long-held view that neurons are passive viral targets. In primary neuronal cultures, IFN-λ treatment results in phosphorylation of the major IFN downstream transcription factor, STAT1, but not STAT2. This contrasts with most other cell types, where the signaling pathway used for IFN-λ is the ISGF3 pathway, which includes both transcription factors. It appears that neurons participate in an IFN-λ signaling pathway that drives limited antiviral gene expression without inducing common inflammation.

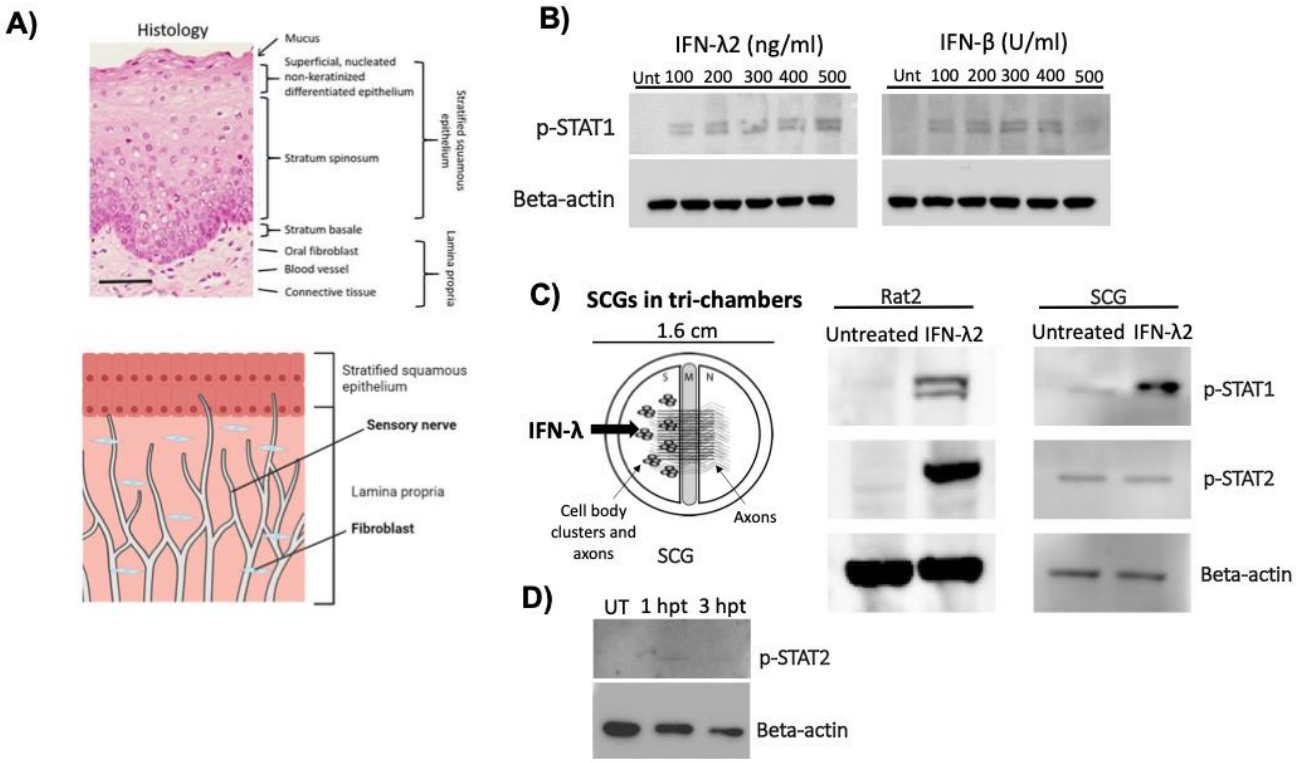

Figure 2.1. STAT activation upon IFN-β and IFN-λ2 treatment in Rat2 cells and SCGs. (**A**) Histological model of tissue from buccal oral mucosa adapted from Edmans et al., Pharmaceutics, 2020 (top) and a diagram model depicting fibroblasts and sensory nerves in the dermis (bottom) [119]. (**B**) Detection of p-STAT1 in Rat2 cells 24 h after treatment with either IFN-β or IFN-λ2 at various concentrations. (**C**) Model of treatment (left) and Western blots of detection of p-STAT1 or p-STAT2 upon IFN-λ2 (200 ng/mL) treatment for 24 h (right). (**D**) Detection of p-STAT2 in SCGs that were treated with IFN-λ2 (200 ng/mL) for 1 or 3 h (hpt) compared to untreated (UT) SCGs. Beta-actin was used as a loading control.

IFN-λ induces differential expression of interferon-stimulated genes (ISG) in primary neurons

Interferons activate a signaling cascade that induces the expression of interferon-stimulated genes (ISGs), which elicit protective responses against a viral threat. ISGs are key regulators of the JAK-STAT pathway that can impact early and late stages of the virus life cycle [21, 25, 120]. STATs serve as transcriptional activators of ISGs. As shown in the previous data above, Rat2 cells and SCGs activate STAT1 and STAT2 differently. To differentiate between ISG induction in neurons, a type I IFN array was used on a 96-well RT-qPCR plate with 84 genes of interest and 2 housekeeping genes. SCGs were either treated or not treated with IFN-λ2 (200 ng/mL) for 24 h prior to harvest and their mRNA levels were analyzed via RT-qPCR (Figure 2.2A). A heat map was constructed based on the mean cycle threshold (Ct) values detected in duplicate control versus IFN-λ treatment conditions demonstrating the activation of a subset of ISGs dependent on exposure to type III IFN. Based on the changes in the Ct values, 21 genes of interest were selected for further investigation.

For these ISGs, we designed primers based on the target sequences in the type-I IFN array. We treated both SCGs and Rat2 cells with IFN-λ2 (200 ng/mL) prior to RNA isolation. This experiment was repeated three times with replicates. Normalized gene expression analyses demonstrated that type III IFN induces a similar response in fibroblasts and primary neurons with differential activation dynamics (Figure 2.2B). The magnitude of ISG induction was detected to be lower overall in SCGs as compared to Rat2 expression. In SCGs, the highest ISG induction was detected to reach approximately 117-fold in the case of Oas2. In Rat2 cells, Oas2 was also the most activated gene and displayed approximately 1400-fold induction upon IFN-λ treatment.

Six ISGs demonstrated a higher fold change in SCGs than Rat2 cells. Stat3, Ifit1, and T7 showed a higher induction in SCGs than Rat2 cells displaying a 2.8-, 15.4-, and 27.8-fold difference, respectively, when compared to induction in Rat2 cells. Cd69 and Isg15 showed a fold change below 1.5-fold (Figure 2.2B). Only one ISG; Cd38 demonstrated a decrease in IFN-λ2-treated SCGs as compared to an increase in IFN-λ2-treated Rat2 cells. Furthermore, we detected that STAT1 expression was induced similarly in both cell types, showing approximately 10-fold induction, whereas STAT2 transcripts were detected to increase 4.6-fold in Rat2 cells and 1.8-fold in SCGs, supporting our differential STAT2 phosphorylation data (Figure 2.1C).

Verification of target ISG induction in Rat2 cells vs. primary neurons upon IFN-λ treatment

Three ISGs were selected for further protein analysis based on the differential gene expression data: Oas1a, IFIT1, and IRF9. Oas1a inhibits protein synthesis by inducing general RNA degradation within infected cells, thus inhibiting viral replication along with IFIT1, which inhibits translation and viral replication. IRF9, a component of the complex known as IFN-stimulated gene factor 3 (ISGF3), is directly involved in the JAK-STAT pathway and is a key component in IFN immune response. These three genes showed a cell-type-specific difference in the induction pattern: Oas1a was detected to be increased in both cell types (at different magnitudes), Ifit1 showed a higher induction in SCGs, and Irf9 demonstrated a higher induction in Rat2 cells. Western blot analyses were performed on IFN-λ2-treated and untreated Rat2 cells and SCGs. Supporting our relative gene expression data, Oas1a expression was detected to be increased in both cell types upon treatment of IFN-λ2, although at a higher level in Rat2 cells (Figure 2.3A). As expected, based on the transcriptional profile, IFN-λ2 (200 ng/mL)-treated Rat2 cells had lower activation of IFIT1 as opposed to SCGs which showed an increase in

protein amounts (Figure 2.3B). Finally, IRF9 demonstrated a slight increase in Rat2 cells upon IFN-λ2 (200 ng/mL) treatment as opposed to untreated or IFN-λ-treated SCGs, validating the transcriptional RT-qPCR analyses.

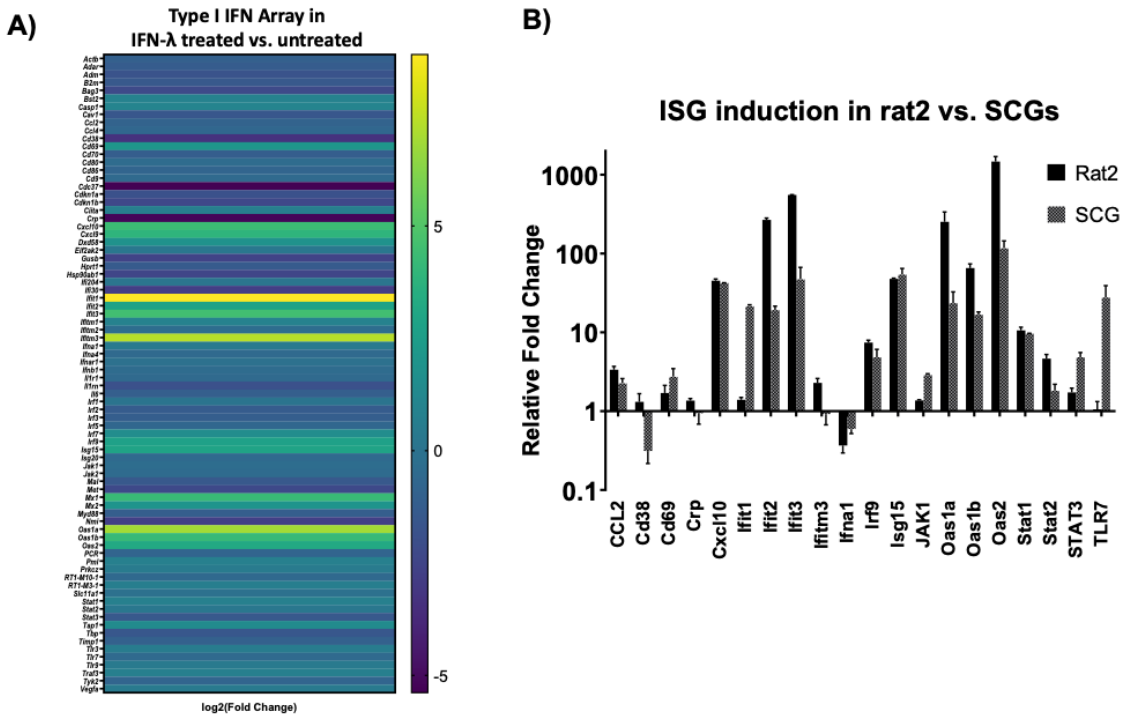

Figure 2.2. Comparative ISG induction upon IFN-λ2 treatment in Rat2 cells and SCGs. (**A**) SCGs were treated with IFN-λ2 or vehicle. Type I IFN array including primer pairs for 85 Interferon stimulated genes (ISG) was used (GAPDH was used as housekeeping gene). Heatmap created using Graphpad Prism 5.0 and performing log2 fold change on normalized gene expression (2^{-ddCt}). Yellow represents higher fold change whereas blue indicates decreased fold change. (**B**) Normalized gene expression (2^{-ddCt}) in SCGs (grey pattern) and Rat2 cells (black) treated with IFN-λ2 (200 ng/mL) for 24 h prior to harvest.

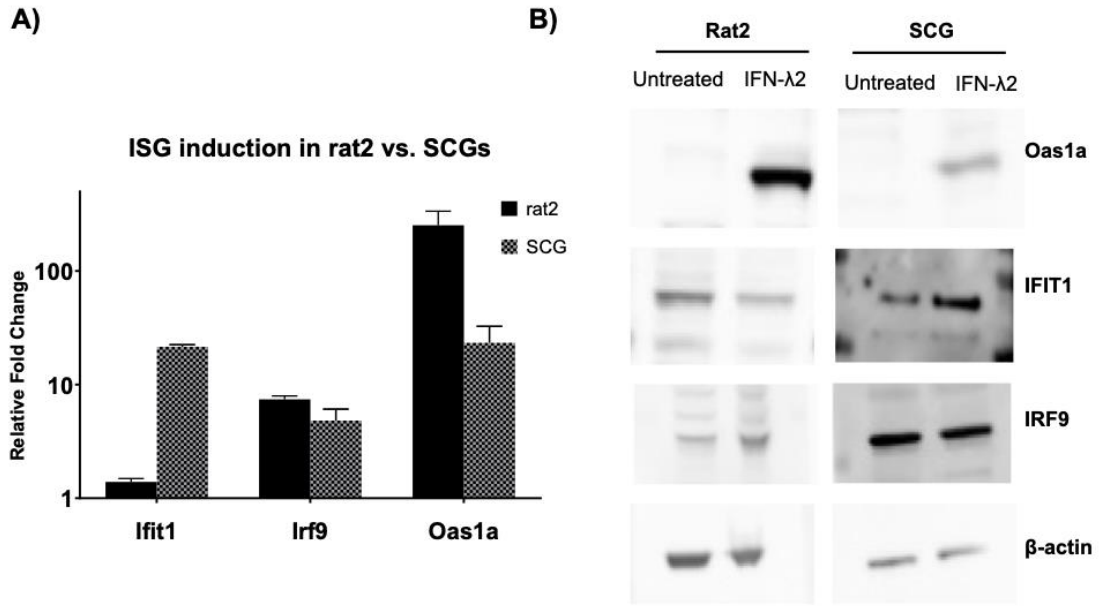

Figure 2.3. Cell-specific induction of different ISGs. (**A**) Normalized gene expression (2^{-ddCt}) of Oas1a, IRF9, and IFIT1. (**B**) Western blots of Rat2 cells and SCGs untreated or treated with IFN-λ2 (200 ng/mL) for 24 h and immunoblotted with respective antibodies: Oas1a, IFIT1, and IRF9. Beta-actin was used as a loading control.

Temporal ISG induction in IFN-λ-treated primary neurons

While the qPCR-based ISG screening focused on a selected subset of antiviral genes, the selective activation of STAT1, but not STAT2, suggested that type III IFN might activate a noncanonical antiviral response different from the well-known ISGF3 (IFN-stimulated gene factor 3) response seen with type I IFN. To gain an unbiased, genome-wide view of this alternative signaling pathway, we conducted RNA sequencing to map the transcriptional landscape of IFN-λ-treated peripheral neurons. We performed RNA-sequencing at early (3 h) and late (24 h) time points after primary SCG neurons were treated with rat IFN-λ2 (200 ng/ml). At 3 h post-treatment, we observed distinct changes in gene expression. Notably, the most significantly downregulated genes included *H19* (a long non-coding RNA implicated in growth control and neural development), *Nos1* (a neuronal nitric oxide synthase involved in neurotransmission), and *Dcx* (a marker of immature neurons involved in neuronal migration) (Figure 2.4A) [121-123]. Conversely, *Ahnak*, a gene involved with membrane repair and calcium signaling, was among the most significantly upregulated (Figure 2.4A) [124, 125]. Gene ontology analysis using *gProfiler* further confirmed these enrichments. By 24 hours post-treatment, a shift toward interferon-stimulated gene (ISG) induction was observed, with 32.6% of the significantly induced genes associated with innate immune response pathways. RSAD2 (viperin) emerged as the most robustly upregulated transcript at this later stage (Figure 2.4B). Other top hits in this later stage included *Mx1* (a GTPase that inhibits viral replication) and *Usp18* (an ISG15 de-conjugating enzyme that acts as a negative regulator of IFN signaling), classic ISGs that are key in facilitating the antiviral response induced by type I and type III IFNs.

(A)

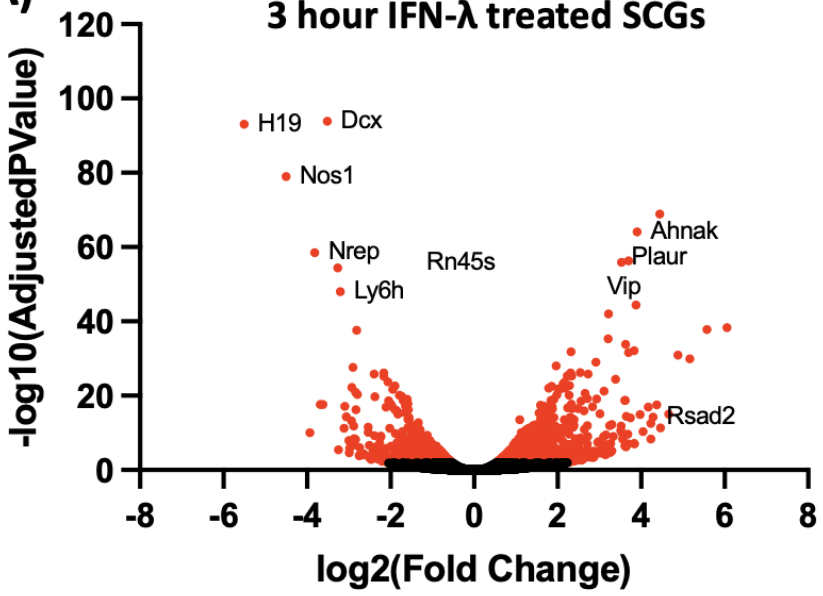

3h post-treatment	Biological Pathway	TnQ	Percent genes expressed
	Innate Immune Response	86	3.20%

(B)

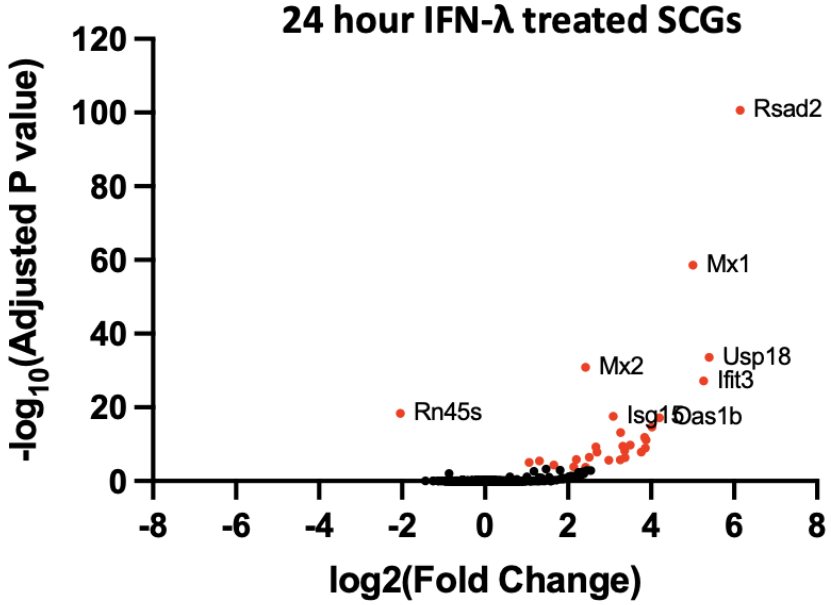

24h post-treatment	Biological Pathway	TnQ	Percent genes expressed
	Innate Immune Response	14	32.60%

Figure 2.4. Delayed ISG activation characterizes the IFN-λ response in peripheral neurons. SCGS were treated with rat IFN-λ2 (200 ng/ml) or vehicle for (**A**) 3 h and (**B**) 24 h. Volcano plots represent differential gene expression normalized to GAPDH. Scattered points represent genes; the x-axis is the log 2-fold change, whereas the y-axis is the statistical significance in differential expression. Red dots highlight genes significantly over- or under-expressed after IFN-λ exposure.

A Venn diagram analysis demonstrated that 40.00% of the genes shared between the 3 h and 24 h treatments were involved in innate immune responses. Additionally, 23.10% of genes were uniquely enriched for antiviral defense functions at 24 h (Figure 2.5A), and GeneVenn identified the specific genes shared between early and late stages of IFN-λ treatment (Figure 2.5B).

(A)

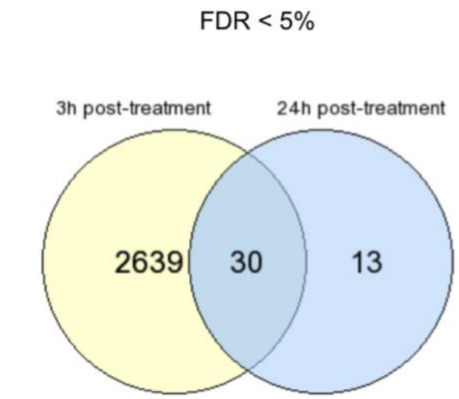

Shared genes	Biological Pathway	TnQ	Percent genes expressed
	Innate Immune Response	12	40.00%

24h post-treatment	Biological Pathway	TnQ	Percent genes expressed
	Defense to Virus	3	23.08%

(B)

FDR < 5% (Shared)	FDR < 5% (24h post-treatment)
Apol9a	Bst2
Cxcl10	Gbp2
Ddx60	Ifgga2l1
Dhx58	Ifitm3
Dtx3l	Isg15
Ifi44	Oas1a
Ifih1	Oasl
Ifit1	Oasl2
Ifit2	Psmb8
Ifit3	Slfn5
Irf7	Sp100
Irgm2	Sp110
Lgals3bp	Xaf1
Lgals9	
Mx1	
Mx2	
Oas1b	
Oas1i	
Parp14	
Parp9	
RT1-A2	
Rig1	
Rn45s	
Rsad2	
Samd9	
Samd9l1	
Slfn13	
Stat1	
Uba7	
Usp18	

Figure 2.5. Differential gene expression profiles at early and late timepoints following IFN-λ treatment in SCGs. (**A**) Venn diagram of differentially expressed genes (DEGs) (FDR <5%) comparing early (3 h) and late (24 h) responses. Shared genes are primarily linked to the innate immune response (40.00%), while the 24 h post-treatment-specific genes are enriched for antiviral defense functions (23.08%). *gProfiler* was utilized to categorize genes. *GeneVenn* was used to identify genes shared after 3 and 24 h post-treatment with IFN-λ. **(B)** Table demonstrating significantly induced genes (FDR <5%) shared between 3 h and 24 h post-treated primary neurons (left) and uniquely enriched genes at 24 h post-treatment (right). *gProfiler* was utilized to categorize genes. *GeneVenn* was used for this analysis.

Dynamic induction comparison of interferon-stimulated genes (ISGs) in IFN-λ- and IFN-β-treated SCGs

To further validate our RNA-sequencing results, we quantified the time-dependent induction of interferon-stimulated genes (ISGs) in primary SCG neurons following treatment with either rat IFN-λ2 (200 ng/ml) or IFN-β (100 U/ml). Normalized gene expression analysis revealed that IFN-λ2 induced a modest, albeit discernible, increase in ISG transcripts at 3 h post-treatment, which became more pronounced by 8 h and 24 h (Figure 2.6A). RSAD2 expression in SCG neurons increased in a time-dependent manner following IFN-λ treatment, with modest induction at 3 h, a significant increase by 8 h, and the highest expression at 24 h ($p < 0.05$ and $p < 0.05$ relative to 3 h, respectively; Figure 2.6A). In contrast, OAS1a and IFIT1 exhibited minimal induction following IFN-λ treatment and did not show statistically significant changes over time points. In comparison, IFN-β induced a higher and earlier expression of ISG transcripts at 3 hours compared to neurons treated with IFN-λ2. IFN-β treatment elicited a rapid and robust ISG response, characterized by a significant increase in RSAD2 expression as early as 8 h ($p < 0.05$) and a further enhancement at 24 h ($p < 0.005$; Figure 2.6.B). OAS1a and IFIT1 were also significantly induced by IFN-β at 24 h compared to 3 h ($p < 0.05$). Importantly, RSAD2 levels were ~3.6-log-fold times higher at 24 h following IFN-β treatment, whereas neurons treated with IFN-λ2 elicited a more moderate ~1.3-log-fold increase (Figure 2.6B). Notably, RSAD2 levels induced by IFN-λ at 24 h were comparable to those induced by IFN-β at 3 h, indicating delayed but sustained ISG activation downstream of IFN-λ signaling.

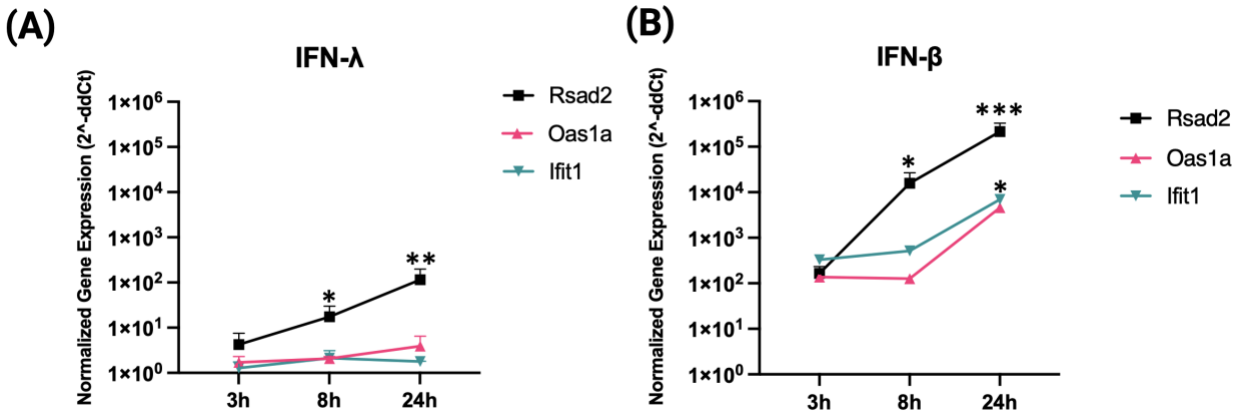

Figure 2.6. Time-course qPCR analysis of ISG induction in IFN-λ-treated SCGs. Normalized gene expression (2^{-ddCt}) in superior cervical ganglion (SCG) neurons following (**A**) rat IFN-λ2 treatment (200 ng/ml) or (**B**) rat IFN-β treatment (100 U/ml) at various times: 3 h-, 8 h- 24 h-post treatment. GAPDH was used as a housekeeping gene. Untreated SCGs served as the control. Statistical significance analyzed via Student's *t* test ($n \geq 3$).

2.3 Discussion

The findings presented in this chapter reveal fundamental cell-type-specific differences in how primary neurons and fibroblasts interpret and respond to type III interferon (IFN-λ) signaling. Although mucosal epithelia have long been recognized as the dominant IFN-λ-responsive barrier against incoming pathogens, our work demonstrates that peripheral neurons also mount robust IFN-λ responses, but through a noncanonical pathway that differs in both signaling mechanism and temporal kinetics from the rapid, JAK-STAT-driven antiviral pathway characteristic of fibroblasts. Specifically, neurons engage STAT1-specific signaling without STAT2 activation, resulting in delayed but sustained ISG induction that prioritizes neuronal survival. These results refine our understanding of early αHV-host interactions at the mucosal-PNS interface and highlight how neurons balance intrinsic and innate immune responses with the need to avoid acute cytotoxic defense.

Rat2 fibroblasts responded to IFN-λ with classical STAT1 and STAT2 phosphorylation, activating the canonical ISGF3 transcription factor broadly described in epithelial and immune cells. This canonical response produced large-magnitude ISG induction, exemplified by dramatic upregulation of Oas2 and widespread activation of antiviral gene networks. Given fibroblasts' role at mucosal entry sites, this rapid, high-amplitude response is consistent with the need to immediately restrict viral replication before virions penetrate deeper tissues.

In contrast, primary neurons engaged a STAT1-dominant signaling cascade. This selective signaling is striking, as it diverges from the canonical IFN-λ biology and instead resembles a modified, neuron-specific antiviral program that limits inflammation while preserving neuronal integrity. STAT1 signaling in neurons must be carefully balanced, as excessive or aberrant STAT1 activation has been implicated in neuronal pathology and

neurodegenerative disorders [126]. The STAT1-dominant response we observed may represent a mechanism to achieve this balance. The mechanism underlying STAT1 selectivity in neurons remains unclear but may involve neuron-specific signaling regulators that preferentially recruit STAT1 homodimers rather than ISGF3 heterotrimers.

The downstream consequences of this signaling divergence were reflected in the distinct ISG expression profiles between the two cell types. Although IFN-λ induced conserved ISGs in both fibroblasts and SCGs, the magnitude and timing differed substantially. Neurons consistently exhibited lower overall fold changes yet showed greater induction of a subset of ISGs, such as IFIT1, STAT3, and TLR7. RNA-sequencing analysis further revealed that the neuronal response operates through a temporally biphasic transcriptional program. Early responses (3 h) centered on genes involved in neuronal structure, signaling, and metabolic adaptation, indicating that IFN-λ initially primes neurons through a protective remodeling state. Only by 24 h did canonical antiviral ISGs dominate the transcriptional landscape, with RSAD2 emerging as the strongest late-induced antiviral effector. This temporal separation reflects a fundamental characteristic of neuron-intrinsic immunity: rather than mounting an immediate antiviral response, neurons first activate homeostatic pathways before committing to sustained ISG expression. The enrichment of innate immune and antiviral defense genes exclusively at late time points supports the interpretation that neurons adopt a sequential response strategy wherein initial cellular adaptation is followed by sustained antiviral expression.

This biphasic, delayed antiviral response stands in sharp contrast with the immediate and potent antiviral response in fibroblasts, This STAT1-specific activation in PNS neurons raises key mechanistic questions: does STAT1-selective signaling confer specific advantages for neurons (e.g., reducing virion particle trafficking and establishment of productive infection), or

does it reflect a developmental or metabolic constraint? What are the specific transcriptional targets of STAT1 homodimers in neurons, and how do they differ from canonical JAK-STAT-driven ISG induction?

The prominent induction of RSAD2 at later timepoints is particularly noteworthy. As a broad-spectrum antiviral effector that has been primarily studied in the context of RNA virus infection, RSAD2's key role in neuronal responses to DNA viruses represents a significant knowledge gap. The following chapter investigates whether RSAD2 functionally restricts αHV replication in neurons.

Together, these results reveal differential IFN-λ responses at the mucosal-PNS interface, where fibroblasts mount rapid antiviral defenses while neurons deploy slower but sustained mechanisms optimized for long-term viability. The cell-type specificity of IFN-λ signaling demonstrated here provides critical context for understanding how αHVs such as HSV-1 exploit neuronal vulnerabilities to access the peripheral nervous system and establish latency through delayed kinetics and STAT1-dependent signaling. The discovery that neurons engage a noncanonical IFN-λ pathway with delayed antiviral gene activation raises critical questions about how neurotropic viruses manipulate, evade, or co-opt this unique signaling environment. The following chapter addresses these questions by examining whether neuronal IFN-λ responses functionally restrict αHV replication and identifying the key antiviral defenses responsible for this restriction.

CHAPTER 3: Global Antiviral Response Against Alpha Herpesvirus Infection: PRV vs HSV-1

Abstract

In the previous chapter, I demonstrated that type III interferons (IFN-λs) activate distinct antiviral programs across cell types, mounting STAT1-dominant, delayed antiviral responses in peripheral sensory neurons. Here, we determined whether these signaling differences translate to functional antiviral activity against αHVs by comparing IFN-λ-mediated restriction of pseudorabies virus (PRV) and herpes simplex virus 1 (HSV-1) in Rat2 fibroblasts and superior cervical ganglion (SCG) neurons. In fibroblasts, IFN-λ pretreatment exhibited a strong antiviral effect, decreasing pseudorabies virus (PRV) replication drastically. In contrast, post-infection treatment only caused modest inhibition, highlighting the importance of early priming. In primary SCG neurons, IFN-λ pretreatment significantly decreased PRV replication, establishing that neurons can indeed mount an effective IFN-stimulated antiviral response against αHV infection. These results establish that IFN-λ generates functional antiviral states in both fibroblasts and PNS neurons.

Notably, while PRV remained highly sensitive to IFN-λ in neurons, HSV-1 was not restricted despite IFN-λ inducing comparable STAT1 phosphorylation and ISG expression. We identified the neurovirulence factor ICP34.5, encoded by simplexviruses (HSV-1 and HSV-2) but absent from varicelloviruses (PRV), as necessary and sufficient for overcoming neuronal IFN-λ restriction. This neuron-specific resistance correlated with the presence of the HSV-1 neurovirulence factor ICP34.5, since infection with an ICP34.5-deficient mutant (Δ34.5) restored IFN-λ sensitivity. These findings reveal that IFN-λ establishes complex antiviral barriers at the mucosal epithelia-PNS junction and identify ICP34.5 as a critical determinant enabling infection.

3.1 Introduction

Having established these cell-type-specific signaling and transcriptional differences between SCGs and fibroblasts, I next asked whether they translate to functional variability in antiviral protection against αHV neuroinvasion. Anatomically, mucosal fibroblasts are among the first cells encountered during peripheral infection, while PNS axons termini innervating these tissues are simultaneously exposed to the cytokines released early after infection. Thus, comparing the effects of IFN-λ treatment on the outcome of αHV infection in fibroblasts and primary neurons provided a means to reconstitute the sequential encounters that incoming virions encounter after mucosal infection and during neuroinvasion.

In this chapter, I examined whether IFN-λ pretreatment functionally restricts PRV replication in both cell types and whether any cell-type-specific differences in antiviral efficacy reflect the distinct signaling pathways identified in Chapter 2. Pseudorabies virus strain Becker (PRV-Be) and the fluorescently tagged PRV180 (expressing mRFP-VP26) were used alongside HSV-17 wt strain and mutants. PRV was selected as an initial model because it shares extensive genomic and biological similarity with HSV-1, including neurotropism, axonal transport, and latency establishment in PNS neurons [127]. PRV efficiently infects compartmentalized neuronal cultures and does not infect humans, enabling safe high-titer experiments [104].

My studies determined that exogenous exposure to IFN-λ treatment prior to PRV infection significantly restricted PRV viral replication (up to 6-log reduction) and primary neurons, with neuronal restriction inversely correlated with viral load (or MOI). Notably, while PRV remained highly sensitive to neuronal IFN-λ pretreatment, HSV-1 exhibited neuron-specific resistance despite the established antiviral response in neurons.

PRV lacks the HSV-1 neurovirulence factor, ICP34.5, which antagonizes PKR-mediated translational arrest [128, 129]. This genomic difference enabled comparative studies to identify ICP34.5-dependent immune evasion mechanisms. The absence of ICP34.5 in PRV provided a genetic tool to establish its necessity for overcoming neuronal IFN-λ defenses. Infection with ICP34.5-deficient HSV-1 (Δ34.5) restored full IFN-λ sensitivity in neurons, while replicating normally in untreated cells, confirming ICP34.5 as necessary for mitigating neuron-specific antiviral responses. IFN-λ creates a cell-specific immune response that differentially affects αHVs based on their immune evasion repertoires.

3.2 Results

Antiviral effect of Type I and Type III IFN in rat fibroblasts against pseudorabies virus (PRV)

Prior studies have demonstrated that both type I and type II IFNs exert antiviral activity against αHV infection in both neuronal and non-neuronal cells [79, 116]. To determine the antiviral potential of IFN-λ2 in Rat2 cells, we infected Rat2 cells with Pseudorabies virus Becker (PRV-Be), a wild-type strain of PRV. PRV is a member of the αHV family that can infect many animals (except humans and higher primates), and its replication cycle is similar to the human pathogen, HSV-1. Therefore, PRV has been used as a model αHV in compartmentalized neuronal culture model [117, 118, 130].

We infected interferon-treated or untreated Rat2 cells with PRV-Be at an MOI of 1 for 24 h. Viral yields between treated and untreated cells infected with PRV were calculated to determine the protective effects of both pre- and post-treatments of type I and type III IFNs. Pre-treated cells were exposed to IFN-β (100 U/mL) or IFN-λ2 (200 ng/mL) for 24 h prior to infection with PRV. Post-treatments were carried out using the same IFN concentration 1 h after the infection.

Cells that were treated with the IFN diluent (0.1% BSA in ddH_2O) served as a control, and the viral supernatants were collected at 24 h post-infection (hpi). Virus yields were calculated as plaque-forming units (pfu) in PK15 cells. In non-treated control Rat2 cells, PRV infection yielded 6.6×10^6 ($\pm 1.4 \times 10^6$) pfu/mL progeny. We detected a significant reduction in the virus yields in the pretreatment condition of both type I and type III IFN, with up to a 3-log decrease in IFN-β ($6.5 \times 10^3 \pm 1.8 \times 10^3$ pfu/mL), and up to a 6-log decrease in IFN-λ2 pretreatment ($2.6 \times 10^1 \pm 1.4 \times 10^1$ pfu/mL) (Figure 3.1). Conversely, post-treatments with either interferon type showed a significant but modest reduction in the virus yield. IFN-λ2 and IFN-β post-treatments yielded $8.4 \times 10^5 \pm 4.6 \times 10^5$ pfu/mL and $2.3 \times 10^6 \pm 1 \times 10^5$ pfu/mL, respectively. This indicates that the introduction of exogenous IFNs (through paracrine signaling) before viral particle invasion primes cells for an antiviral response. If the viral infection is initiated prior to interferon exposure, the host cell's antiviral response is less restrictive.

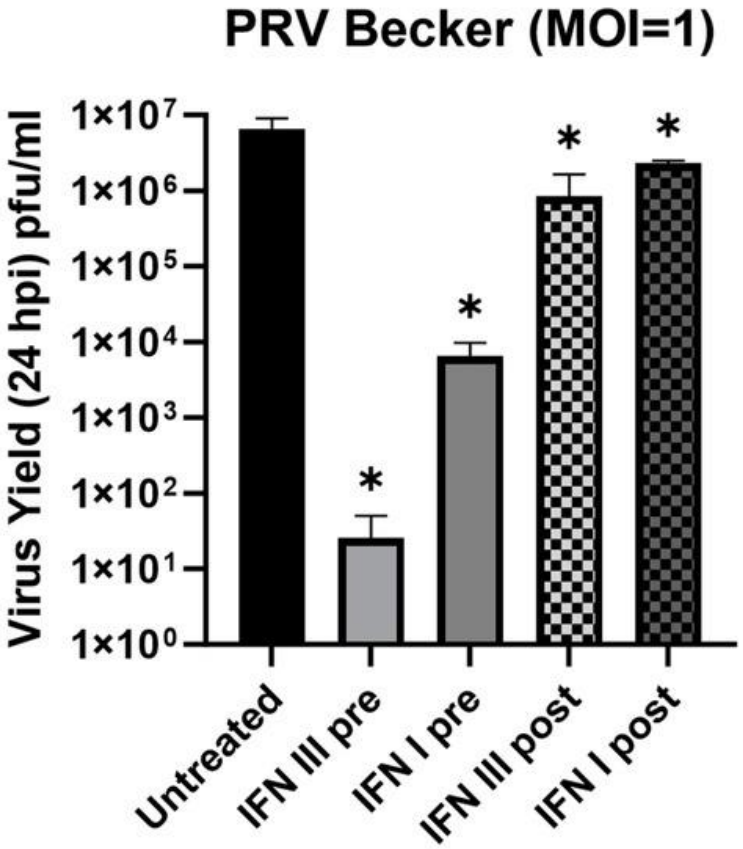

Figure 3.1. Antiviral effect of IFN-λ in Rat2 cells. Rat2 cells pre- and post-treated with IFN-β (100 U/mL) or IFN-λ2 (200 ng/mL) for 24 h prior to infection PRV-Becker (MOI = 1). Harvest of these cells was performed 24 hpi. Statistical significance analyzed via Student's *t* test (n ≥ 3) is indicated as follows: ns, not significant; *, $p < 0.05$.

Antiviral effect of IFN-λ in primary SCG neurons against pseudorabies virus (PRV)

A similar approach was followed using primary SCG neurons to determine the antiviral potential of IFN-λ2 pretreatment. In these experiments, we used PRV-180, a red capsid recombinant of PRV-Becker (mRFP-VP26) that allows for fluorescent imaging and observation of infected cells prior to harvest [131]. First, we infected SCGs at a high MOI (MOI 10) since PRV productive infections initiate efficiently at this MOI in primary neurons. The SCGs were treated with IFN-λ2 (200 ng/mL) in the S-compartment for 24 h prior to infection. SCGs were infected with PRV-180 (10^5 pfu, MOI 10) in the S-compartment for 24 h before harvest (Figure 8A). Virus yields demonstrated a 10-fold decrease in IFN-λ2 pre-treated SCGs, but this did not reach statistical significance (Figure 3.2A). In untreated SCGs, PRV-180 infection resulted in $1.2 \times 10^4 \pm 4.3 \times 10^3$ pfu/mL, and IFN-λ2 pre-treated SCGs yielded $1.9 \times 10^3 \pm 6.4 \times 10^2$ pfu/mL of infectious progeny in 24 hpi.

To investigate the effect of IFN-λ2 against a lower dose of PRV infection, we infected the neurons with PRV-180 at an MOI of 1 (10^4 pfu), after a pretreatment with IFN-λ2 (200 ng/mL). We detected a significant reduction in the virus yield in IFN-λ2 pre-treated samples (Figure 3.2B). At the MOI of 1, control SCGs yielded $2 \times 10^3 \pm 4.9 \times 10^2$ pfu/mL, whereas IFN-λ2 pre-treated neurons yielded $1.2 \times 10^2 \pm 5.1 \times 10^1$ pfu/mL virus with a 17-fold mean difference, implying that the antiviral effect of type III IFNs in primary neurons is more significant at low MOI infections.

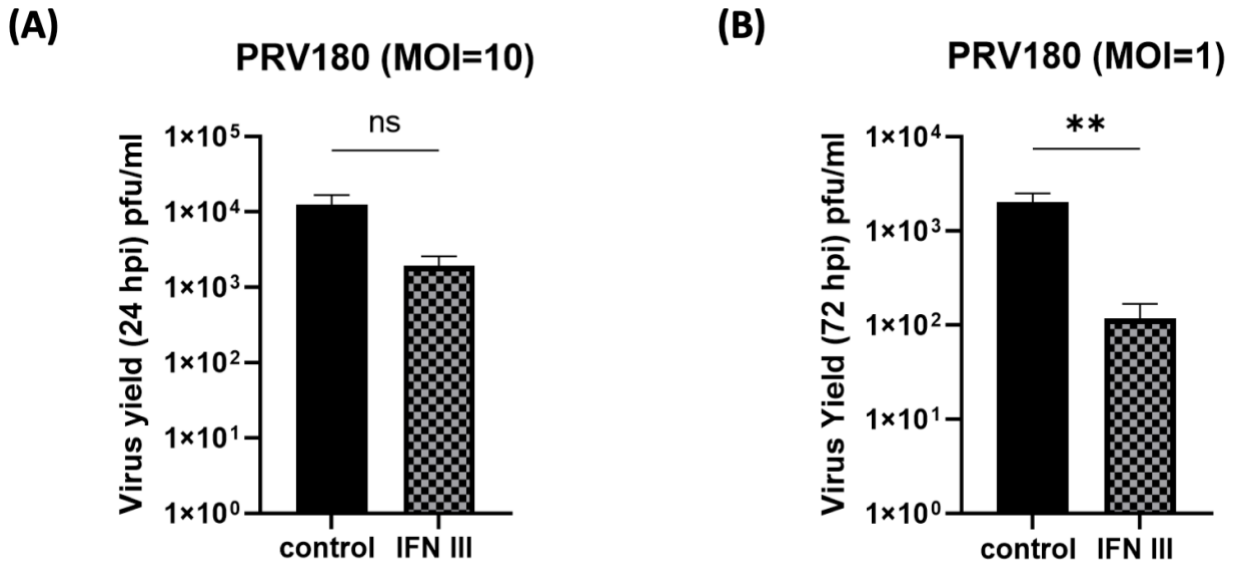

Figure 3.2. Antiviral effect of IFN-λ in SCGs. (**A**) SCGs pre-treated with IFN-λ2 (200 ng/mL) for 24 h prior to infection with PRV-180 (10^5 PFU) for 24 h. (**B**) SCGs pre-treated with IFN-λ2 (200 ng/mL) for 24 h prior to infection with PRV-180 (10^4 PFU) for 24 h. Statistical significance analyzed via Student's *t* test ($n \geq 3$) is indicated as follows: ns, not significant; **, $p < 0.005$.

HSV-1 mitigates the IFN-λ-induced antiviral response in neurons

Following the establishment that type III interferon induced an antiviral state in peripheral neurons and prevented PRV infection, the second question of interest was whether this neuronal antiviral state was able to limit the human pathogen HSV-1 infection. To determine whether the IFN-λ antiviral program was virus-agnostic, we next compared PRV and HSV-1 infection with identical neuronal IFN-λ conditions.

For these experiments, we used a recombinant HSV-1 strain 17 expressing mRFP-VP26 (OK14). Surprisingly, we did not observe a significant reduction in OK14 viral yield after 48 hours post-infection (hpi) when superior cervical ganglion (SCG) neurons were pretreated with 200 ng/ml of IFN-λ (Figure 3.3A). In contrast, Rat2 fibroblasts pretreated with rat IFN-λ2 exhibited a significant (~210-fold) reduction in OK-14 titers after 24 hpi ($p < 0.05$; Figure 3.3B).

SK-N-SH cells (a human neuroblastoma-derived cell line with neuronal characteristic) were used without differentiation to assess species-specific (human vs rat) differences in neuronal IFN-λ responsiveness [132]. These cells were maintained in an undifferentiated state to determine the intrinsic capacity of human neuronal cells to respond to type III IFNs, independent of differentiation. This comparison was crucial as human and rat neurons may differ significantly between interferon receptor expression and downstream signaling pathways. SK-N-SH cells pretreated with human IFN-λ2 (200 ng/ml, 24 h) showed no significant suppression of OK-14 replication (Figure 3.3C). However, human dermal fibroblasts (HDFs) pretreated with human IFN-λ2 exhibited a strong reduction in viral yield (~25-fold), with suppression reaching highly significant levels ($p < 0.00005$; Figure 3.3D). Overall, these results suggest that IFN-λ demonstrates antiviral activity against HSV-1 in fibroblasts but not in neuronal cells, and that the degree of inhibition varies among different species of fibroblasts.

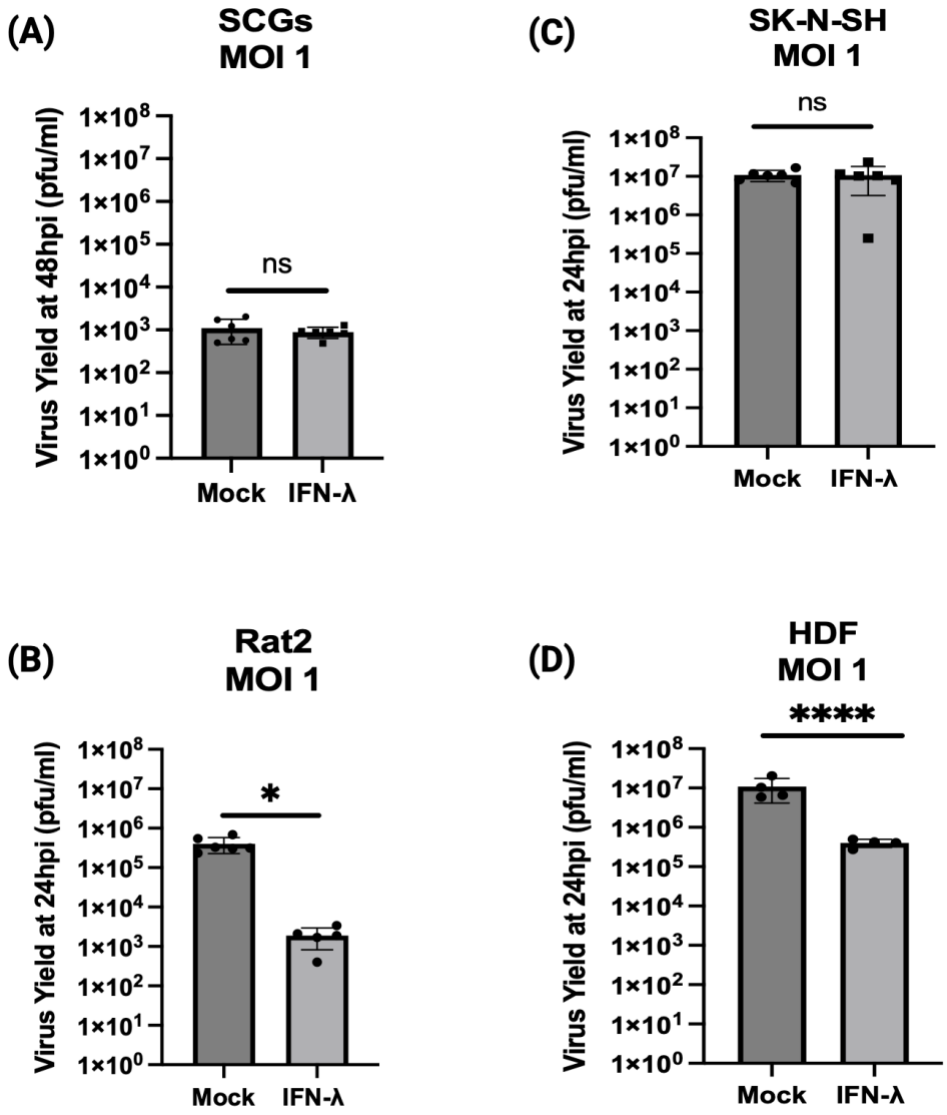

Figure 3.3. Differential antiviral activity of IFN-λ across neuronal and non-neuronal cell types following HSV-1 infection. (**A**) SCGs were pre-treated with rat IFN-λ2 (200 ng/mL) for 24 h prior to infection with OK-14 (MOI 1). (**B**) SK-N-SH cells were pre-treated with human IFN-λ2 (200 ng/mL) for 24 h prior to infection with OK-14 (MOI 1). (**C**) Rat2 cells were pre-treated with rat IFN-λ2 (200 ng/mL) for 24 h prior to infection with OK-14 (MOI 1). (**D**) HDFs pre-treated with human IFN-λ2 (200 ng/mL) for 24 h prior to infection with OK-14 (MOI 1). Statistical significance analyzed via Student's *t* test ($n \geq 3$) is indicated as follows: ns, not significant; *, $p < 0.05$, ****, $p < 0.00005$.

ICP34.5 suppresses IFN-λ-induced antiviral response during HSV-1 infection

Our results show that HSV-1 invades SCGs and effectively suppresses the IFN-λ-mediated antiviral responses, while PRV remains susceptible to it. We further explored this difference between the viruses by monitoring viral protein expression during infection. PRV and HSV-1 are both αHVs, they share a highly conserved genomic structure and encode many homologous genes. However, there are differences in key genomic regions, specifically the inverted repeat (IR) sequences, which are flanked by the unique long (UL) and unique short (US) regions of the viral genome, and contain genes that regulate viral pathogenesis and immune evasion. PRV contains IRs that are relatively compact compared to HSV-1 and lacks certain immunomodulatory genes present in HSV-1, such as ICP34.5, a multifaceted protein essential for mitigating immune responses and counteracting host antiviral pathways. Although both viruses can establish latency, the absence of ICP34.5 in PRV may increase sensitivity to interferon-stimulated responses (Figure 3.4A). Specifically, HSV-1 encodes the multifunctional neurovirulence factor ICP34.5, which combats host antiviral defenses, whereas PRV's genome lacks this gene [133-135]. Based on this difference, we hypothesized that the absence of ICP34.5 would make HSV-1 more vulnerable to IFN-λ-induced antiviral activity. To test this, we assessed the replication of an HSV-1 mutant lacking ICP34.5 (Δ34.5) and compared it to its revertant, 34.5R, developed by the Thompson Lab [136].

In SCG neurons pretreated with rat IFN-λ2 (200 ng/ml, 24 h), the replication of Δ34.5 was significantly reduced compared to untreated controls. This indicates that ICP34.5 is essential for HSV-1 to evade the IFN-λ-mediated antiviral response in neurons effectively ($p < 0.05$; Figure 3.4B). Notably, in the absence of IFN-λ, Δ34.5 replicated at equal or even higher titers than the revertant virus, 34.5R, indicating that this mutant does not have a baseline replication

defect in SCG neurons (Figure 3.4C). Similarly, in human SK-N-SH cells, pretreatment with IFN-λ2 also resulted in a notable decrease in Δ34.5 titers (Figure 3.4D), confirming the neuron-specific, rather than species-specific, resistance of HSV-1. Likewise, in the absence of IFN-λ, Δ34.5 replicated at similar titers to 34.5R-infected SK-N-SH cells (Figure 3.4E). Overall, these findings suggest that the differential sensitivity of HSV-1 and PRV to IFN-λ is linked to the presence of ICP34.5, which enables HSV-1 to suppress host antiviral defenses in neuronal cells.

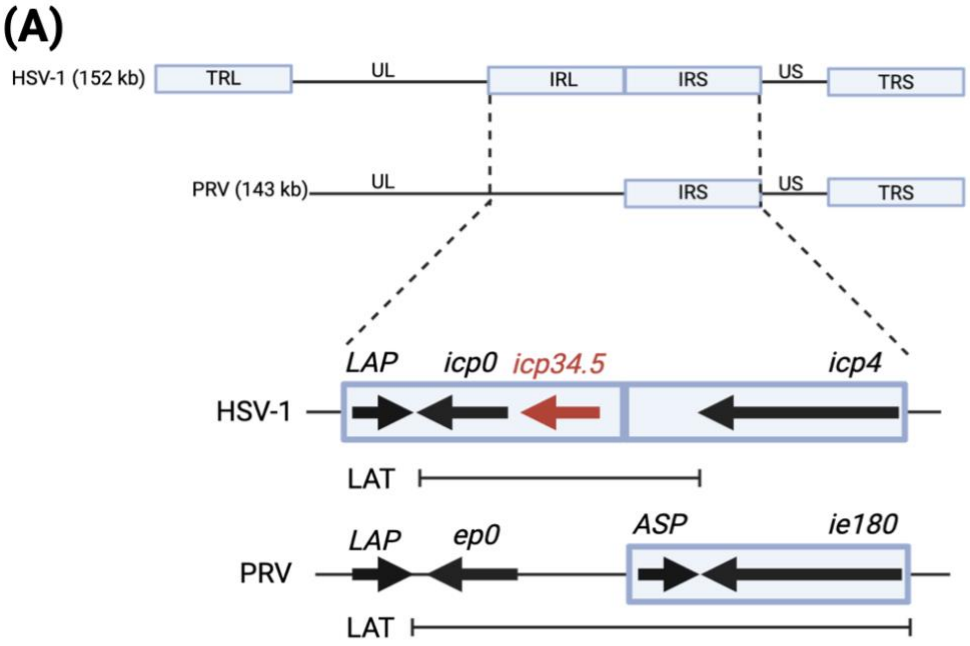
(A)
HSV-1 (152 kb)
TRL
UL
IRL
IRS
US
TRS
PRV (143 kb)
UL
IRS
US
TRS
LAP
icp0
icp34.5
icp4
HSV-1
LAT
LAP
ep0
ASP
ie180
PRV
LAT

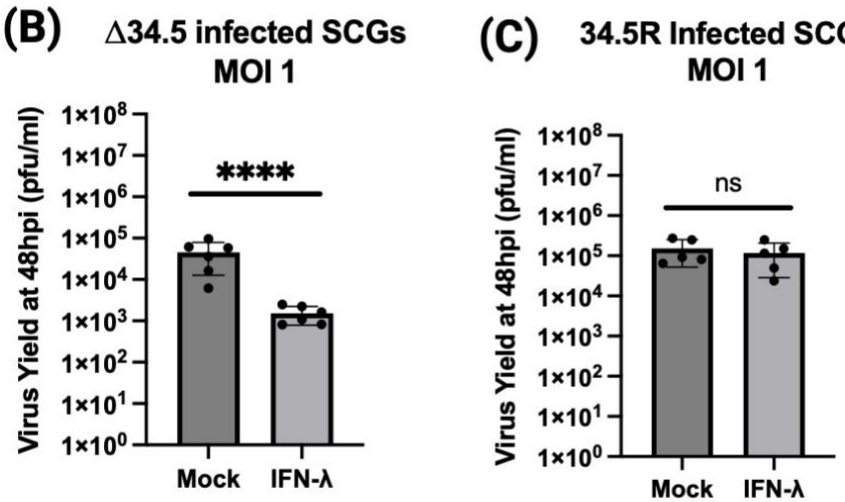
(B) Δ34.5 infected SCGs
MOI 1
Virus Yield at 48hpi (pfu/ml)
****
Mock
IFN-λ
(C) 34.5R Infected SCGs
MOI 1
Virus Yield at 48hpi (pfu/ml)
ns
Mock
IFN-λ

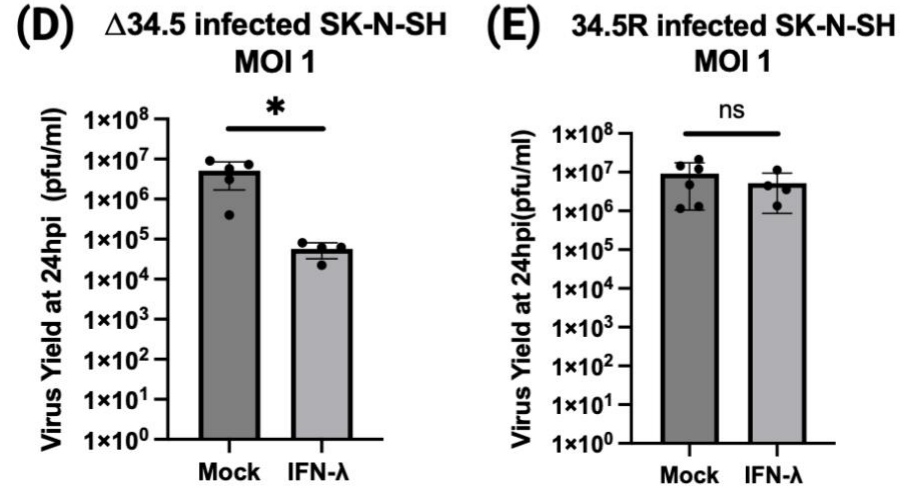
(D) Δ34.5 infected SK-N-SH
MOI 1
Virus Yield at 24hpi (pfu/ml)
*
Mock
IFN-λ
(E) 34.5R infected SK-N-SH
MOI 1
Virus Yield at 24hpi(pfu/ml)
ns
Mock
IFN-λ

Figure 3.4. Loss of ICP34.5 renders HSV-1 more susceptible to IFN-λ-mediated restriction in neuronal cells. (**A**) Schematic comparison of the HSV-1 and PRV genomes, highlighting genes involved in viral replication and immune evasion. HSV-1 encodes ICP34.5 (highlighted in red), not found in the PRV genome. (**B**) SCGs were pre-treated with rat IFN-λ2 (200 ng/mL) for 24 h prior to infection with Δ34.5 for 48 h. (**C**) SCGs were pre-treated with rat IFN-λ2 (200 ng/mL) for 24 h prior to infection with 34.5R for 48 h. (**D**) SK-N-SH cells were pre-treated with human IFN-λ2 (200 ng/mL) for 24 h prior to infection with Δ34.5 for 24 h. (**E**) SK-N-SH cells were pre-treated with human IFN-λ2 (200 ng/mL) for 24 h prior to infection with 34.5R for 24 h. Statistical significance analyzed via Student's *t* test ($n \geq 4$) is indicated as follows: ns, not significant; *, $p < 0.05$, ****, $p < 0.00005$.

3.3 Discussion

This chapter's findings demonstrate that type III IFNs (IFN-λs) are crucial for establishing a robust antiviral defense in both fibroblasts and peripheral neurons, although the dynamics and antiviral potential of this response differ significantly across cell types and infecting viruses. Recognizing these differences is key to understanding how neurotropic viruses navigate biological barriers during mucosal infection and neuroinvasion.

In fibroblasts, pretreatment with IFN-λ results in a pronounced antiviral effect, reducing pseudorabies virus (PRV) replication, implicating IFN-λ's role in establishing a highly effective antiviral state when cells are primed before viral entry. Fibroblasts reside in dermal and submucosal connective tissues immediately beneath the mucosal epithelial barriers, positioning them as a critical secondary defense layer that limits viral dissemination to deeper tissues, including PNS neurons. While PRV remains highly susceptible to the antiviral state induced by IFN-λ and post-infection treatment (minimal effect on viral replication) highlights a fundamental principle: once viral immediate-early and early proteins accumulate, they rapidly antagonize the host cell's antiviral defenses, rendering cells vulnerable despite IFN priming. This timing dependency has important implications for elucidating natural infection dynamics, as IFN-λ produced by infected epithelia likely primes neighboring uninfected cells, including PNS neuron axons, before virions spread, creating a protective barrier that influences the viral dose ultimately reaching the neuronal cell body.

In primary neurons, pretreatment with IFN-λ significantly reduces PRV replication at low multiplicities of infection (MOI), suggesting a viral load threshold beyond which neuronal antiviral defenses are overwhelmed [81]. This MOI-dependent protection reveals a critical threshold phenomenon: neuronal antiviral defenses, characterized by IFN-λ mediated ISG

induction, effectively suppress low-dose infections but are overwhelmed with high viral genomes simultaneously enter neurons. This threshold is biologically relevant for neuroinvasion, as the number of incoming viral capsids determines the fate of infection. Low viral doses favor genome silencing and latency establishment, whereas high doses promote productive replication through sheer numerical advantage and rapid accumulation of viral immune antagonists. The capacity of IFN-λ to restrict low-dose infections suggests that epithelial IFN-λ production may play a critical role in limiting neuroinvasion efficiency during productive infection, potentially reducing the number of virions that establish latency in the cell body nucleus. Future studies examining whether IFN-λ priming influences the latency-to-productive infection ratio will be essential for understanding how mucosal immune responses shape long-term infection outcomes.

The most notable findings of this chapter are the differential sensitivity of PRV and HSV-1 to neuronal IFN-λ responses. While PRV remained highly sensitive to IFN-λ-mediated restriction in neurons, HSV-1 replicated efficiently despite inducing comparable STAT1 phosphorylation and ISG expression. This disparity demonstrated the fundamental difference in how these two αHVs interact with neuron-specific immune defenses. Specifically, HSV-1's resistance to IFN-λ is neuron-specific as opposed to a general viral phenotype. Both Rat2 fibroblasts and human dermal fibroblasts displayed significant IFN-λ-mediated viral replication suppression during HSV-1 infection, demonstrating that fibroblasts retain the capacity to restrict HSV-1 (Figure 3.3). Additionally, this neuron-specific resistance is conserved across species as both rat SCGs and human SK-N-SH neuroblastoma cells failed to restrict HSV-1, ruling out species-specific differences. These findings indicate that HSV-1 has evolved specialized mechanisms to overcome antiviral defenses unique to neurons.

Indeed, the absence of ICP34.5 in PRV and its presence in simplexviruses (HSV-1 and HSV-2) provided a natural genetic tool to dissect its role in overcoming neuronal IFN-λ responses, while highlighting differences in αHVs neuroinvasion. The molecular basis for ICP34.5's ability to overcome neuronal IFN-λ defenses involves multiple complementary mechanisms that collectively disable host antiviral responses. First, ICP34.5 recruits protein phosphatase 1α (PP1α) to dephosphorylate eIF2α, thereby reversing the translational shutoff imposed by protein kinase R (PKR) and other stress-activated eIF2α kinases during viral infection [128, 137]. This function is critical because eIF2α phosphorylation normally blocks both viral and cellular protein synthesis as a protective antiviral mechanism [138]. By restoring translation, ICP34.5 enables continued viral protein synthesis despite activation of PKR and potentially allows viral proteins to antagonize ISG effector functions. Second, ICP34.5 inhibits autophagy by binding Beclin-1, preventing autophagosome formation and the subsequent degradation of viral components [87, 89]. Manivanh et al. demonstrated that ICP34.5 blocks TANK-binding kinase 1 (TBK1)-mediated phosphorylation of interferon regulatory factor 3 (IRF3), thereby attenuating type I interferon production in trigeminal neurons (TG) [139]. Together, these functions position ICP34.5 as a regulator that counteracts the innate immune response. Notably, this chapter showed that infection with an ICP34.5-deficient HSV-1 mutant (Δ34.5) restored sensitivity to neuronal IFN-λ pretreatment, demonstrating that ICP34.5 is both necessary and sufficient for HSV-1 to overcome neuron-specific antiviral defenses. Importantly, Δ34.5 replicated wild-type levels of virus yield in intreated neurons, confirming that its IFN-λ sensitivity reflects loss of immune evasion capacity rather than baseline replication defects.

Several critical questions remain unanswered. First, which specific neuronal ISG(s) mediate IFN-λ restriction of PRV? While RSAD2 is a strong candidate, other ISGs, including IFIT1,

STAT3, and TLR7, which showed preferential induction in neurons (Chapter 2), may also contribute to the immune response. Genetic studies analyzing individual ISGs in primary neurons, either via knockdown or knockout, may be necessary to establish their relative contributions. Additionally, does ICP34.5-mediated eIF2α dephosphorylation disrupt specific ISG protein localization, post-translational modifications (e.g., phosphorylation, ubiquitination), or oligomerization required for antiviral activity? Third, why is ICP34.5-mediated resistance neuron-specific? Do neurons express unique ISG targets particularly vulnerable to ICP34.5, or do neuronal ISGs rely more heavily on translational control mechanisms that ICP34.5 disrupts? Comparative ISG profiling of neurons and fibroblasts during HSV-1 infection may reveal cell-type-specific vulnerabilities. Fourth, what compensatory mechanisms, if any, does PRV employ in the absence of ICP34.5? PRV encodes alternative PKR antagonists such as IE180, which inhibits the phosphorylation of eIF2α; however, these viral proteins are clearly insufficient to overcome neuronal IFN-λ responses, suggesting HSV-1's evolutionary advantage against neuron-specific defenses [37, 140].

Collectively, this chapter summarizes the role of IFN-λ in creating a potent antiviral response with rapid, high-magnitude restriction in fibroblasts and slower, but sustained responses in PNS neurons (Figure 3.5). However, these defenses are not universally effective. While varicelloviruses like PRV remain vulnerable to neuronal IFN-λ immune response, simplexviruses, encoding ICP34.5, have evolved specialized countermeasures that neutralize neuron-specific antiviral mechanisms. This evolutionary divergence explains the enhanced neurotropism of HSV-1 and HSV-2 and their capacity to establish lifelong latent infections in human PNS neurons.

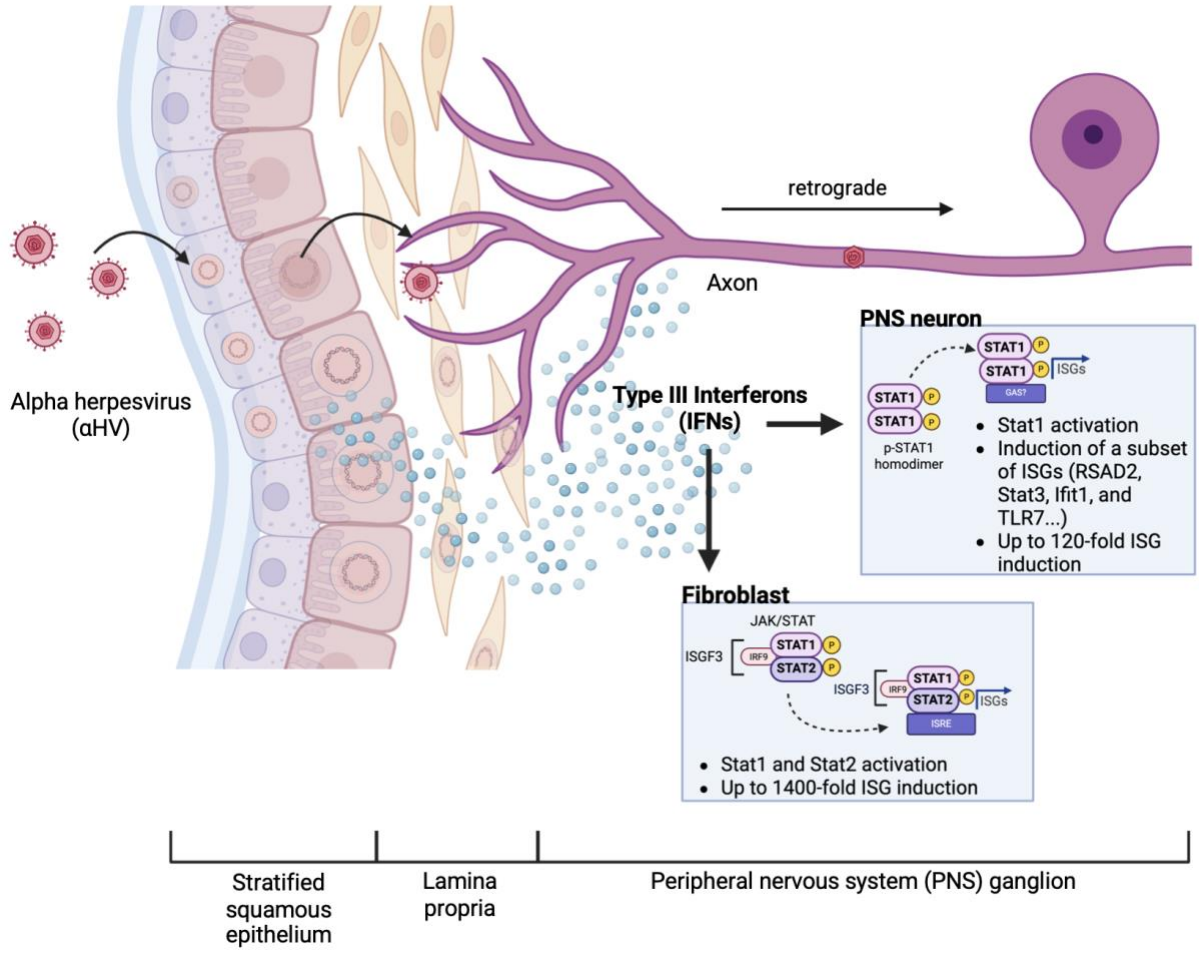

Figure 3.5. αHV infection triggers differential Type III interferon responses in peripheral nervous system neurons and fibroblasts. Alpha herpesvirus (αHV) virions infect the mucosal epithelium at the peripheral tissue site. Virions travel through the lamina propria and enter PNS axon termini, where they undergo retrograde axonal transport to the neuronal cell body. During infection, Type III interferons (IFN-λ) are produced and secreted in the microenvironment. These cytokines signal to two distinct resident cell populations with different responses. In PNS neurons (top panel), IFN-λ induction leads to STAT1 phosphorylation and homodimerization, resulting in transcriptional activation of a subset of interferon-stimulated genes (ISGs), including RSAD2, Stat3, Ifit1, and TLR7, achieving up to 120-fold ISG induction. In contrast, fibroblasts (bottom panel) exhibit robust JAK/STAT pathway activation involving both STAT1 and STAT2. ISGF3 (Interferon-Stimulated Gene Factor 3) complex formation, comprised of STAT1/STAT2 heterodimers with IRF9, drives potent transcriptional responses with up to 1400-fold ISG induction. This differential signaling demonstrates cell-type-specific innate immune responses within the mucosal epithelium-PNS axis during αHV infection. Created on Biorender.com.

CHAPTER 4: IFN-λ-induced RSAD2 Contributes to a Neuron-Specific Antiviral Barrier

Abstract

Interferon-stimulated genes (ISGs) form the backbone of intrinsic antiviral immunity, yet only a small subset possesses well-defined biochemical activities capable of directly inhibiting viral replication. RSAD2 (also known as viperin) is a unique ISG that directly inhibits viral RNA synthesis through its radical SAM (s-adenosyl methionine)-dependent enzymatic conversion of cytidine triphosphate (CTP) into 3′-Deoxy-3′,4′-didehydro-cytidine triphosphate (ddhCTP), a chain-terminating nucleotide analog that blocks viral RNA synthesis [32, 141, 142]. Although RSAD2 has been studied extensively in fibroblasts and immune cells, its function in neurons, the primary targets of αHV infections, remains to be elucidated. This chapter identifies RSAD2 as a central antiviral effector of the neuronal type III IFN (IFN-λ) response and demonstrates that herpes simplex virus 1 (HSV-1) overcomes this defense through ICP34.5-mediated antagonism. While extensively characterized in immune cells and hepatocytes, RSAD2 expression and function in neurons remain less understood [143]. IFN-λ treatment robustly induces RSAD2 in rat superior cervical ganglion (SCG) neurons and human neuroblastoma cells (SK-N-SH), localizing to distinct punctate perinuclear structures resembling ER-derived membranes. This RSAD2 response occurred rapidly in human neuronal cells and more gradually in primary neurons, consistent with the delayed yet durable IFN-λ signaling identified in earlier whole-transcriptomic analyses (Chapter 2).

The functional significance of RSAD2 was revealed through comparative analysis of pseudorabies virus (PRV) and herpes simplex virus type 1 (HSV-1). While PRV remains highly sensitive to IFN-λ-mediated restriction in neurons, HSV-1 replicates efficiently despite

comparable ISG induction, due to the activity of its neurovirulence factor ICP34.5. In neurons infected with ICP34.5-deficient HSV-1 (Δ34.5), RSAD2 expression remains high, its punctate perinuclear localization is preserved, eIF2α phosphorylation persists, and late viral protein synthesis is severely impaired.

Genetic validation using siRNA-mediated RSAD2 knockdown partially rescued Δ34.5 replication, confirming that RSAD2 is essential in IFN-λ-mediated antiviral restriction. Together, these findings identify RSAD2 as a neuron-specific antiviral effector whose spatial organization and enzymatic activity are disrupted by HSV-1 through ICP34.5-mediated antagonism. This chapter reveals a critical interface between the innate neuronal immunity and viral immune evasion, demonstrating how simplexviruses have evolved specialized strategies to overcome RSAD2-dependent neuronal immune response and establish PNS neuroinvasion.

4.1 Introduction

Interferon-stimulated genes (ISGs) constitute a critical component of the cell's intrinsic and innate immune defense against viral infections. Despite their importance, only a small subset of ISGs has been characterized to possess well-defined biochemical mechanisms that directly inhibit viral replication. Among these, RSAD2 (radical S-adenosyl methionine domain-containing 2), commonly known as viperin, stands out for its broad-spectrum antiviral activity and a unique enzymatic mode of action [142]. The selection of RSAD2 as the central focus of this chapter was motivated by several converging lines of evidence establishing it as the prime candidate for mediating neuronal IFN-λ restriction. Transcriptomic analysis shows that RSAD2 is the most upregulated gene in neurons after 24 h of IFN-λ treatment (Chapter 2). This suggests RSAD2 plays a key role in PNS neurons' type III IFN immune response. Additionally, unlike

many immune proteins that regulate signaling pathways, RSAD2 directly interferes with viral replication through its catalytic activity [31]. Following type I and type III interferon signaling, RSAD2 is rapidly upregulated and functions as an immediate antiviral effector, positioning it at the frontline of cellular defense against diverse viruses.

Structurally, RSAD2 contains a radical S-adenosyl-L-methionine (SAM) enzyme domain with a 4Fe-4S cluster, a cofactor typically associated with metabolic enzymes rather than classic immune effectors [30, 141]. This unusual structural feature provided the first clue that RSAD2 functions enzymatically rather than through protein-protein interactions of typical immune regulators. RSAD2 catalyzes the conversion of cytidine triphosphate (CTP), a canonical nucleotide, to synthesize 3'-deoxy-3',4'-didehydro-CTP (ddhCTP), an antiviral ribonucleotide analog that terminates viral RNA synthesis [31, 32, 144]. This chain-terminating analog inhibits viral RNA-dependent RNA polymerases, effectively blocking the elongation of nascent viral RNA chains [145]. RSAD2 is an immune effector that synthesizes an antiviral nucleotide, conceptually similar to therapeutic nucleoside analogs to HSV-1 such as acyclovir, but produced naturally by host cells [146].

RSAD2's subcellular localization is functionally critical for its antiviral activity. The protein predominantly localizes to membranes derived from the endoplasmic reticulum (ER), lipid droplets, and mitochondria-associated membranes through its N-terminal amphipathic αhelix, which anchors RSAD2 to membrane surfaces [147]. This membrane association positions RSAD2 at advantageous cellular sites frequently used by viruses for replication and assembly. For αHVs, which undergo secondary envelopment at trans-Golgi network or ER-derived membranes to acquire their final lipid envelope, RSAD2's strategic localization positions it to interfere with late stages of the viral lifecycle. Whether RSAD2 localizes similarly in

neurons- and whether this localization is maintained or disrupted during αHV infection- remains unexplored but represents a critical determinant of its antiviral efficacy.

Much of the mechanistic understanding of RSAD2 comes from studies utilizing rapidly dividing cell lines or primary cells not involved with the nervous system. RSAD2 was first identified in a 2001 study by Chin, K. C., and Crewell, P. during human cytomegalovirus (HCMV) infection of macrophages, and was designated as cytomegalovirus-induced gene 5 (cig5) [148]. The studies revealed that RSAD2 transcripts are robustly induced within hours of HCMV infection, and that RSAD2 relocalizes to perinuclear degradative compartments post-infection, suggesting a role in disrupting viral assembly or promoting degradation of viral components [148]. Subsequent mechanistic investigations demonstrated that RSAD2 inhibits the late stages of the HCMV replication cycle by blocking virion envelopment and modulating host lipid metabolism, including cholesterol and fatty acid biosynthesis required for the acquisition of the viral envelope and efficient virion assembly.

RSAD2's antiviral activity was further shown to extend to the flaviviruses, retroviruses, influenza virus, and numerous other viruses, making RSAD2 a pan-antiviral effector with broad-spectrum activity [149, 150]. In the case of influenza virus, RSAD2 prevents viral budding from the plasma membrane by disrupting lipid raft formation. For HIV-1, RSAD2 inhibits virion release and reduces viral infectivity through poorly defined mechanisms potentially involving disruption of Gag protein trafficking. Against hepatitis C virus (HCV), RSAD2 directly interacts with the NS5A nonstructural protein and disrupts replication complex assembly. This diversity of mechanisms suggests that RSAD2 may function through both its enzymatic activity, such as ddhCTP production, and through direct protein-protein interactions that disrupt viral processes. While these studies strongly implicated RSAD2 as an important intrinsic restriction factor, they

have been performed in fibroblasts, hepatocytes, macrophages, or epithelial cells [148, 151, 152]. The function of RSAD2 in neurons, specifically in the PNS, serve as primary cellular targets of αHV infection that remain to be investigated.

Importantly, most mechanistic studies on RSAD2 have focused on RNA viruses, especially flaviviruses, orthomyxoviruses, and retroviruses, where RSAD2's production of ddhCTP directly inhibits viral RNA-dependent RNA polymerases (RdRp) that synthesize viral genomes and transcripts [31, 32]. Although RSAD2 has been implicated in restricting certain DNA viruses including human cytomegalovirus (HCMV), its role in blocking alpha herpesviruses has not been well documented [148]. RSAD2 might block herpesviruses through mechanisms that do not involve direct inhibition of DNA replication or transcription. Some evidence indicates that RSAD2 disrupts lipid metabolism pathways vital for herpesvirus envelope formation and virion assembly at ER-derived membranes [153]. RSAD2 has also been shown to interact with and sequester cellular proteins potentially required for membrane trafficking, which could interfere with the transport of viral glycoproteins to assembly sites. Additionally, RSAD2-induced changes in cellular metabolism may cause ER stress and phosphorylation of eIF2α, creating a hostile environment for herpesvirus replication.

While RSAD2 has been extensively characterized in the context of HCMV and RNA virus infections, essentially no mechanistic studies have examined its function during simplex virus infections in peripheral neurons, even though HSV-1 must evade intrinsic neuronal barriers to establish lifelong latent infection in sensory ganglia. This chapter addresses whether RSAD2 restricts αHV replication through direct nucleotide incorporation, metabolic disruption, stress-response induction, or a combination of these pathways.

HSV-1 encodes unique neurovirulence factors absent from many other herpesviruses, most notably ICP34.5, which antagonizes host antiviral responses through multiple complementary mechanisms. ICP34.5 recruits protein phosphatase 1α (PP1α) to dephosphorylate eIF2α and reverse translational shutoff, binds Beclin-1 to inhibit autophagy, and inhibits TBK1-mediated IRF3 phosphorylation to attenuate interferon production [134, 135, 154]. Unlike PRV, that lack ICP34.5 homologues and remain sensitive to neuronal IFN-λ restriction (Chapter 3), HSV-1 encoding ICP34.5 replicates efficiently in IFN-λ-treated neurons, implicating ICP34.5 as a potential RSAD2 antagonist. [155, 156].

Overall, the findings presented in this chapter demonstrate that RSAD2 serves as a primary neuronal antiviral effector downstream of IFN-λ signaling, and that HSV-1's capacity to invade PNS neurons depends critically on ICP34.5-mediated antagonism of RSAD2 function through disruption of both its spatial organization and its downstream effects on translational control. Elucidating RSAD's role in neuronal immune response has key implications. If RSAD2 mediates antiviral defense, its enzymatic activity could prevent αHV neuroinvasion during infection. Understanding how ICP34.5 antagonizes RSAD2 may aid drug development, as small molecules disrupting their interaction or PP1α inhibitors that stabilize eIF2α phosphorylation could restore neuronal defenses.

4.2 Results

IFN-λ triggers strong neuronal RSAD2 induction and perinuclear localization across different species

Since RSAD2 was detected as the highest induced ISG in the RNA-seq analysis, we further evaluated RSAD2 protein expression and subcellular localization patterns following IFN-λ treatment in primary neurons and human neuronal cell lines. In SCG neurons exposed to rat IFN-λ2 (200 ng/ml, 24 h), immunofluorescence staining revealed distinct RSAD2 puncta localized predominantly in the perinuclear region, with minimal presence in untreated controls (Figure 4.1A). Western blot analysis corroborated these findings, indicating a robust induction of RSAD2 protein at 24 hours post-treatment, utilizing Beta-actin as a loading control (Figure 4.1B). As RSAD2 has been shown to be expressed in the central nervous system (CNS), it was expected that protein levels would also increase in PNS neurons [157].

To analyze interferon-stimulated gene (ISG) kinetics in human neuronal cells, SK-N-SH cells were treated with 200 ng/mL IFN-λ2 for 3, 8, and 24 hours. qPCR measurements showed RSAD2 as the most highly induced ISG, peaking at 24 hours with greater fold-change and sustained upregulation compared to OAS1 and IFIT1 (Figure 4.2). In human SK-N-SH neuronal cells, IFN-λ treatment induced a delayed antiviral transcriptional response. RSAD2 expression increased over time, reaching a significant elevation at 24 h post-treatment compared to 3 h ($p < 0.05$; Figure 4.2). In contrast, OAS1a and IFIT1 exhibited modest, variable increases following IFN-λ treatment and did not show statistically significant changes across time points.

A comparable temporal pattern was observed in human SK-N-SH cells, where immunofluorescence analysis revealed perinuclear RSAD2 puncta as early as 3 hours, with a pronounced increase by 24 h (Figure 4.1C). Notably, in both SCGs and SK-N-SH cells, RSAD2

perinuclear localization remained sustained across all examined time points, indicating that this spatial pattern is a stable and conserved feature of IFN-λ signaling in neuronal contexts. Immunoblotting confirmed upregulation of RSAD2 protein at both time points, 3 h and 24 h post-treatment (Figure 4.1D). These results collectively demonstrate that IFN-λ significantly upregulated RSAD2 protein expression in both rodent and human neuronal cells.

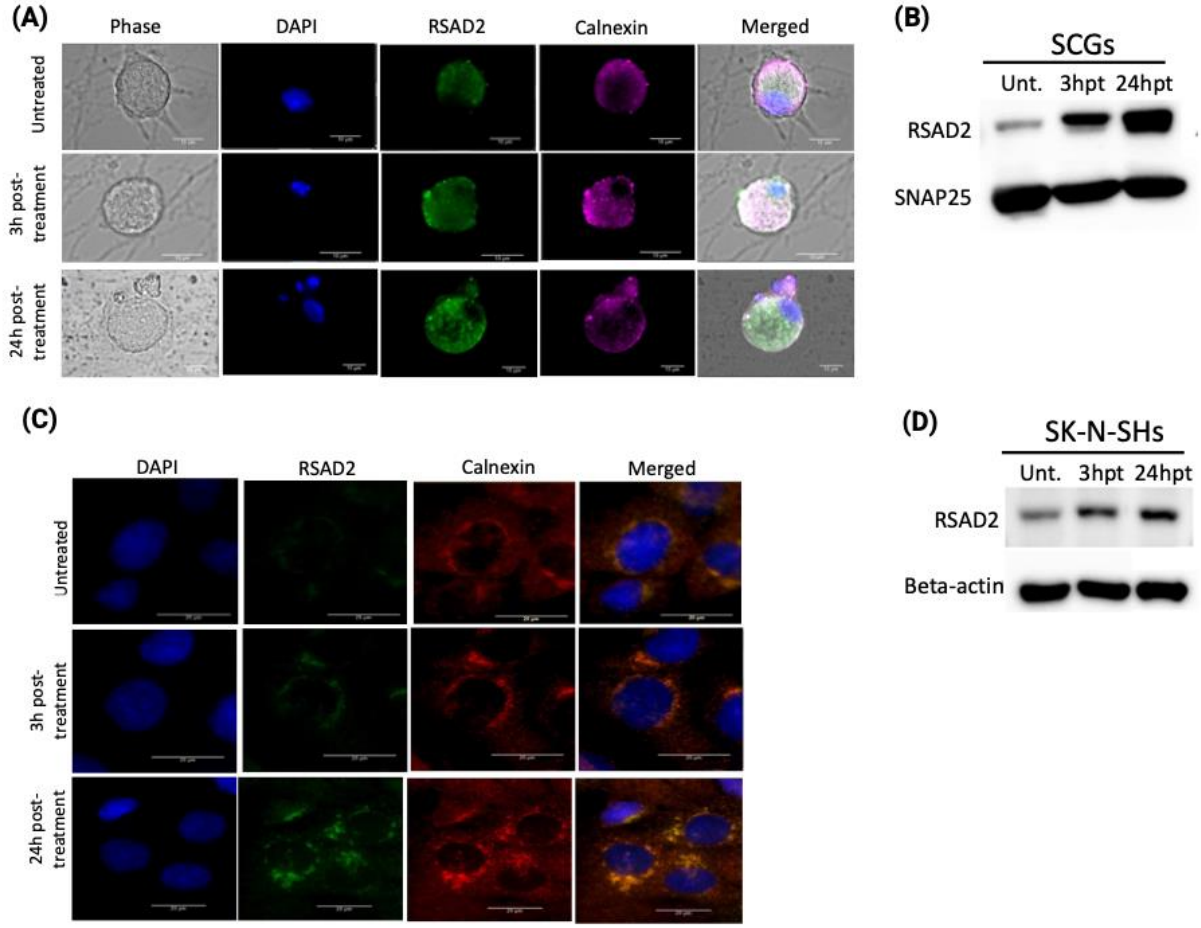

Figure 4.1. RSAD2 expression increases after IFN-λ treatment. (**A**) Immunofluorescence staining of RSAD2 in SCG cell bodies after 3 h- and 24 h-post-treatment with rat IFN-λ2 (200 ng/ml). Representative images are shown (scale bars, 10 μm). (**B**) Immunoblotting of RSAD2 in SCGs treated with rat IFN-λ2 (200 ng/ml) for 3 h- and 24 h-post-treatment. SNAP25 was used as a loading control. (**C**) Immunofluorescence staining of RSAD2 in SK-N-SH cells treated with human IFN-λ2 (200 ng/ml) for 3 h- and 24 h-post-treatment (bars, 20 μm). (**D**) Immunoblotting of RSAD2 in SK-N-SH cells treated with human IFN-λ2 (200 ng/ml) for either 3 h- or 24 h-post-treatment. Beta-actin was used as a loading control.

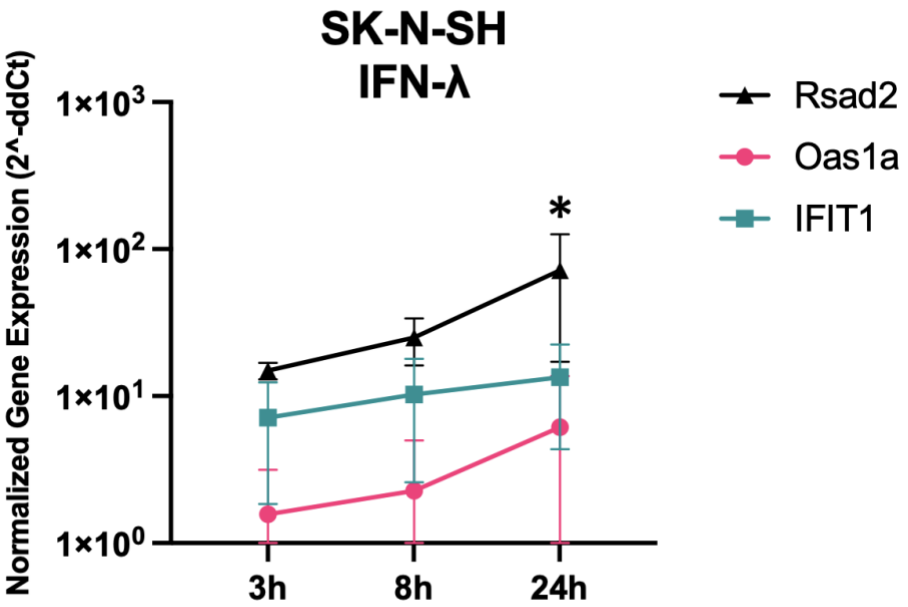

Figure 4.2. IFN-λ-induced ISG expression kinetics in SK-N-SH cells. Normalized gene expression (2^{-ddCt}) in SK-N-SH cells following human IFN-λ2 (200 ng/mL) treatment for 3 h-, 8 h- and 24 h-post-treatment. Statistical significance analyzed via Student's *t* test ($n \geq 3$).

HSV-1 infection alters RSAD2 expression through ICP34.5 protein

After observing robust RSAD2 induction in response to IFN-λ, we next sought to determine how viral infection modulates RSAD2 expression in the presence or absence of the HSV-1 neurovirulence factor ICP34.5. For these experiments, we compared HSV-1 OK14 and PRV180 infections to previously published HSV-1 mutants; ICP34.5 deletion: Δ34.5 and its revertant, 34R, initially constructed by Dr.Thompson and Dr. Sawtell and kindly shared with us by Dr. Leib and Drayman (Figure 4.3A) [136].

Immunofluorescence staining analyses of RSAD2 protein in SCGs demonstrated that Δ34.5-infected neurons largely maintained RSAD2 protein levels and perinuclear localization. In contrast, neurons infected with 34.5R showed less punctate organization with RSAD2 dispersed diffusely, including within the neuronal nucleus. This diffusion of RSAD2 may suggest disruption of spatial organization (Figure 4.3B). Specifically, RSAD2 gene expression was markedly increased in SCGs 24 h after infection with the HSV-1 Δ34.5 mutant, reaching levels comparable to those observed during PRV180 infection (Figure 4.3C) [29]. In primary SCG neurons infected with wild-type HSV-1 (OK14), RSAD2 expression remained low and did not significantly change across infection, with mean values of 21.4 ± 0.9, 17.3 ± 0.9, and 18.5 ± 3.9 at 3, 8, and 24 hpi, respectively (Figure 4.3C). In contrast, infection with the ICP34.5-deficient virus (Δ34.5) resulted in substantially higher RSAD2 expression at all timepoints, reaching 49.6 ± 28.0, 53.1 ± 24.8, and 86.4 ± 32.1 at 3, 8, and 24 hpi. RSAD2 levels were significantly elevated in Δ34.5-infected neurons compared to OK14 at 24 hpi ($p < 0.05$), indicating that ICP34.5 suppresses RSAD2 induction during HSV-1 infection, and that loss of ICP34.5 permits sustained and amplified RSAD2 expression in neurons.

Neurons infected with 34.5R showed reduced RSAD2 expression in comparison. Additionally, Δ34.5-infected neurons largely maintained RSAD2 protein levels throughout infection, whereas 34.5R-infected neurons demonstrated reduced expression of RSAD2 (Figure 4.3D). To determine whether IFN-λ differentially affects viral protein expression in the absence of ICP34.5, immunoblot analysis was performed using antibodies against ICP4 (IE), ICP8 (E), and poly HSV-1 (L). In IFN-λ pre-treated neurons, Δ34.5 infection demonstrated reduced IE and E protein levels compared to 34.5R-infected neurons (Figure 4.3D). Late protein expression decreased when SCGs were infected with Δ34.5, suggesting that ICP34.5 is critical for maintaining temporal regulation of viral gene expression under IFN-λ pressure, and its absence may lead to dysregulated late gene expression (Figure 4.3D).

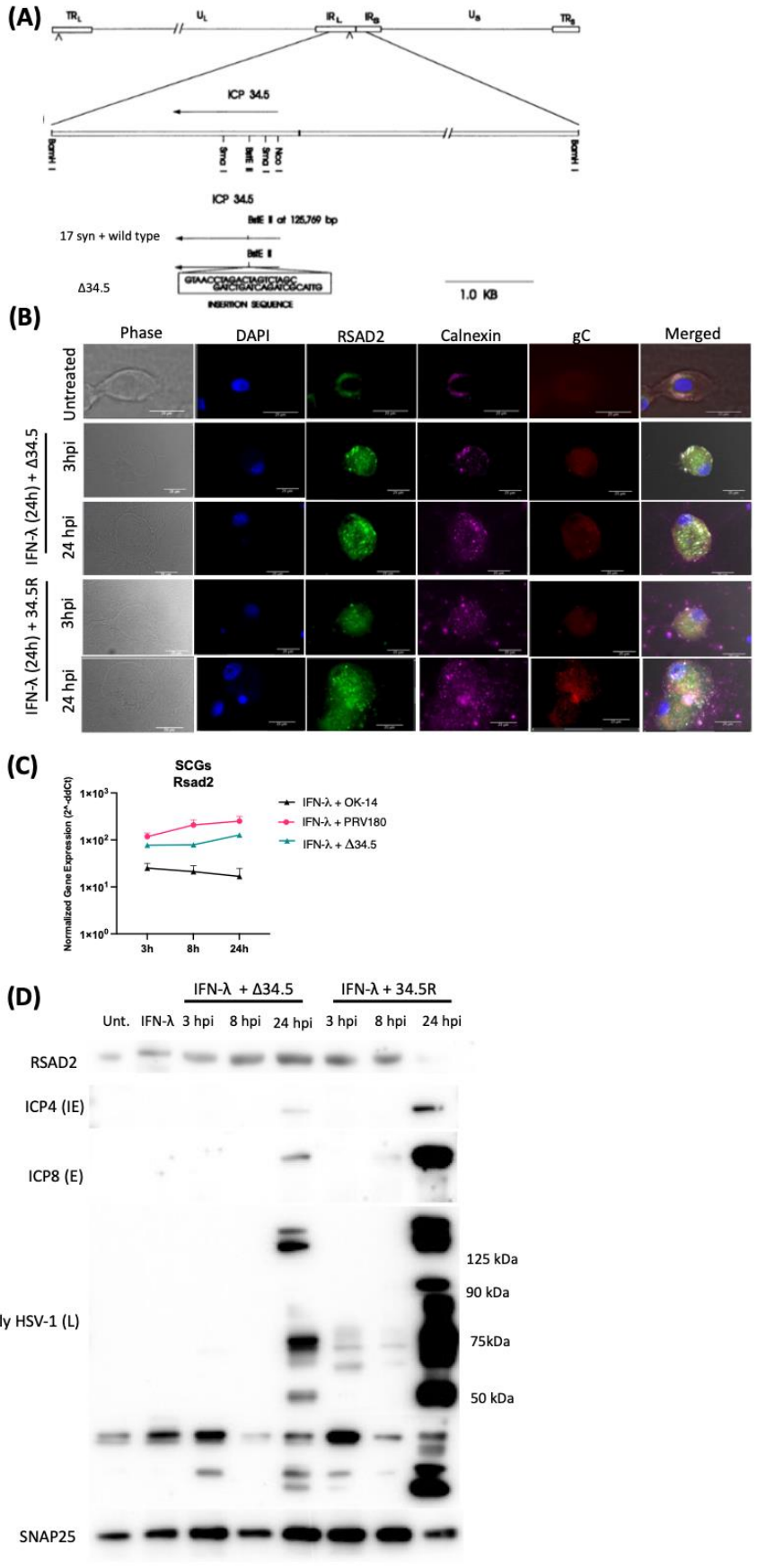
(A)
ICP 34.5
17 syn + wild type
Δ34.5
1.0 KB
(B)
Phase
DAPI
RSAD2
Calnexin
gC
Merged
Untreated
IFN-λ (24h) + Δ34.5
3hpi
24 hpi
IFN-λ (24h) + 34.5R
3hpi
24 hpi
(C)
SCGs
Rsad2
Normalized Gene Expression (2^-ddCt)
IFN-λ + OK-14
IFN-λ + PRV180
IFN-λ + Δ34.5
3h
8h
24h
(D)
IFN-λ + Δ34.5
IFN-λ + 34.5R
Unt.
IFN-λ
3 hpi
8 hpi
24 hpi
3 hpi
8 hpi
24 hpi
RSAD2
ICP4 (IE)
ICP8 (E)
poly HSV-1 (L)
125 kDa
90 kDa
75kDa
50 kDa
SNAP25

Figure 4.3. ICP34.5 suppresses RSAD2 expression and enhances viral protein expression in primary neurons. (**A**) To generate the HSV-1 mutant 17termA, a 20-bp linker (5′-GTAACCTAGACTAGTCTAGC-3′ and complementary sequence 5′-GTTACGCTAGACTAGTCTAG-3′) was inserted into the BstEII restriction site (bp 125,769) within the BamHI S+Q fragment of the HSV-1 strain 17syn+ genome. Schematic representation of the HSV-1 genome in the prototypic P-isomer configuration, showing the unique long (UL) and unique short (US) regions flanked by terminal repeat long (TRL), internal repeat long (IRL), internal repeat short (IRS), and terminal repeat short (TRS) regions. Arrowheads indicate the locations of the ICP34.5 gene. Expanded view of the BamHI S+Q region, illustrating the location and transcriptional orientation of ICP34.5 and the primary latency-associated transcript (LAT). Relevant restriction sites used for mutant construction are indicated with corresponding base-pair coordinates. The restored virus, 17termAR, was generated by cotransfection of 17termA viral DNA with the wild-type 17syn+ BamHI S+Q fragment, restoring the native sequence at the insertion site. Figure adapted from Bolovan, et al. (1994) [136]. (**B**) SCGs were pretreated with rat IFN-λ2 (200 ng/ml, 24 h) prior to infection with either 34.5R or Δ34.5 at MOI 1. Cells were fixed at 24 hpi and stained for RSAD2 expression (scale bars, 10 μm). (**C**) Normalized gene expression (2^{-ddCt}) of RSAD2 in SCGs following infection with Δ34.5, or 34.5R at MOI 1 for 3 h or 24 hpi. Statistical significance was assessed using unpaired two-tailed t tests with Welch's correction. (**D**) Immunoblotting of SCGs pretreated with rat IFN-λ2 (200 ng/ml) for 24 h and infected with either 34.5R or Δ34.5 at MOI 1 for 3 h, 8 h, or 24 h prior to harvest. Lysates were probed with antibodies against RSAD2, ICP4 (immediate early), ICP8 (early), poly-HSV-1 (late), and SNAP25 (loading control).

Neuronal IFN- λ response does not affect viral gene transcription

To assess the effect of IFN-λ pretreatment on viral gene expression, we pretreated superior cervical ganglia (SCGs) with IFN-λ2 (200 ng/ml, 24 h). Then, cells were infected with HSV-1 (OK14) or Δ34.5 at an MOI of 1. Viral transcripts: immediate-early (ICP27), early (ICP8), and late (gC) were measured by qPCR at 3 h, 8 h, and 24 h after infection and normalized to GAPDH, a housekeeping gene. At 24 hours post-infection (hpi), the Δ34.5 mutant virus showed significantly increased gC transcript levels compared to OK14 ($p < 0.05$; Figure 4.4A). This indicates that IFN-λ pretreatment did not inhibit viral gene expression in the ICP34.5-deficient mutant (Δ34.5) during infection. SK-N-SH cells underwent the same treatment protocol (IFN-λ2 pretreatment followed by OK14 or Δ34.5 infection at MOI of 1). Notably, at 24 hpi, Δ34.5-infected cells showed a significant increase in gC transcript levels compared to OK14 ($p < 0.05$; Figure 4.4B). These findings suggest that IFN-λ alone does not directly impair viral gene expression.

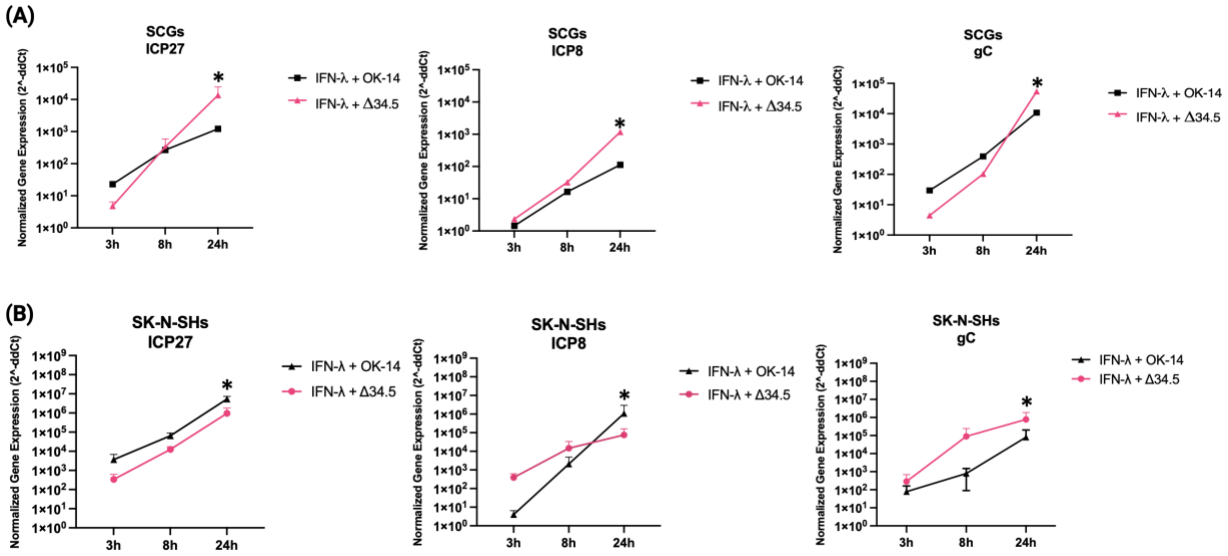

Figure 4.4. Neuronal IFN-λ pretreatment does not alter HSV-1 gene expression significantly. (**A**) qPCR quantification of viral immediate-early (ICP27), early (ICP8), and late (gC) gene expression in SCG neurons pre-treated with rat IFN-λ2 (200 ng/ml) for 24 h and infected with wild-type HSV-1 (OK14) or Δ34.5 at MOI 1 for either 3 h-, 8 h-, or 24 hpi. Statistical significance was performed using Student's *t* test: *, $p < 0.05$ (n=3 replicates). (**B**) Similar analysis performed with SK-N-SH cells pre-treated with human IFN-λ2 (200 ng/ml) for 24 h and infected with OK14 or Δ34.5 at MOI 1. Statistical significance was assessed using Student's *t* test: *, $p < 0.05$ (n=3 replicates).

ICP34.5 modulates RSAD2 expression to counteract neuronal antiviral responses

To examine the intracellular distribution and regulation of RSAD2 during HSV-1 infection in human neuronal cells, SK-N-SH cells were pretreated with their respective IFN-λ2 (200 ng/ml, 24 h) and infected with either the revertant virus, 34.5R, or the ICP34.5-deficient mutant (Δ34.5). SK-N-SH cells were analyzed at 3 hpi and 24 hpi by immunofluorescence and immunoblotting. In 34.5R-infected cells, RSAD2 staining detection decreased at later timepoints of 24 hpi in comparison to earlier timepoints at 3 hpi (Figure 4.5A). In contrast, Δ34.5-infected cells displayed a more punctate, perinuclear distribution of RSAD2 that persisted at both early and late time points (Figure 4.5A). In several infected cells, RSAD2 remained concentrated around the nuclear envelope, suggesting that loss of ICP34.5 preserves its subcellular localization, potentially by preventing viral disruption of host protein trafficking or organelle organization.

A similar pattern appeared in the steady state expression of genes in SK-N-SH cells, where RSAD2 upregulation occurred only after Δ34.5 infection with IFN-λ pretreatment, not with wild-type virus (Figure 4.5B). These results were confirmed by immunoblot analyses of RSAD2 protein levels. In SK-N-SH neurons, RSAD2 expression decreased during OK14 infection, with significantly lower levels at 24 hpi than at 3 hpi ($p < 0.05$; Figure 4.5B). In contrast, RSAD2 expression was maintained during Δ34.5 infection, resulting in significantly higher RSAD2 levels at 24 hpi compared to OK14 ($p < 0.05$; Figure 4.5B).

To further explore viral infection progress in these cells, we examined HSV-1 viral protein expression. Cells infected with the ICP34.5 revertant strain (34.5R) showed strong late protein expression at both 8 hpi and 24 hpi, consistent with efficient replication (Figure 4.5C). In contrast, Δ34.5-infected cells displayed reduced viral protein accumulation. These results suggest

that ICP34.5 by altering the localization and reducing the amounts of RSAD2 protein, promotes HSV-1 late gene expression in primary rat neurons and human neuronal cells.

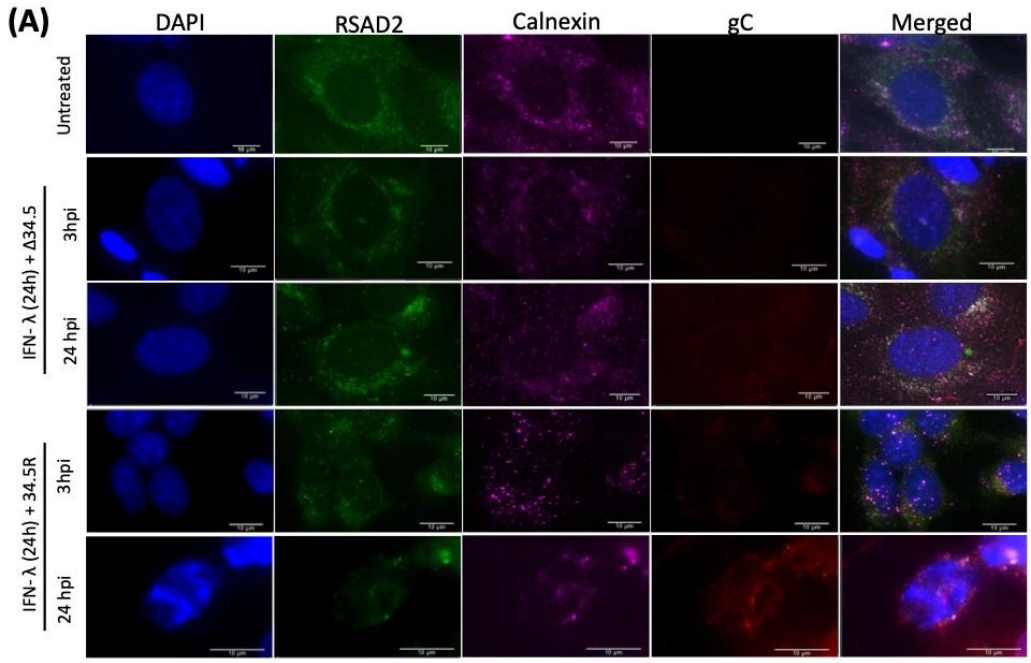
(A)
DAPI
RSAD2
Calnexin
gC
Merged
Untreated
IFN-λ (24h) + Δ34.5
3hpi
24 hpi
IFN-λ (24h) + 34.5R
3hpi
24 hpi

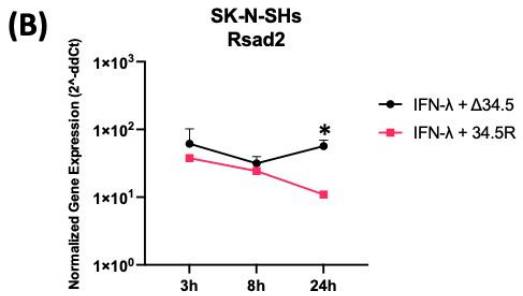
(B)
SK-N-SHs
Rsad2
Normalized Gene Expression (2^-ddCt)
1×10^3
1×10^2
1×10^1
1×10^0
3h
8h
24h
*
IFN-λ + Δ34.5
IFN-λ + 34.5R

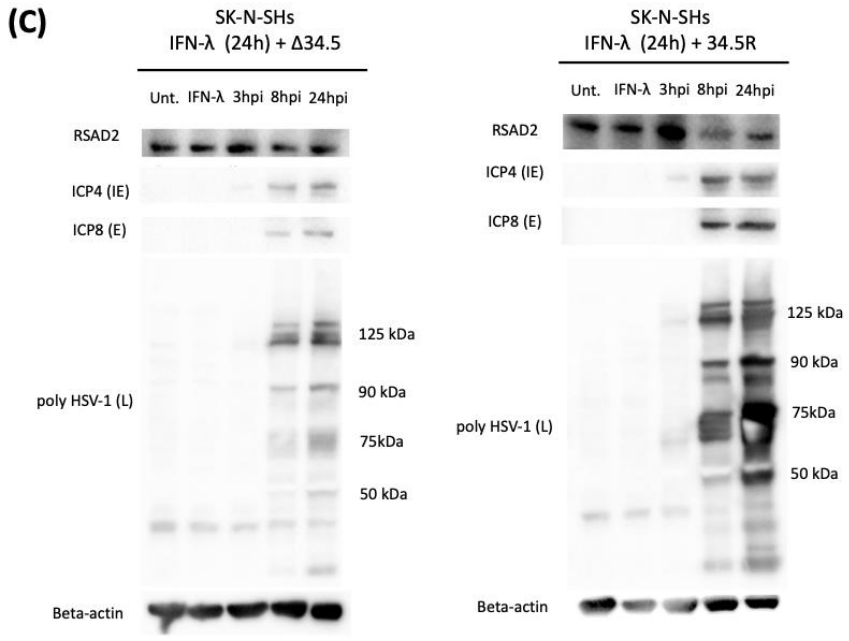
(C)
SK-N-SHs
IFN-λ (24h) + Δ34.5
Unt.
IFN-λ
3hpi
8hpi
24hpi
RSAD2
ICP4 (IE)
ICP8 (E)
poly HSV-1 (L)
125 kDa
90 kDa
75kDa
50 kDa
Beta-actin
SK-N-SHs
IFN-λ (24h) + 34.5R
Unt.
IFN-λ
3hpi
8hpi
24hpi
RSAD2
ICP4 (IE)
ICP8 (E)
poly HSV-1 (L)
125 kDa
90 kDa
75kDa
50 kDa
Beta-actin

Figure 4.5. ICP34.5 modulates host antiviral responses and supports late gene expression in HSV-1-infected SK-N-SH cells. (**A**) Immunofluorescence staining of SK-N-SH cells pretreated with human IFN-λ2 (200 ng/ml, 24 h) prior to infection with either 34.5R or Δ34.5 at MOI 1. Cells were fixed at 3 hpi and 24 hpi and stained for RSAD2 expression. Scale bars are 10 μm. (**B**) Normalized gene expression of RSAD2 in SK-N-SH cells following infections with either Δ34.5 or 34.5R at MOI 1 across three timepoints: 3, 8, and 24 hpi. Statistical significance was determined using an unpaired Student's *t* test; *, $p < 0.05$. (**C**) Immunoblotting of SK-N-SH cells pretreated with human IFN-λ2 (200 ng/ml) for 24 h and infected with either 34.5R or Δ34.5 at MOI 1 for 3, 8, and 24 h. Beta-actin was used as a loading control.

RSAD2 accumulation on the endoplasmic reticulum sustains p-eIF2α-mediated translational arrest in the absence of functional ICP34.5

To examine whether IFN-λ pretreatment affects host stress-response pathways targeted by ICP34.5, we assessed eIF2α phosphorylation in SCG neurons infected with the Δ34.5 or revertant strain (34.5R). Neurons were pretreated with rat IFN-λ2 (200 ng/ml, 24 h) and harvested at 24 hpi for immunoblot analysis. PNS neurons pre-treated with IFN-λ and infected with Δ34.5 demonstrated sustained p-eIF2α expression, whereas those infected with 34.5R displayed a gradual reduction in detection levels (Figure 4.6A and 4.6B).

Immunoblot analysis was performed to assess eIF2α phosphorylation in human SK-N-SH cells to determine whether the sustained p-eIF2α observed in SCGs was similarly maintained in a human neuronal cell model (Figure 4.7A). Variance-robust ANOVA tests revealed a significant overall treatment effect (Brown-Forsythe ANOVA: $F^*(6, 12.39) = 15.28$, $p < 0.0001$; Welch's ANOVA: $W(6, 6.178) = 12.05$, $p = 0.0036$). Using Games-Howell post hoc testing to account for unequal variance, Δ34.5 infection resulted in significantly increased eIF2α phosphorylation at 8 hpi ($p < 0.05$; Figure 4.7B). At 24 hpi, Δ34.5-infected cells showed significantly higher phosphorylated eIF2α levels compared to 34.5R-infected cells ($p < 0.05$; Figure 4.7B). In contrast to the sustained response in Δ34.5-infected cells, eIF2α phosphorylation declined significantly over time in 34.5R-infected cells (3 hpi vs 24 hpi, $p < 0.05$; Figure 4.7B). Together, these results indicate that ICP34.5 promotes dephosphorylation of eIF2α during late infection, whereas its absence leads to sustained activation of the host translational stress response.

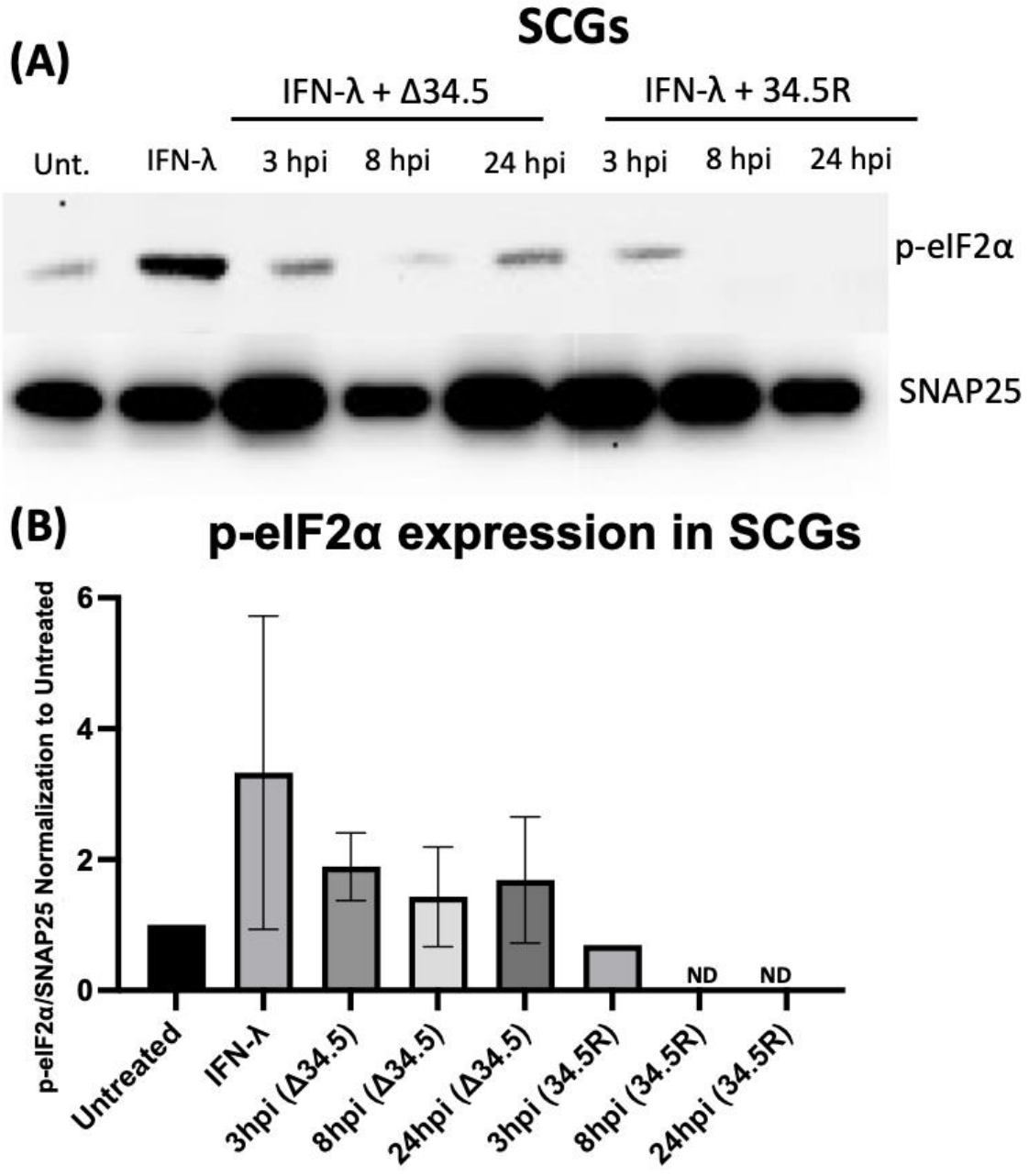

Figure 4.6. eIF2α phosphorylation sustains in IFN-λ-treated SCGs during Δ34.5 infection. SCGs were pretreated with rat IFN-λ2 (200 ng/mL, 24 h) and subsequently infected with either the HSV-1 ICP34.5-revertant strain (34.5R) or the ICP34.5-deficient mutant (Δ34.5) at MOI 1. (**A**) Cells were harvested 3-, 8-, and 24 h post-infection for immunoblot analysis. Immunoblots were probed with antibodies against phosphorylated eIF2α (p-eIF2α). SNAP25 was used as a loading control (n=2 triplicates). (**B**) p-eIF2α levels were normalized to SNAP25 and demonstrate efficient p-eIF2α depletion (n=2 triplicates; ND = not detected). Bars represent mean ± SEM.

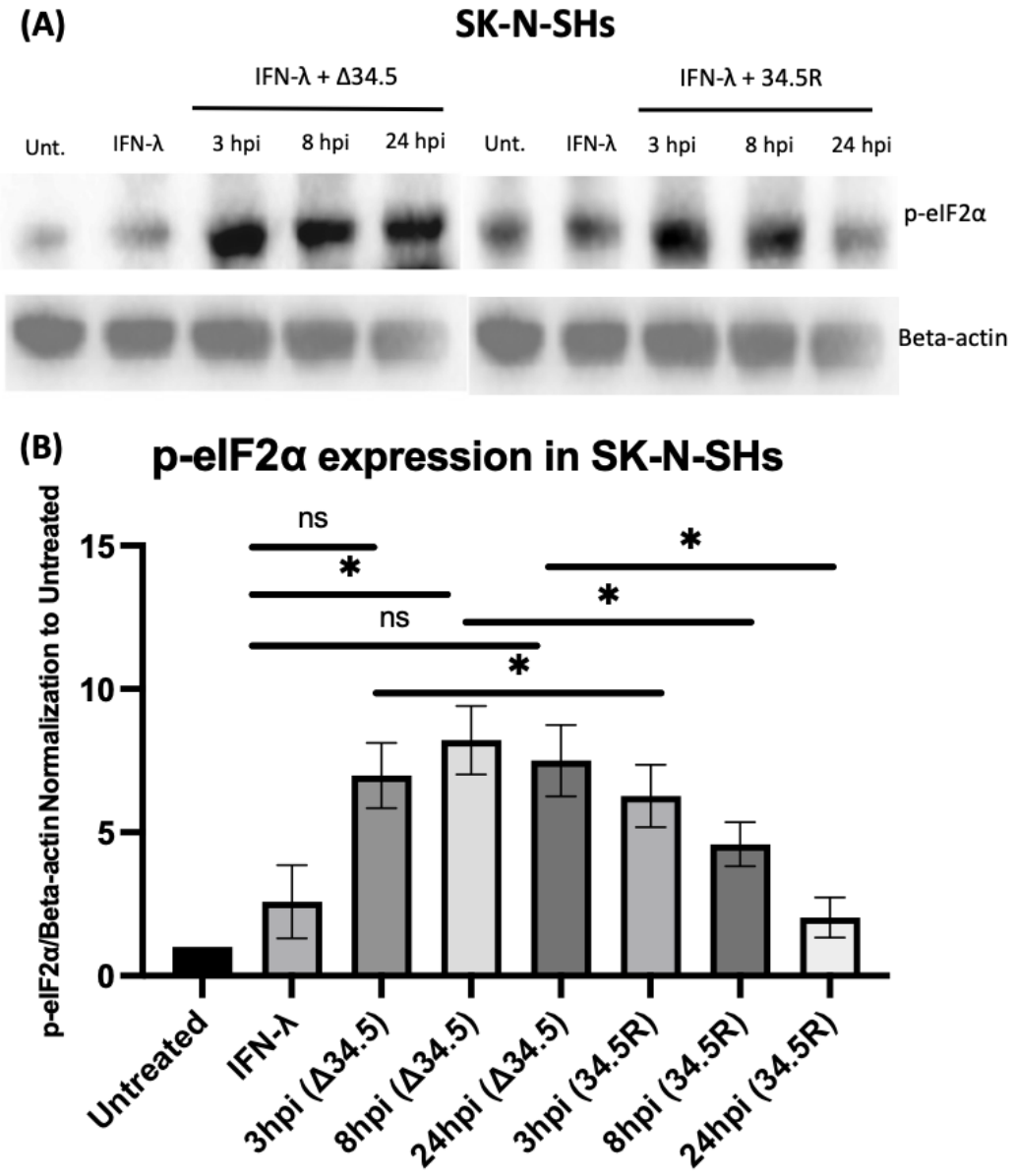

Figure 4.7. eIF2α phosphorylation sustains during ICP34.5-deficient HSV-1 infection in IFN-λ-treated human neuronal cells. SK-N-SH cells were pretreated with human IFN-λ2 (200 ng/mL, 24 h) and subsequently infected with either the HSV-1 ICP34.5-revertant strain (34.5R) or the ICP34.5-deficient mutant (Δ34.5) at MOI 1. (**A**) Cells were harvested 3, 8, and 24 h post-infection for immunoblot analysis. Immunoblots were probed with antibodies against phosphorylated eIF2α (p-eIF2α). Beta-actin was used as a loading control (n=3). (**B**) p-eIF2α levels were normalized to Beta-actin and demonstrate efficient p-eIF2α depletion (n=3 triplicates). Bars represent mean ± SEM. Individual points indicate biological replicates. Statistical significance was determined using Brown-Forsythe and Welch one-way ANOVA followed by Games-Howell's multiple comparisons test. *, $p < 0.05$; ns, not significant.

RSAD2 functions as a key antiviral effector of IFN-λ-mediated response in PNS neurons

To directly assess the role of RSAD2 in mediating IFN-λ-dependent restriction of HSV-1, we performed RNA interference experiments in primary SCG neurons utilizing siRNA magnetofection. Immunoblot analysis confirmed efficient silencing of RSAD2 following transfection with a rat RSAD2-specific siRNA compared to a non-targeting (NT) control. Band intensities normalized to SNAP25 demonstrated a significant reduction in RSAD2 protein levels, validating the knockdown efficiency (Figure 4.8A).

We next evaluated the functional impact of RSAD2 depletion on viral replication during IFN-λ treatment. SCGs were pretreated with rat IFN-λ2 (200 ng/mL, 24 h) and subsequently infected with the HSV-1 Δ34.5 mutant for 24 h at MOI 10. Due to unequal variance across treatment groups, viral titers were analyzed using Brown-Forsythe and Welch one-way ANOVA. Both tests revealed a significant overall effect of treatment, indicating that viral replication differed among experimental conditions (Brown-Forsythe ANOVA: $F^*(3, 12.82) = 5.949$, $p = 0.0090$; Welch ANOVA: $W(3, 7.734) = 6.916$, $p = 0.0139$). Games-Howell's post hoc analysis demonstrated that IFN-λ significantly reduced viral replication relative to untreated neurons ($p < 0.05$; Figure 4.8B). Notably, RSAD2 knockdown (siRSAD2) restored virus yield similar to untreated levels despite IFN-λ pretreatment ($p < 0.05$; Figure 4.8B). These findings demonstrate that RSAD2 contributes to the antiviral effect of IFN-λ in neurons and plays a central role in restricting HSV-1 in the absence of ICP34.5.

(A)

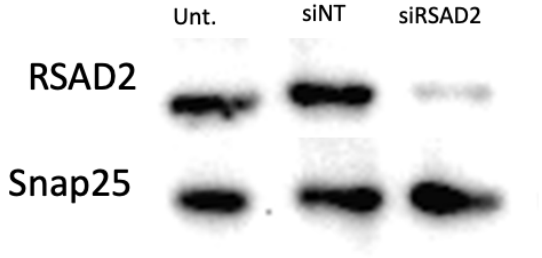
Unt.
siNT
siRSAD2
RSAD2
Snap25

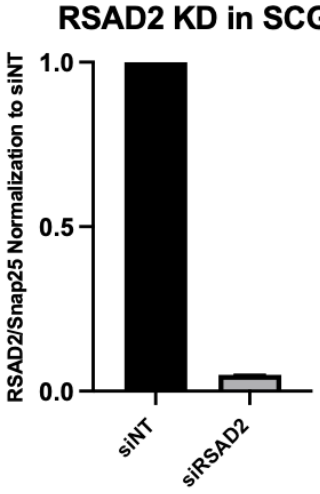
RSAD2 KD in SCGs
RSAD2/Snap25 Normalization to siNT
1.0
0.5
0.0
siNT
siRSAD2

(B)

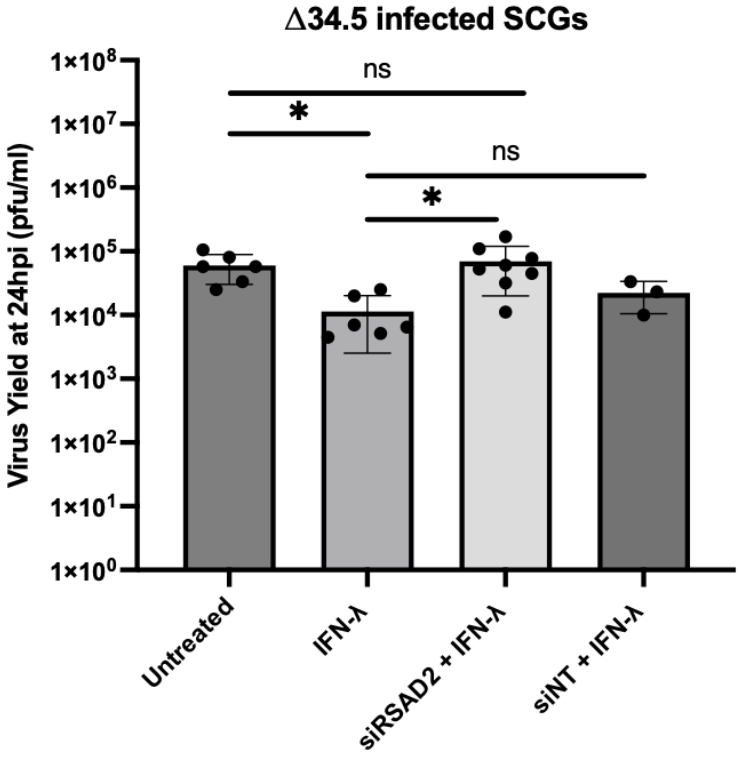
Δ34.5 infected SCGs
Virus Yield at 24hpi (pfu/ml)
1×10^8
1×10^7
1×10^6
1×10^5
1×10^4
1×10^3
1×10^2
1×10^1
1×10^0
ns
*
ns
*
Untreated
IFN-λ
siRSAD2 + IFN-λ
siNT + IFN-λ

Figure 4.8. RSAD2 knockdown restores ICP34.5-deficient HSV-1 replication in IFN-λ-treated SCGs. (**A**) Representative immunoblot showing RSAD2 protein levels in SCGs following transfection with nontargeting (NT) or RSAD2-specific siRNA. Quantification of the bands shown below the blot using ImageJ. RSAD2 levels were normalized to SNAP25 and demonstrate efficient RSAD2 depletion (RSAD2, 0.061 ± 0.003 SEM relative to NT control; unpaired Student's *t* test, **, $p < 0.005$). (**B**) SCGs were transfected with nontargeting (siNT) or rat RSAD2-specific siRNA (siRSAD2) for 48 h and pretreated with rat IFN-λ2 (200 ng/mL) for 24 h prior to infection with the HSV-1 Δ34.5 mutant at an MOI of 10. Viral titers were quantified at 24 h post-infection. Bars represent mean ± SEM. Individual points indicate biological replicates. Statistical significance was determined using Brown-Forsythe and Welch one-way ANOVA followed by Games-Howell's multiple comparisons test. *, $p < 0.05$; ns, not significant.

4.3 Discussion

This chapter further characterizes RSAD2 (viperin) as an antiviral effector mediating IFN-λ restriction of αHV and demonstrates that HSV-1 can overcome this defense through ICP34.5 antagonism in PNS neurons. Our results demonstrate that RSAD2 is strongly induced by IFN-λ in peripheral neurons, localizes to punctate perinuclear ER-associated structures, and effectively restricts αHV replication as demonstrated by RSAD2 functional assays (Figure 4.6). However, HSV-1 encoding ICP34.5 disrupts RSAD2's spatial organization and reverses its downstream effects on translation, allowing productive infection in IFN-λ-primed neurons. These findings directly address the central questions from Chapters 2 and 3 and establish the molecular basis of simplexvirus neurotropism.

The differential RSAD2 induction observed between rat superior cervical ganglion (SCG) neurons and human SK-N-SH neuroblastoma cells raises important questions about species-specific and developmental regulation of innate immunity. IFN-λ treatment induced RSAD2 protein accumulation in human SK-N-SH cells within 24 h, with prominent perinuclear puncta clearly visible by immunofluorescence. Likewise, rat primary SCG neurons exhibited similar induction; albeit with weaker staining intensity and less pronounced punctate localization indicating that RSAD2 regulation may differ with neuronal developmental state or species-specific innate immune programming. Rat and human IFN-λ receptors (IFN-λR1/IL-10R2) exhibit sequence divergence that may influence ligand binding affinity or downstream signaling strength [21]. Also, the developmental or differentiation state may influence RSAD2 responsiveness: SK-N-SH cells are transformed neuroblastoma cells with retained proliferative capacity, whereas primary SCG neurons are fully differentiated, post-mitotic cells. Transformed

cells may exhibit enhanced interferon responsiveness or altered chromatin states that facilitate rapid ISG induction compared to quiescent primary neurons [158].

Species-dependent differences in RSAD2 antiviral function have documented mouse RSAD2 displaying more potent activity against HSV-1 than human RSAD2 [151]. This species-specific variation in RSAD2 antiviral potency suggests that αHVs and RSAD2 have co-evolved, with viruses adapting to the RSAD2 variants present in their natural host species. The finding that both rat and human neurons restrict HSV-1 Δ34.5 despite quantitative differences in RSAD2 induction indicates that the RSAD2-ICP34.5 antagonistic relationship is functionally conserved across species, supporting its fundamental importance in antiviral activity. While we observed quantitative differences in RSAD2 induction between rat SCG neurons and human SK-N-SH cells, the biological significance of these differences remains uncertain. Future comparative studies using primary human sensory neurons (e.g., dorsal root ganglia from organ donors) will be necessary to determine whether the enhanced RSAD2 response observed in SK-N-SH cells reflects genuine species differences or artifacts of transformation and cell line adaptation.

HSV-1 deploys multiple complementary strategies to neutralize RSAD2, highlighting its relevance as a viral restriction factor and suggesting evolutionary selection pressure. The HSV-1 virion host shutoff protein (vhs), encoded by UL41, is a multifunctional endoribonuclease that nonspecifically degrades host mRNAs to shut off cellular protein synthesis and redirect the translational machinery toward viral proteins. Studies have demonstrated vhs targets RSAD2 mRNA and deplete RSAD2 protein during infection [152]. Shen et al. demonstrated that RSAD2 strongly inhibits UL41-null HSV-1 replication, supporting the idea that the virus actively suppresses RSAD2 [152]. ICP34.5 serves as another HSV-1 countermeasure, disrupting RSAD2 localization and reversing eIF2α phosphorylation to restore late protein synthesis. However, in

IFN-λ-primed neurons where RSAD2 protein is pre-induced and accumulated before viral entry, vhs-mediated mRNA degradation is insufficient to eliminate pre-existing RSAD2 protein, which has a relatively long half-life (about 6-9 hours in many cell types) [159]. Under these conditions, ICP34.5 provides a complementary and perhaps more critical mechanism by disrupting RSAD2 function at the protein level.

This work further identifies HSV-1 ICP34.5 as a neuron-specific antagonist of RSAD2. First, ICP34.5 disrupts RSAD2's spatial organization. In IFN-λ-primed neurons infected with wild-type HSV-1, RSAD2 puncta rapidly dispersed from perinuclear foci to diffuse into the cytoplasm, coinciding with a reduction in total RSAD2 protein levels (Figure 4.3). This behavior is consistent with previous studies showing that ICP34.5 directly disrupts the spatial organization of RSAD2 [160].

Second, ICP34.5 reverses RSAD2's downstream effects on translation by recruiting protein phosphatase 1α (PP1α) to dephosphorylate eIF2α. Our immunoblot analysis confirmed this mechanism, demonstrating that Δ34.5-infected SK-N-SH cells maintained high levels of phosphorylated eIF2α and exhibited severely impaired late viral protein synthesis (Figure 4.5C and Figure 4.7). In contrast, revertant 34.5R infections showed eIF2α dephosphorylation and late protein production. Primary neurons exhibited a more complex phenotype. Immunoblot analysis of IFN-λ pre-treated neurons infected with Δ34.5 or 34.5R demonstrated viral protein levels were elevated when ICP34.5 was present, suggesting that indeed ICP34.5 is essential for temporal gene expression during HSV-1 infection (Figure 4.3D). Primary neurons may respond differently to p-eIF2α-mediated translational stress than neuroblastoma cells, potentially due to differences in basal PKR activity or virion assembly efficiency. This two-pronged antagonism, spatial disruption of RSAD2 plus functional reversal of its downstream effects on translation,

demonstrates the selective pressure RSAD2 imposes on HSV-1 and explains why viruses lacking these countermeasures (e.g., PRV) remain vulnerable to neuronal IFN-λ responses.

We next performed loss-of-function studies in neurons to further investigate RSAD2's essential role in the immune response. siRNA-mediated RSAD2 knockdown in IFN-λ-primed SCG neurons partially restored replication of Δ34.5 HSV-1. This finding demonstrates that RSAD2 contributes to the antiviral response against HSV-1 and that ICP34.5 mitigates this. This strongly suggests that RSAD2 and ICP34.5 function as opposing determinants of infection outcome in neurons. In Δ34.5 infection, RSAD2 remains localized in perinuclear antiviral compartments, maintains high mRNA levels, and potently restricts infection. When ICP34.5 is present, these antiviral functions collapse, enabling the virus to proceed with genome replication and late gene expression despite the IFN-λ primed state.

A central question in Chapter 3 was to dissect how different αHVs interact with neuronal RSAD2-mediated defenses. PRV provided a critical comparison due to the lack of an ICP34.5 homologue, enabling direct assessment of RSAD2 function in the absence of viral impact. This chapter shows that PRV maintained RSAD2 expression during infection at 3 hpi, 8 hpi, and 24 hpi when neurons were primed with IFN-λ for 24 h. While RSAD2 localization during PRV infection was not explored in this chapter, the parallels between PRV and d34.5 HSV-1 sensitivity (both lacking ICP34.5) strongly suggest that PRV is unable to overcome RSAD2-mediated defenses. This finding has critical implications for understanding αHV evolution and neurotropism.

PRV, despite being a highly neurotropic swine virus, does not naturally infect higher primates and displays a limited range of hosts. VZV, which also lacks ICP34.5, establishes latency in human dorsal root ganglia but requires higher viral loads and demonstrates limited

spread in PNS neurons. The absence of ICP34.5 in varicelloviruses may render them more vulnerable to IFN-λ-mediated responses, partially explaining their distinct neurobiological properties compared to simplexviruses. αHVs have evolved sophisticated viral programs to overcome neuronal RSAD2-mediated responses, enabling efficient neuroinvasion and establishment. The differential sensitivity of PRV (restricted) versus HSV-1 (resistant) to IFN-λ represents that RSAD2 and other ISG restriction is potent and effective when viral countermeasures are absent but can be overcome by viruses encoding specialized antagonists such as ICP34.5.

The differential antiviral response of IFN-β (type I IFN) compared to IFN-λ (type III IFN) as observed in Chapter 3 warrants further discussion in the context of RSAD2. Specifically, IFN-β triggers a rapid onset of interferon-stimulated gene (ISG) expression, including a strong induction of RSAD2, resulting in a high-magnitude response. In contrast, IFN-λ induces a slower but more sustained response over a longer period. This pattern of response mirrors what has been observed in epithelial cells, but in neurons, these responses are more pronounced. Neurons seem to be predisposed to a response that is dampened in intensity but maintained over an extended duration when stimulated by IFN-λ. The variations in receptor levels, the speed of signal transduction, or the accessibility of chromatin regions for ISGs could all play roles in this reduced sensitivity. The delayed yet persistent response to IFN-λ might actually be advantageous for neurons, as an overt or rapid activation of antiviral pathways could cause cytotoxic stress and damage. The finding that IFN-λ induces sustained RSAD2 expression suggests that type III IFNs may be particularly effective at establishing neuron-specific long-lasting antiviral response.

In contrast to the strong IFN-λ-mediated restriction observed in PRV infection, HSV-1 remained largely resistant in both rodent primary neurons and human neuronal models. This

resistance was not observed in fibroblasts, where IFN-λ effectively suppressed HSV-1 replication, demonstrating that the evasion mechanism is neuron-specific rather than species-specific. Based on the findings in this chapter, I proposed a model for how IFN-λ establishes RSAD2-mediated antiviral response in neurons and how HSV-1 overcomes them via ICP34.5 antagonism (Figure 4.9). In this model, IFN-λ produced by infected epithelial cells at mucosal barriers diffuses to adjacent tissues and primes uninfected cells, including PNS neuron axon terminals innervating at these sites. IFN-λ binding to receptors, IFNLR1/IL10B, activates STAT1-selective signaling (Chapter 2), leading to transcription of ISGs, including RSAD2. RSAD2 protein accumulates and localizes to punctate perinuclear ER-derived membrane domains through its N-terminal amphipathic αhelix. When HSV-1 infects IFN-λ primed neurons, RSAD2 activity and associated ER stress activate PERK and PKR, leading to eIF2α phosphorylation that enforces translational arrest. HSV-1 overcomes this barrier by deploying ICP34.5 to dismantle RSAD2's structural organization while simultaneously subverting the integrated stress response to restore viral translation. Together, RSAD2 and ICP34.5 define a neuron-specific antagonistic mechanism that determines whether HSV-1 commits to productive replication or is suppressed in a type III IFN-primed environment.

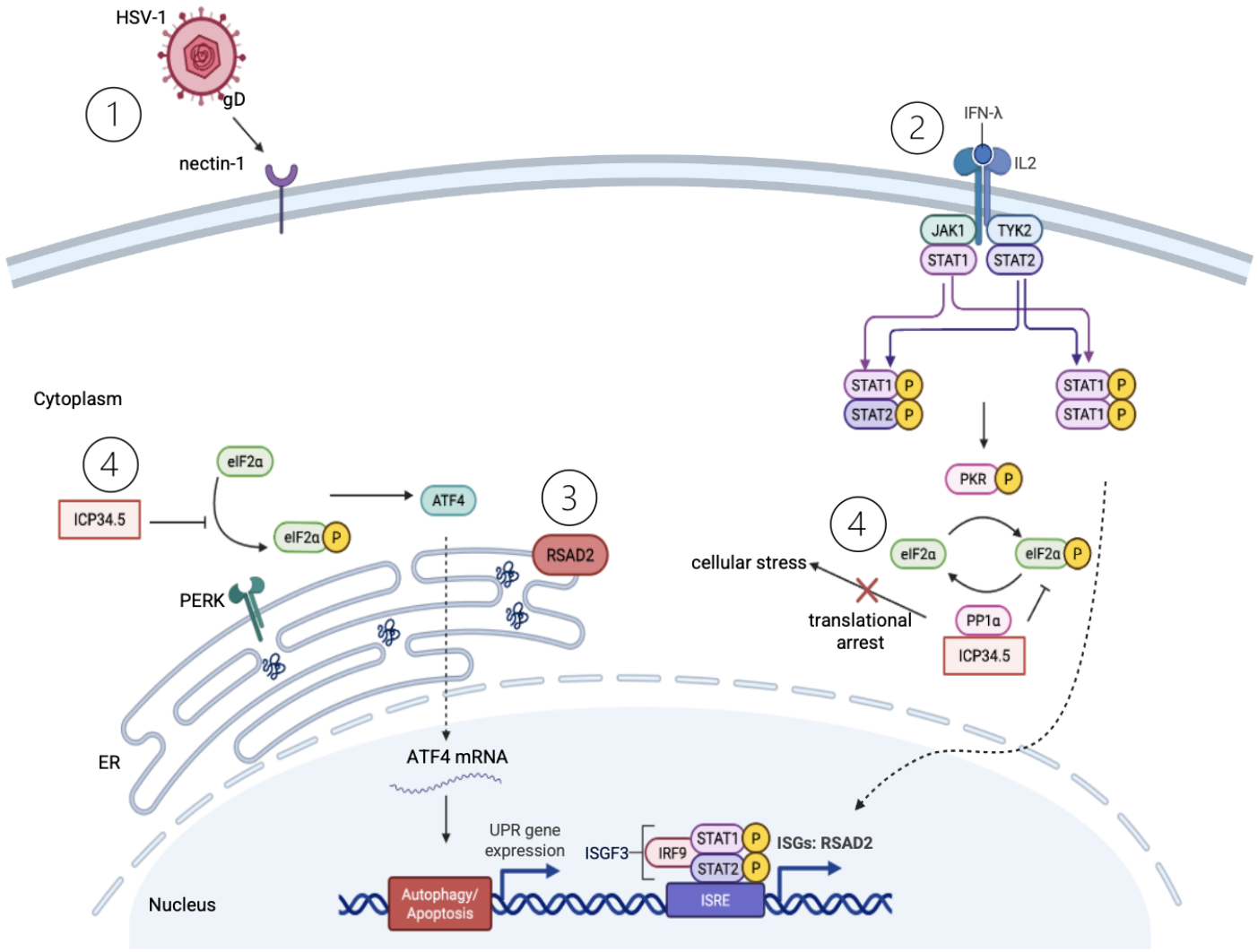

Figure 4.9. Proposed model of ICP34.5-mediated regulation of RSAD2 during IFN-λ-induced antiviral responses in neurons. (**1**) HSV-1 enters via nectin-1 and gD-mediated attachment, activating innate immunity. (**2**) IFN-λ binds its receptor, triggering the phosphorylation of JAK1/TYK2 and STAT1/2, which form ISGF3 and promote the expression of ISGs, such as RSAD2 (viperin). (**3**) RSAD2 localizes to the endoplasmic reticulum (ER), restricting viral replication by altering lipid metabolism, inducing translational shut off and disrupting assembly. (**4**) HSV-1 ICP34.5 counteracts this by recruiting PP1α to dephosphorylate eIF2α, inhibiting translational shutoff, and interfering with ER stress response, thus limiting RSAD2 antiviral activity.

CHAPTER 5: Axonal Responses to IFN-λ Suppress αHV Retrograde Transport and Productive Infection

Abstract

Neuroinvasion by αHVs begins when virions released from infected mucosal epithelia encounter peripheral neuronal axons that have already been exposed to inflammatory cytokines. These early cytokine signals may function as an advanced warning system, enabling axons to initiate intrinsic antiviral defenses before viral particles reach the soma. Here, we investigated how type III interferon (IFN-λ), a prominent mucosal antiviral cytokine, shapes early neuronal responses to incoming virions. Using compartmentalized superior cervical ganglion (SCG) cultures, we found that local IFN-λ treatment of axons within the N-compartment significantly reduced retrograde transport of PRV180 (mRFP-VP26) capsids, following infection at MOI 10, indicating that IFN-λ establishes a localized axonal antiviral state. Reduced number of virion movement correlated with delayed infection, as axonal IFN-λ pretreatment diminished PRV180 signal at 24 hpi; however, by 48 hpi, virus infection overcomes the antiviral restriction at this MOI.

To determine the signaling mechanism underlying this restriction, we examined IFN-λ-induced JAK-STAT activation using immunofluorescence microscopy and Western blot analysis. Chapter 2 demonstrated that global (cell body and axon) exposure to IFN-λ triggered strong STAT1 phosphorylation and nuclear accumulation, but minimal STAT2 activation. Notably, when IFN-λ was applied exclusively to axons, p-STAT1 accumulated locally within neurites without nuclear translocation, demonstrating that axons autonomously sense IFN-λ and initiate non-canonical STAT1-dependent signaling independent of the soma. To confirm that STAT1 phosphorylation was required for axonal IFN-λ-mediated restriction, we inhibited

STAT1 using fludarabine. Fludarabine treatment selectively blocked p-STAT1 accumulation in axons and abolished the antiviral activity of IFN-λ against PRV180. Under these conditions, PRV180 capsid movement, cell body accumulation, and viral yields were comparable to untreated control neurons, confirming that STAT1 activation in axons is both necessary and sufficient for IFN-λ-mediated restriction of retrograde viral transport. Collectively, these findings identify that the axonal STAT1 signaling axis may limit α-herpesvirus retrograde transport and neuroinvasion, revealing a key cytokine-driven type III IFN checkpoint at the mucosal epithelial-PNS junction.

5.1 Introduction

Life-long infection by αHVs such as HSV-1 requires successful neuroinvasion: virions released from epithelial cells must gain access to PNS neurons via axonal termini and engage the retrograde transport motors to reach the neuronal nucleus, where infection is established. Infected epithelial cells rapidly mount an immune response, including cytokine release such as type I and type III IFNs, to nearby uninfected cells, including PNS neurons. These cytokine signals function as an advanced warning system, enabling neurons to initiate antiviral defenses before virions physically contact axons. One question central to αHV neuroinvasion is whether axons can autonomously detect and trigger local antiviral responses that restrict viral entry and retrograde transport independent of transcriptional programs in the soma.

Prior studies using compartmentalized primary cultures of neurons show that axons can sense cytokines and respond with or without direct input from the cell body [79]. This early axonal response may determine whether viral particles are able to reach the nucleus through retrograde transport or are held back in the axons. Should only a small number of virions be able

to reach the soma these genomes may never start a productive infection and are immediately silenced [81]. Thus, axonal exposure to IFNs represents a critical immune checkpoint that determines the infection outcome.

Although neurons express the type I IFN receptor (IFNAR1/2) and can initiate STAT1-mediated antiviral signaling, they produce and secrete type I IFN at a substantially lower level than epithelial cells [20, 161]. Nonetheless, type I IFN pretreatment has been shown to protect neurons from productive HSV-1 infection, promote latency, and decrease reactivation frequency in multiple experiment systems [16, 17, 100]. When type I IFN is directly applied to axons within compartmented chambers (N-compartment), p-STAT1 accumulates locally in the axon and is sufficient to block retrograde capsid transport, thereby reducing the number of viral genomes reaching the neuronal nucleus [79]. This axon autonomous response occurs independently of the cell body, revealing that peripheral axons can initiate localized antiviral response upon cytokine detection. If early mucosal defenses fail, delayed immune signals (e.g. interferon-γ made by immune-cell infiltrators) activate p-STAT1 and direct its nuclear translocation in the infected neuron, upregulating antiviral gene programs, including apoptosis if necessary [12, 14, 17]. Thus, neuronal interferon signaling consists of at least two phases: early axon-localized responses, followed by late nuclear responses including ISG expression.

Despite these insights into type I IFN signaling in axons, the role of type III IFNs (IFN-λ) in axonal immune response remains to be elucidated. IFN-λ is the predominant interferon produced at mucosal epithelial barriers, including oral, genital and respiratory epithelia, where αHV initiate primary infection [21, 28, 162, 163]. Unlike ubiquitously expressed type I IFN receptor (IFNAR1/IFNAR2), IFN-λ signals through a distinct receptor complex (IFNLR1/IL-

10B) with restricted tissue expression being most abundant in mucosal tissue and showing lower but detectable expression in neurons [21].

Importantly, all previous characterizations of neuronal IFN-λ responses in this thesis examined responses in whole neurons (both the cell body and axon). Whether IFN-λ can establish axon-independent antiviral responses comparable to those observed with type I IFNs remained unknown. Given that IFN-λ is the primary interferon produced at mucosal sites where αHVs initiate infection, and that PNS axons directly innervate these mucosal tissues, it is critical to understand whether axonal IFN-λ provides a frontline defense against neuroinvasion and to define the spatial organization of neuronal immunity.

This chapter investigates whether IFN-λ establishes a local axonal antiviral response that restricts αHV neuroinvasion. Using compartmentalized primary neuron cultures that physically separate the cell body (S-compartment) from the axons (N-compartment), the following studies investigate these central questions: Does local IFN-λ treatment restrict retrograde transport of incoming viral capsids? Can axons activate STAT1 phosphorylation without signaling from the soma? Lastly, is axonal accumulation of p-STAT1 sufficient for IFN-λ-mediated restriction of capsid transport?

5.2 Results

Reduced viral particle motility after IFN-λ pretreatment

To assess whether IFN-λ treatment influences viral particle transport within the axon, the N-compartments of compartmentalized sympathetic neuron (SCG) cultures were pre-treated with 200 ng/mL rat IFN-λ2 for 24 hours. Subsequently, the transport of recombinant pseudorabies

virus (PRV180), engineered to express mRFP-VP26 capsid protein, was monitored within the distal axonal (N) compartment (Figure 5.1A). Live-cell microscopy (63X) was used to study retrograde transport in axons of untreated or IFN-λ-pretreated neurons infected with PRV180 at MOI 10 (Figure 5.1B) between 15 min and 1 hpi. Quantitative analysis using *ImageJ* to determine the percentage of virions displaying directed movement over a 60-second interval revealed that IFN-λ significantly reduces the number of virus particles capable of sustained retrograde transport (Figure 5.1C). These observations support a model in which IFN-λ locally primes neurons and establishes an initial axonal antiviral state.

Delayed productive infection upon axonal IFN-λ treatment at MOI 1

Following our observation that local IFN-λ exposure in axons decreases virion motility, we further examined whether this reduction would affect the overall infection efficiency. To assess whether IFN-λ treatment influences the establishment of a productive retrograde infection in neuronal cell bodies, we pre-treated the N-compartment of compartmentalized sympathetic neuron (SCG) cultures with 200 ng/mL of rat IFN-λ2 or vehicle for 24 hours. After this pretreatment, the cultures were infected with PRV180 at a multiplicity of infection (MOI) of 1 (Figure 5.2A). To visualize the connectivity between axons in the N-compartment and the soma in the S-compartment, we used Dio, a lipophilic dye that allows detailed observation of neural connections. Infection progression was monitored in the S-compartment at 24 h and 48 h post-infection (Figure 5.2B). We observed that pretreatment with IFN-λ reduced retrograde PRV180 infection at 24 hours post-infection, but this delay was restored by 48 h as the virus infection overcame IFN-λ-mediated restriction (Figure 5.2C). These results suggest that local exposure to IFN-λ can delay the establishment of productive retrograde infection, potentially affecting the spread and efficiency of viral infection within neural pathways.

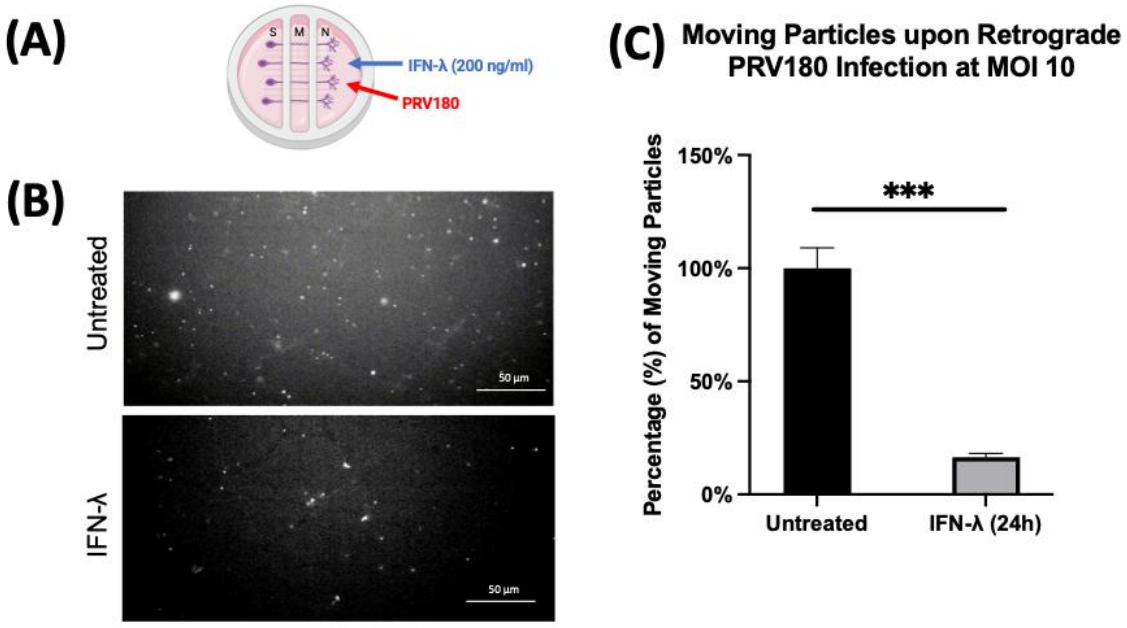

Figure 5.1. IFN-λ pretreatment reduces retrograde axonal transport of incoming PRV particles in SCG neurons. (A) Schematic of the compartmentalized SCG neuron culture system showing IFN-λ2 pretreatment (200 ng/mL, 24 h) applied to the soma (S) compartment prior to PRV-180 infection of the distal axonal (N) compartment**. (B)** Representative live-cell images of axonal PRV-180 particles (mRFP-VP26 capsid) imaged at 63X magnification in untreated and IFN-λ-pretreated neurons in black-and-white over a period of 15 minutes to 1 h. Scale bars are 50 µm; n = 3 replicates. **(C)** Quantification of virion transport dynamics using *ImageJ* particle-tracking analysis over a 60-second recording period. Statistical significance analyzed via Student's *t* test (n ≥ 3) is indicated as follows: ***, $p < 0.0005$.

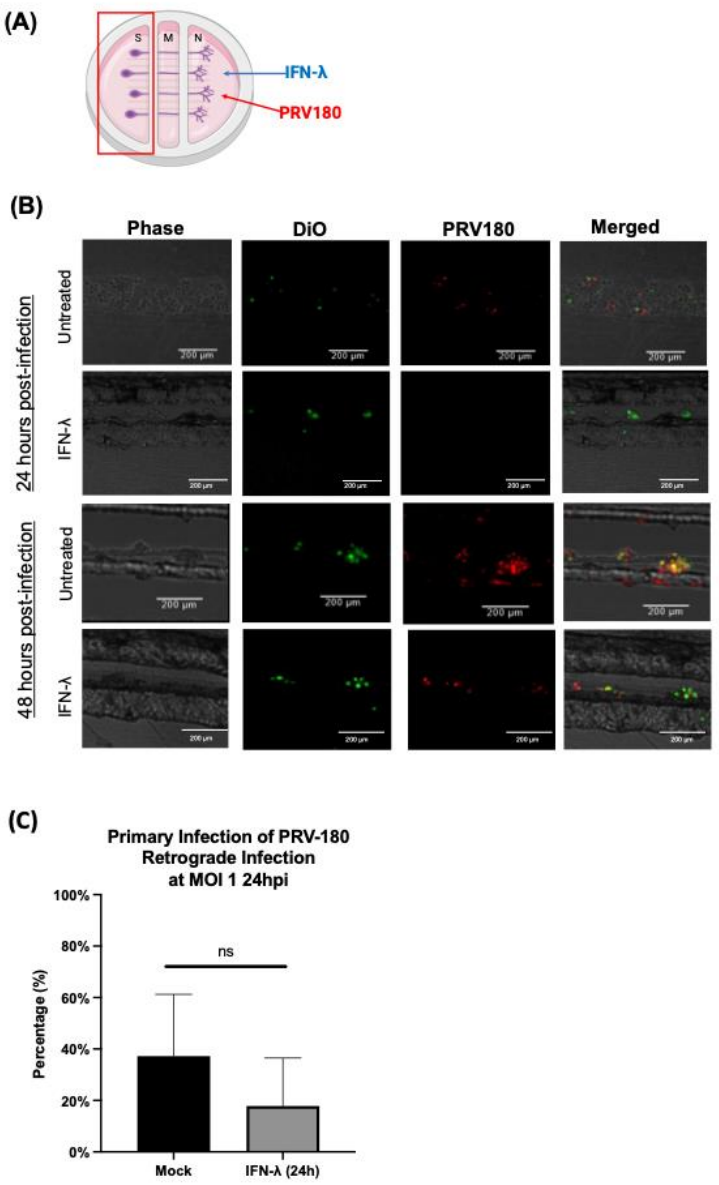

Figure 5.2. IFN-λ pretreatment in axons delays productive retrograde PRV infection. (**A**) Schematic of compartmentalized SCG cultures showing DiO labeling (green) in the N-compartment to confirm axonal connectivity with soma in the S-compartment. The N-compartment was pre-treated with 200 ng/mL rat IFN-λ2 for 24 h before infection with PRV180 (MOI 10). The red box surrounds the area imaged (S-compartment) (**B**) Representative fluorescence images at 24 and 48 hpi taken at 63X objective. Scale bar is set to 200 µm. (**C**) Primary infection of PRV180 was determined by normalizing red capsid fluorescence with DiO after 24 hpi. Statistical significance analyzed via Student's *t* test, ns: not significant ($n \geq 3$).

Local IFN-λ exposure induces axonal p-STAT1 accumulation independent of soma signaling

We previously showed that global IFN-λ treatment activates canonical JAK-STAT signaling in SCG neurons, leading to strong STAT1 phosphorylation in primary neurons (but not STAT2) [29] (Figure 5.3A and 5.3B). Under global treatment conditions, p-STAT1 was primarily localized in neuronal nuclei, similar to the pattern observed with IFN-β–treated SCGs, which aligns with previous findings that both cytokines induce classical ISGF3-dependent transcriptional programs after neuron-wide exposure [79] (Figure 5.3C). To investigate whether axons alone can sense type III IFN and trigger a localized signaling response, we selectively exposed only the neurite (N) compartment of SCG tri-chambers to exogenous IFN-λ2 (200 ng/mL, 24 h) (Figure 5.3D). Immunofluorescence analysis showed accumulation of p-STAT1 within axons after treatment, suggesting that distal axons can independently phosphorylate and retain STAT1 in response to local IFN-λ (Figure 5.3E). These results distinguish localized axonal IFN-λ signaling from the classical soma-driven response and demonstrate that distal axons can autonomously activate STAT1 without involving the cell body's transcriptional machinery.

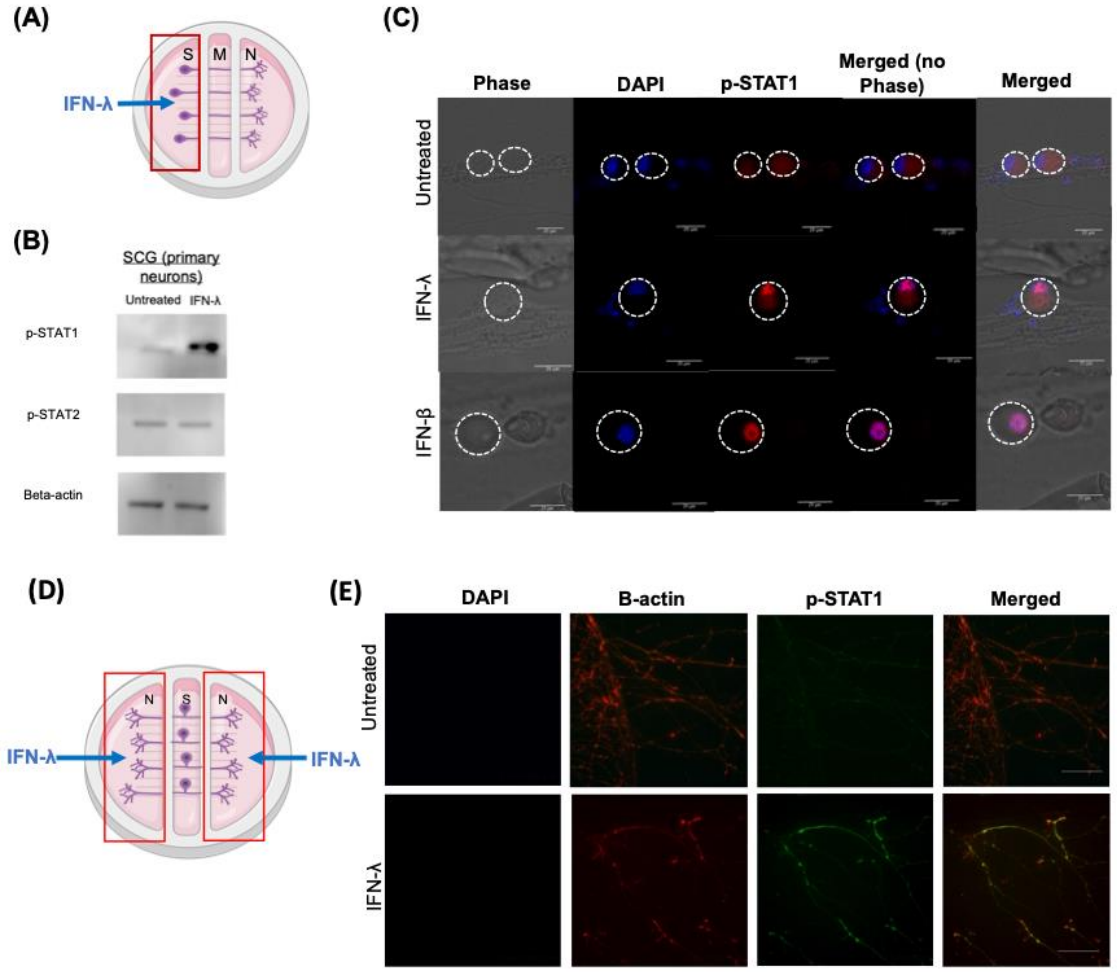

Figure 5.3. STAT1 phosphorylation is induced in SCGs in response to global or local IFN-λ treatment. (**A**) Schematic design demonstrating the treatment of SCGs globally with rat IFN-λ2 (200 ng/mL, 24 h). (**B**) SCG neurons were globally treated with rat IFN-λ2 (200 ng/mL, 24 h) and blotted for p-STAT1, p-STAT2, or Beta-actin (control). (**C**) Immunofluorescence staining of p-STAT1 nuclear localization in SCGs treated with IFN-λ and IFN-β; DAPI was used as a control to stain the nucleus, and p-STAT1 can be observed in red. (**D**) SCG neurons were cultured in the M-compartments of the tri-chambers, and only the neurite (N) compartment received IFN-λ2 treatment (200 ng/mL, 24 h), while the cell bodies remained untreated. (**E**) Axonal p-STAT1 was visualized by immunofluorescence to evaluate local activation of STAT1. P-STAT1 can be observed under green fluorescence and Beta-actin was used as a cytoplasmic control in red. DAPI was used to stain nuclei blue. Images were taken at 63X, and the scale bars are 20 μm.

Inhibition of STAT1 phosphorylation abolishes the IFN-λ–dependent antiviral response in axons

To determine whether IFN-λ–mediated restriction of αHV infection requires STAT1 activation, we first validated pharmacological inhibition of p-STAT1 using fludarabine, a known STAT1 inhibitor [164, 165]. Rat embryonic fibroblast (REF) cells were pre-treated with 50 μM fludarabine for 24 h, followed by IFN-λ2 exposure. In REF cells, fludarabine effectively blocked STAT1 phosphorylation, eliminating the p-STAT1 signal normally induced by IFN-λ (Figure 5.4A). In contrast, p-STAT2 activation remained intact despite inhibitor treatment, indicating that fludarabine selectively suppresses STAT1 without interfering with upstream IFN-λ receptor signaling. We next assessed whether axonal p-STAT1 is required for the antiviral activity of IFN-λ in sympathetic neurons. The neurite (N) compartment of the tri-chamber was pre-treated with 50 μM fludarabine or vehicle for 24 h, followed by localized rat IFN-λ2 exposure (200 ng/mL, 24 h), and subsequently infected with PRV180 (MOI 1) for 30 hours (Figure 5.4B). Axonal IFN-λ pretreatment in the presence of the vehicle significantly reduced PRV180 infection, supporting previous findings that distal IFN-λ signaling primes axons to limit retrograde neuroinvasion. Inhibition of p-STAT1 in the axonal compartment abolished this antiviral effect, with viral titers in fludarabine-treated axons similar to those in untreated infected SCGs (Figure 5.4C). This indicates that p-STAT1 activation in distal axons is essential for IFN-λ–mediated restriction of PRV180, with STAT1 being crucial for this intrinsic antiviral pathway.

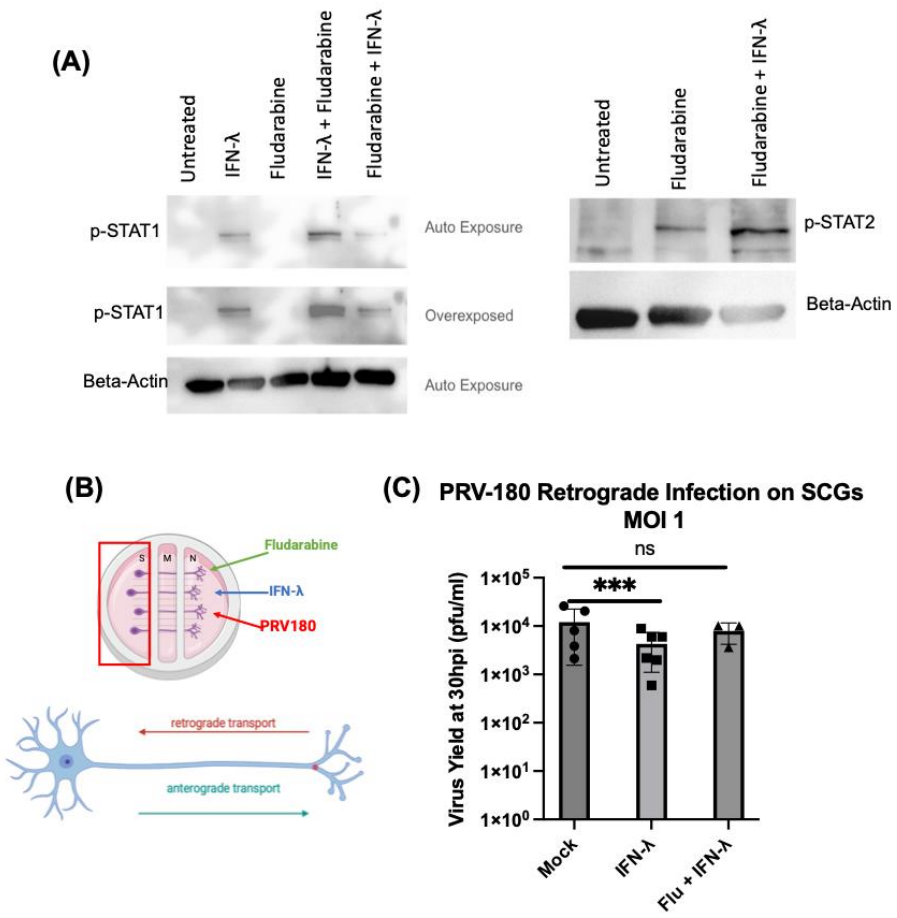

Figure 5.4. Fludarabine inhibition of STAT1 activation abolishes IFN-λ-dependent antiviral protection in axons. (**A**) Rat2 fibroblasts were pre-treated with 50 μM fludarabine followed by IFN-λ2 stimulation. Immunoblotting confirmed that p-STAT1 induction was effectively blocked by fludarabine, whereas p-STAT2 activation remained intact. (**B**) Schematic of the tri-chamber experimental design. The neurite (N) compartment was treated with fludarabine, followed by IFN-λ2 (200 ng/mL, 24 h), and subsequently infected with PRV180. (**C**) Viral titers from SCG neurons show that inhibition of STAT1 prevents IFN-λ–mediated antiviral restriction. Fludarabine-treated axons displayed PRV180 yields comparable to untreated, infected controls, demonstrating that p-STAT1 is required for IFN-λ–dependent suppression of retrograde viral infection. Statistical significance analyzed via Student's *t* test (n ≥ 3) is indicated as follows: ns, not significant; ***, $p < 0.0005$.

5.3 Discussion

Our findings demonstrate that type III interferon (IFN-λ) initiates a localized, axonal antiviral response that restricts aHV neuroinvasion before viral capsids reach cell bodies. Exposing distal axons to IFN-λ locally was enough to decrease PRV180 capsid movement and delay productive infection by inducing robust STAT1 phosphorylation in the axonal compartment. These results establish that axons function as autonomous sensors of antiviral type III IFN, forming an innate barrier against neuroinvasion at the mucosal-PNS interface. This axon-specific antiviral state operates by restricting the transport of incoming capsids, thereby reducing the number of capsids reaching the nucleus.

This spatial restriction has significant biological consequences. Since axons have finite dynein motor capacity and multiple cargo compete for retrograde transport machinery, even modest reductions in capsid transport efficiency can produce substantial decreases in the viral load delivered to the soma [166]. During αHV infection, virions must compete with the endogenous cargoes for access to dynein motors [167]. The molecular basis of this competition centers on viral capsid-dynein interactions. During primary infection, PRV and HSV-1 inner tegument proteins UL36 and UL37 form a crucial complex with the host motor, dynein and are essential for transporting entering viral capsids from the periphery to the nucleus on microtubules.[167]. This pUL36/pUL37 complex, together with outer capsid protein VP26, mediates direct physical interactions with dynein light chains and dynactin subunits, enabling capsids to hijack the host's retrograde transport machinery. Any host defense mechanism that disrupts these capsid-dynein interactions, such as axonal accumulation of STAT1 phosphorylation, can therefore function as a potent antiviral by preventing viral particles from completing their journey.

The mechanism underlying axonal IFN-λ restriction centers on local STAT1 phosphorylation. Previous studies on type I interferons demonstrated that phosphorylated STAT1 can accumulate non-canonically within axons, where it interferes with retrograde transport and slows the progression of incoming virions toward the soma [79]. Our findings extend this model to type III interferons by showing that IFN-λ alone is sufficient to induce p-STAT1 locally within distal axons, even without cell body exposure or nuclear translocation (Figure 5.3). This compartmentalized signaling occurs independently of cell body, indicating that axons possess functional IFN-λ receptors (IFNLR1/IL-10B) and signaling pathways necessary to initiate local antiviral response. The spatial restriction of p-STAT1 to axons distinguishes localized axonal signaling from global IFN-λ treatment, in which p-STAT1 accumulates to neuronal nuclei and activates canonical ISG transcription (Chapter 2). This indicates that SCG neurons deploy two distinct IFN-λ signaling modes: a local axonal checkpoint, mediated by p-STAT1 retention in the axon to restrict virion transport, and a global soma response that induces transcriptional antiviral defenses.

Studies in compartmentalized sensory neurons support this dual-mode model by showing that type I, type II, and type III IFNs all trigger robust phosphorylation of STAT1 and STAT3 within axons when applied locally [79]. However, only type II IFNs produce retrograde signaling that drives nuclear STAT localization in the distant soma. Notably, type I and type III IFNs produce a strictly local axonal signaling response that does not propagate back to the cell body. This reveals a broader principle: peripheral neurons interpret type I and type III IFNs as axon-restricted antiviral cues, enabling them to mount rapid, non-transcriptional defenses.

Although both type I (IFN-β) and type III (IFN-λ) IFNs induce axonal p-STAT1 and restrict capsid transport, important differences may exist in their efficacy, kinetics, or

downstream mechanisms. The biological differences between type I and type III IFNs relates to the spatial distribution of IFNs during natural infection. IFN-β is produced systemically whereas IFN-λ is predominantly produced at mucosal epithelia and likely acts locally on innervating axon termini.

The functional importance of neuronal STAT1 signaling *in vivo* is supported by studies using neuron-specific STAT1 knockout mice. Rosato and Leib generated mice with conditional STAT1 deletion in neurons ($STAT1^{-/-}$) and examined HSV-1 replication in corneal tissues following infection [168]. These studies revealed elevated viral titers, confirming that STAT1 signaling is critical for restricting viral replication and establishing latency *in vivo*. Our pharmacological inhibition studies utilizing fludarabine reinforce that STAT1 phosphorylation is both necessary and sufficient for IFN-λ-mediated axonal restriction. Fludarabine selectively inhibits STAT1 phosphorylation, enabling specific investigation of STAT1's functional requirement. When applied to the axonal (N) compartment, fludarabine abolished IFN-λ-mediated restriction of PRV180, restoring viral titers to levels comparable to untreated controls (Figure 5.4C). Inhibition of STAT1 phosphorylation suppresses IFN-λ-mediated restriction of virion transport. It restores infection to untreated levels, demonstrating that STAT1 acts as a direct effector of the axonal antiviral state.

The mechanism by which axonal p-STAT1 restricts capsid transport remains to be elucidated but likely involves several non-mutually exclusive pathways. P-STAT1 may directly or indirectly interfere with dynein motor complex assembly, reducing the efficiency of retrograde transport. Previous studies have demonstrated that STAT1 proteins can interact with cytoskeletal regulators and motor proteins [169, 170]. Additionally, p-STAT1 may trigger local translation of specific ISGs within axons from pre-existing mRNAs that were transcribed in the

soma and trafficked to axonal compartments [171]. Axons contain localized translational machinery and can synthesize proteins from transported mRNAs in response to local signaling [172, 173]. Distinguishing these mechanisms will require future studies examining p-STAT1 interactome in axons, local protein synthesis during type III IFN treatment, and assessing metabolic changes associated with axonal STAT1 activation. Additionally, testing OK14 (HSV-1 expressing mRFP-VP26) will determine whether this restriction is specific to PRV180 or represents a broader antiviral mechanism.

Collectively, this chapter establishes that type III IFNs create a spatially compartmentalized antiviral defense in PNS neurons, with distinct responses in the axons. The axonal checkpoint described here, mediated by local STAT1 phosphorylation, limits viral capsid transport before genomes reach the nucleus. This reduces the number of virions arriving at the nucleus and suggests a bias toward non-productive or latent infection states. This axon-autonomous response complements the broader transcriptional antiviral response discussed in earlier chapters, offering a detailed and layered understanding of neuronal antiviral defenses.

CONCLUSION

Summary

α-Herpesviruses must successfully overcome a complex series of intrinsic and innate immune barriers within the peripheral nervous system (PNS) to establish lifelong latency in PNS neurons. While mucosal epithelial cell responses to type III interferons (IFN-λ) have been well characterized, substantially less was understood regarding how PNS neurons respond to IFN-λ signaling or how neurotropic viruses have evolved to mitigate neuron-specific defenses. This dissertation defines the neuron-specific IFN-λ response at transcriptional, subcellular, and functional levels before and after αHV infection.

Neurons use a distinct IFN-λ signaling program

In Chapter 2, I demonstrated that primary superior cervical ganglion (SCG) neurons employ a predominantly STAT1-driven IFN-λ response, in contrast to fibroblasts, which activate the canonical JAK-STAT pathway involving both STAT1 and STAT2. Neurons initiate the induction of antiviral interferon-stimulated genes (ISGs) with a delayed onset, and early transcriptional changes are notably enriched for processes related to neuronal homeostasis and cytoskeletal regulation whereas longer exposure to type III IFNs induced relevant ISG expression such as *Isg15*, *Oas1a*, *Mx1*, and *Rsad2*. These findings suggest that the neuronal IFN-λ response has been evolutionarily tuned to balance robust intrinsic and innate immune response with the preservation of neuronal structural integrity, function, and homeostasis.

IFN-λ establishes cell-type-specific antiviral thresholds

In Chapter 3, I demonstrated that IFN-λ pretreatment (24 h prior to infection) confers potent protection against pseudorabies virus (PRV) infection in both fibroblasts and SCG neurons. In contrast, HSV-1 exhibited robust resistance to IFN-λ in neurons despite equivalent receptor expression and STAT1 activation, while remaining partially sensitive in fibroblasts. Using the well-characterized ICP34.5-deficient HSV-1 mutant virus, Δ34.5, I demonstrated that genetic deletion of this gene, renders HSV-1 acutely sensitive to neuronal IFN-λ pretreatment, similar to PRV. These results suggest that IFN-λ creates a two-tier antiviral barrier, acting quickly in fibroblasts, and with delayed but sustained efficacy in neurons, and that HSV-1 has evolved specific mechanisms to overcome the neuronal layer of this defense.

RSAD2 functions as a critical neuron-specific antiviral effector directly antagonized by HSV-1 ICP34.5

Chapter 4 identified RSAD2 as a central antiviral factor mediating IFN-λ restriction of αHVs in PNS neurons and defined the molecular basis by which HSV-1 overcomes this defense via ICP34.5-mediated antagonism. Transcriptomic analysis from Chapter 2 identified RSAD2 as the most highly upregulated ISG in neurons treated with IFN-λ for 24 h. Immunofluorescence microscopy and Western blot analysis further confirmed robust RSAD2 protein accumulation in both primary rat SCG neurons and human SK-N-SH neuroblastoma cells. RSAD2 localized to distinct punctate perinuclear structures consistent with ER-associated membranes, positioning it strategically at sites where αHVs undergo secondary envelopment.

Comparative infection studies showed that wild-type HSV-1 encoding ICP34.5 dramatically altered RSAD2's subcellular distribution, causing dispersal of perinuclear RSAD2 puncta throughout the cytoplasm and reducing total RSAD2 protein levels by 24 hpi. Neurons infected with ICP34.5-deficient HSV-1 mutant, Δ34.5, or pseudorabies virus (PRV) which also lacks the ICP34.5 homologue, maintained robust RSAD2 expression. Additionally, neurons infected with Δ34.5 demonstrated preserved contracted perinuclear localization of RSAD2 throughout infection (3 hpi and 24 hpi). In wild-type HSV-1 infections, ICP34.5 disrupted RSAD2's spatial organization and reversed its downstream functional consequences. RSAD2 activity induces sustained phosphorylation of eukaryotic translation initiation factor 2 alpha (eIF2α), triggering integrated stress responses and translational arrest that restrict viral late protein synthesis. ICP34.5 counteracts this defense by recruiting protein phosphatase 1 alpha (PP1α) to dephosphorylate eIF2α, restoring translational capacity and enabling productive viral replication despite RSAD2 presence.

RSAD2 was revealed to be a causal necessity for neuronal antiviral defense against αHV invasion by performing siRNA-mediated RSAD2 knockdown experiments in primary SCG neurons. RSAD2 depletion rescued replication of Δ34.5 viral titers in IFN-λ pretreated neurons. These loss-of-function studies establish RSAD2 as an essential component of neuronal immune response induced by type III IFNs.

These findings further reveal implications for αHV neurotropism and evolution. PRV, a varicellovirus that lacks ICP34.5 homologues, remains acutely sensitive to IFN-λ in neurons; however, HSV-1 (a simplexvirus) resists this defense. This suggests that acquisition of ICP34.5 represents a key evolutionary adaptation enabling simplexviruses to efficiently invade and

establish latency within the PNS. RSAD2 induces a coordinated antiviral checkpoint whereby its enzymatic activity and stress-induced translational arrest restrict viral replication. HSV-1's deployment of ICP34.5 to simultaneously dismantle this immune response highlights the selective pressure RSAD2 exerts on neurotropic herpesviruses.

IFN-λ activates local STAT1-specific signaling in axons

Chapter 5 revealed that IFN-λ establishes a spatially compartmentalized response, creating an immune barrier against αHV neuroinvasion at the mucosal epithelia-PNS junction. Using tri-chambers that physically separate neuronal cell bodies (S-compartment) from axons (N-compartment), I performed experiments applying IFN-λ locally in axons to differentiate the global response (whole neuron) from the local (axons). Live-cell microscopy and quantitative particle-tracking analyses demonstrated that IFN-λ -pretreated axons exhibited fewer viral particles retrogradely moving than untreated controls, with a measurable reduction in the percentage of particles moving within the first hour of infection. This transport restriction translated into a delayed productive infection phenotype: PRV180 fluorescence signal in cell bodies was delayed until 48 hpi, confirming that axonal IFN-λ exposure creates a functional barrier that limits the number of viral genomes reaching the cell body. In contrast, in epithelial cells, IFN-λ predominantly restricts viruses at the cell surface or within the cytoplasm to limit viral replication. The neuronal IFN-λ antiviral response exploits the extended axonal compartment to intercept and limit viral genomes before they reach the replication machinery in the cell body nucleus.

Immunofluorescence microscopy further demonstrated that IFN-λ treatment in axons induced accumulation of p-STAT1. To establish whether STAT1 phosphorylation is necessary

and sufficient for axonal IFN-λ-mediated retrograde transport restriction, a pharmacological STAT1 inhibitor, fludarabine, was utilized. Notably, when fludarabine was applied to the axonal N-compartment before local IFN-λ treatment and PRV180 infection, the antiviral protective effect of IFN-λ was inhibited, confirming that STAT1 axonal phosphorylation is essential for IFN-λ-mediated restriction of virion particle movement from the axon to the neuronal nucleus, functioning as a direct effector of the axonal antiviral state.

Future Directions

Comparative analysis of type I IFNs versus type III IFNs

Previously, a critical, but underexplored comparative question concerned whether type I and type III IFNs employ identical or distinct mechanisms to restrict nervous system virus infections. Given that Chapter 2 demonstrated neurons respond to IFN-λ with STAT1-dominant signaling, side-by-side kinetic analysis quantifying STAT1 phosphorylation during type I versus type III IFN treatment may assess its antiviral potency against HSV-1. Examining neurotoxicity and measuring endogenous interferon levels in infected PNS neurons via ELISA would determine whether IFN-λ's delayed kinetics represent an evolutionary trade-off favoring delayed, sustained protection over immediate maximal restriction. Additional studies may involve temporal dynamics of pSTAT1 accumulation through time-course experiments to identify therapeutic windows.

Defining the molecular interface between RSAD2 and ICP34.5

While this thesis confirms that ICP34.5 interferes with the accumulation and function of RSAD2, the precise molecular mechanism underlying this interaction remains unclear. Future research should aim to determine whether ICP34.5 directly interacts with RSAD2, affects the

stability of its 4Fe-4S cluster, influences the production of ddhCTP, or reorganizes ER-associated membrane domains. Employing structural and proteomic approaches will be crucial for elucidating the nature of this antagonism and understanding how ICP34.5 modulates RSAD2 activity at the molecular level.

Quantifying RSAD2 enzymatic activity in neurons

Measuring ddhCTP levels directly in primary neurons remains a major technical challenge due to their low abundance, rapid turnover, and the difficulty of extracting intact nucleotide pools from highly polarized cells [110]. Developing targeted metabolomic methods, especially LC-MS/MS techniques optimized for small-volume neuronal samples, would enable accurate quantification of ddhCTP and related intermediates [174]. Using these assays could further clarify whether RSAD2 activity in neurons mainly causes chain termination of viral RNA, modulates the integrated stress response through sensors like ZAK (known as MAPKKK20 or MLK7) or GCN2 (general control nonderepressible 2), or involves other neuron-specific metabolic pathways [175]. These measurements would provide vital evidence linking RSAD2 enzyme activity to functional antiviral effects in neurons and help determine if ddhCTP production uniquely contributes to neuronal intrinsic immunity.

Dissecting axonal IFN-λ signaling and its impact on αHV neuroinvasion

The findings presented in Chapter 5 establish that axonal IFN-λ signaling restricts retrograde virion movement via pSTAT1 accumulation in the axons; however, the precise molecular mechanism remains unanswered. Future studies must distinguish whether pSTAT1 directly interferes with dynein motor recruitment to viral capsids or if it affects the biophysical

properties of transported cargo. Proximity labeling approaches such as APEX2-tagged STAT1 expressed in primary neurons may enable an unbiased identification of proteins in close spatial proximity to axonal pSTAT1 during infection. To further confirm whether cargo transport is affected, mass spectrometry analysis of dynein motor components, such as the dynein light chains DYNLL1, would elucidate whether pSTAT1 directly disrupts αHV virion motor interactions.

Another question concerns whether ISGs are translated locally within axons and whether axonally synthesized antiviral proteins can contribute to the restriction of retrograde transport. Although Chapter 5 demonstrates that axonal accumulation of pSTAT1 occurs without nuclear translocation and is therefore independent of transcription at the level of STAT1 signaling, axons contain ribosomes, translation machinery, and mRNA granules that facilitate local protein synthesis from existing or locally transcribed mRNAs [176]. Determining whether RSAD2 or other ISGs are synthesized locally in axons would be fundamental to our understanding of compartmentalized neuronal immunity. Complementary single-molecule fluorescence in situ hybridization (RNAscope) can directly visualize ISG mRNAs within axonal compartments and quantify mRNA puncta density in axons versus the soma after IFN-λ treatment.

Concluding Remarks

The findings in this dissertation establish that type III interferons (IFN-λ) function as a critical immune factor linking mucosal epithelial immunity with intrinsic neuronal antiviral response, creating a spatially and temporally coordinated barrier against αHV neuroinvasion. At mucosal surfaces, IFN-λ is produced by infected epithelial cells and diffuses locally to prime the axon termini of sensory neurons that densely innervate these tissues. The localized IFN-λ

establishes an immediate, independent axonal checkpoint mediated by phosphorylated STAT1 (p-STAT1), restricting retrograde virion transport. This response enables neurons to elicit a potent immune defense at sites of viral entry.

Latency is influenced by multiple factors, including the multiplicity of infection (MOI), distance from infection site, and the timing and magnitude of host immune response [14, 60, 81]. A critical but often overlooked variable is the effective viral genome copy number that reaches the neuronal nucleus during primary infection. By restricting the efficiency of virion particle trafficking during retrograde transport, mucosal IFN-λ effectively reduces the MOI experienced by the neuronal nucleus, even when peripheral infection involves high viral titers. This may explain the paradox that most HSV-1 primary infections establish latency rather than cause neurological disease, despite replicating to high titers in epithelial tissues [13]. The mucosal-PNS interface, enriched in both IFN-λ-producing epithelial cells and IFN-λ-responsive axons, functions as a neurological barrier that permits infection while restricting its magnitude.

The ability of αHVs to overcome neuronal defenses fundamentally determines their fitness and capacity for lifelong persistence. HSV-1 and HSV-2, which encode ICP34.5, successfully navigate immune responses elicited by neurons during infection. ICP34.5 disrupts RSAD2's perinuclear localization, inhibits eIF2α phosphorylation to restore viral translation, and potentially interferes with axonal antiviral signaling, enabling productive infection and efficient latency establishment in PNS neurons. RSAD2 and ICP34.5 represent a critical evolutionary determinant of simplex virus neurotropism.

In contrast, pseudorabies virus (PRV), a veterinary varicellovirus, lacks ICP34.5 and remains highly sensitive to IFN-λ pretreatment, exhibiting impaired axonal transport, reduced

viral replication, and diminished neuroinvasion efficiency. This heightened sensitivity underscores a fundamental evolutionary divergence between simplexviruses and varicelloviruses in how neuronal immune barriers are encountered and overcome. While PRV (and possibly the human varicellovirus, varicella-zoster virus, VZV) has evolved alternative strategies to persist within the nervous system, these mechanisms appear less effective at neutralizing IFN-λ-mediated neuronal restriction during early infection and require further investigation. The acquisition of ICP34.5 thus represents a key evolutionary innovation that enhanced simplexvirus neurotropism and persistence in the face of robust mucosal and neuronal immune responses.

This dissertation highlights IFN-λ as a potent alternative to type I IFNs that prevents neuroinvasion during primary infection. By elucidating the molecular mechanisms that regulate the balance between viral persistence and neuronal restriction, it lays a foundation for advancing next-generation interventions to prevent neuroinvasion, decrease recurrent disease, and bolster neuron-intrinsic immunity against a family of pathogens that have co-evolved with humans.

Materials and Methods

Cells

Wild-type Rat2 cells were used as a fibroblast cell model (ATCC). The cells were cultured in Dulbecco Modified Eagle medium (DMEM) (Cytiva parent company Danaher Corporation, Washington, DC, USA), 1% penicillin-streptomycin (PS) (Cytiva parent company Danaher Corporation, Washington, DC, USA), and 10% fetal bovine serum (FBS) (Genessee, Burlington, MA, USA). Human dermal fibroblasts (HDFs) were obtained from the Nir Drayman Laboratory (University of California, Irvine) and grown in DMEM, 1% PS, and 10% FBS. Porcine kidney epithelial cell line (PK15) was grown in DMEM, 1% PS, and 5% FBS. Human Dermal Fibroblasts (HDFs) were acquired from the Bert Semler Laboratory (University of California, Irvine) and grown in DMEM, 1% PS, and 20% FBS. The Nir Drayman lab (University of California, Irvine) provided the human neuroblastoma cell line, SK-N-SH cells, grown in DMEM, 1% PS, and 20% FBS.

Immunofluorescent staining

Primary superior cervical ganglion (SCG) neurons were cultured on poly-D-lysine– and laminin-coated glass coverslips and processed for immunofluorescence following the experimental treatments described in each figure. Neuronal cells and SK-N-SH cells were fixed in 4% paraformaldehyde (Electron Microscopy Sciences, Hatfield, PA, USA) for 15 minutes at room temperature, washed three times in PBS, permeabilized with Methanol for 5 minutes at -20C, and blocked in 5% BSA in PBS for 1 hour. Primary antibodies were diluted in blocking buffer and incubated overnight at 4°C, including anti-RSAD2 (Invitrogen, Waltham, MA, USA; 1:500), anti-pSTAT1 (Cell Signaling Technology, Danvers, MA, USA; 1:200), anti-pSTAT2 (Millipore Sigma, Burlington, MA, USA; 1:200), and when applicable, anti-gC (Abcam,

Cambridge, UK; 1:300). Following primary incubation, cells were washed in PBS and incubated with Alexa Fluor-conjugated goat anti-mouse or goat anti-rabbit secondary antibodies (Thermo Fisher Scientific, Waltham, MA, USA; 1:500) for 1 hour at room temperature. Nuclei were stained with DAPI (1 μg/mL) for 1 h at RT, along with secondary antibodies at 1:1000, and coverslips were mounted using Polygel mountant (Thermo Fisher Scientific). Confocal images were acquired using a Leica microscope with 20X or 63X oil-immersion objectives under consistent settings for each comparison. Image analysis was performed using standardized thresholding and background subtraction to ensure uniform quantification across samples.

Interferon treatment

Recombinant rat IFN-λ2 (200 ng/mL) was added directly to neuronal cultures or rat epithelial cell lines for 24 hours prior to infection or 1 h post-infection (VWR, Radnor, PA, USA). SK-N-SH cells were treated with human IFN-λ2 (200 ng/mL, 24 h) (Thermo Fisher, Waltham, MA, USA).

Primary Neuronal Culture

Superior cervical ganglion (SCG) in Campenot tri-chambers were used for all primary neuronal cultures 35mm tissue culture dishes (Corning, Corning, NR, USA) were coated with poly-DL-ornithine (Millipore Sigma, Burlington, MA, USA) and mouse laminin (Life Technologies Carlsbad, CA, USA) to promote neuronal adherence. SCG were isolated from 16- or 17-day Sprague Dawley rat embryos (Jackson Laboratories, Bar Harbor, MA, USA), as described by Curanovic et al. [104]. Tri-chambers were attached to coated 35 mm dishes with autoclaved silicone grease. The chambered dishes were filled with neurobasal medium (Gibco, Billings, MT, USA) + 50X B-27 supplement (Gibco, Billings, MT, USA) + 100X Penicillin-Streptomycin-Glutamine (Gibco, Billings, MT, USA) + 1000X murine nerve growth factor

(Gibco, Billings, MT, USA). SCG were seeded in the S-compartments of the chambers. SCG were also seeded in the S-compartments of the chambers or in 12-well plates. After two days, 1 μM Cytosine β-D-arabinofuranoside (Ara-C, Millipore Sigma, Burlington, MA, USA) was added to select against any mitotic cells. Two days after Ara-C addition, the medium was removed from chambers and replaced with fresh neuronal medium. Neuronal medium was changed every five to seven days. All animal work was performed in accordance with the Institutional Animal Care and Use Committee of the University of California, Irvine Research Board under protocol; AUP-21-008.

Real-Time qPCR

Neuronal cell bodies were collected from the S compartment of 3–5 chambers and total RNA was extracted using RNeasy Mini-Kit (Qiagen, Hilden, Germany) for both neurons and Rat2 cells. cDNA synthesis was carried out using SuperScript III (Life Technologies Carlsbad, CA, USA) first-strand synthesis kit with an oligo(dT) primer. A 96-well Type I IFN array (BioRad Laboratories, Hercules, CA, USA) containing 86 genes commonly induced by type I IFNs was performed in duplicate using neuronal cDNA. Kapa Sybr Fast qPCR (Roche Holding AG, Basel, Switzerland) master mix was prepared for RT-qPCR using Bio-Rad and Applied Biosystems RT-qPCR Thermocycler. Amplification was performed using the following conditions: 95 °C for 3 min, 40 cycles of 95 °C, 3 s, and 60 °C, 30 s. Following RT-qPCR of type I IFN array replicates, only 80 genes were analyzed using comparative Ct analysis. The following genes were not included in data analysis as they did not consistently pass the thresholds in replicate: Nos2, Socs1, Il10, Ccl5, Tnfsf10. GAPDH was used as the housekeeping gene to normalize Type I IFN array data.

Of these 80 genes, 22 genes of interest were chosen for the following analysis based on their normalized gene expression. Triplicates were prepared and fold changes were calculated using the comparative Ct method (2^{-ddCt}) normalized to GAPDH in treated and untreated samples of both primary neurons and Rat2 cells. Primers were ordered from Integrated DNA Technologies (IDT, Coralville, IA, USA), as shown below in Table 1.

Gene	Forward Primer	Reverse Primer
Actb	CGTCCACCCGCGAGTACAACC	CGACGACGAGCGCAGCGATATCG
CCL2	GCTAATGCATCCACTCTC	GTTTAACATTACTTAAGGC
Cd38	GCGTAGTCTTCATTGGTGATG	CGCTGACATCATCTTGGGACGC
Cd69	CGCAGTCTACAGAAGCAAC	GACTGAAACACTGGATTGGGC
Crp	GGGGCAGGAGCAGGACTCG	CATAGACTGCATTGATCTG
Cxcl10	GGCTTCCCAATTCTCTAAGAGC	GAGCAGGCTGGGGCATGGC
Gapdh	GCAACAATGTCCACTTTGTC	GCCTGGTTACCAGGGCTGC
Ifit1	CGCTACGCAGCCAAGTATTTCC	CTGTTGCTTGTAACAGAGCCC
Ifit2	GCTGAGTGCTTTGACACAGC	GCTCTCCAATGATTCCTTAC
Ifit3	GCAACTGCAGAATACAGG	CTTATTCATGTACTCCATAG
Ifitm3	CCCCCAGTGGCAGCGTTCACG	GAACAGTCCGACAGAGCC
Ifna1	GCCAGTAGGGAGTCTTCCTGG	GCTTGGGATGCAACCCTCC
Irf9	CCAACCTGCCACTCTCGC	CCTTGCACTTTCTCTTGGCC
Isg15	GGTCCCCTGAAACTAAGG	GCTGACCCAGTGAGTCTCTC
Jak1	CGAAGGCAGAAACTCCATG	CGGAACCTCTACCACGAGAAC
Oas1a	CGAATGTATCTCCCTGGGG	GCATAGACCGTGAGCAGC
Oas1b	GCGCCAATTCAGGAAGTACAGC	CCCAACCCACAATTCTACG
Oas2	GGTGATGATCGATGTGCTG	CTGGTCTTGGAACTGTTTG
Stat1	GCATTTAAAGTCATATTCATC	CCGTGATGTTAGATAAAC
Stat2	GGAGTGGGTGGGAAACGGG	GCAACATCTCCCACTGCGCC
Stat3	GCAGGAATCGGCTATACTGC	CCTGGCGCCTTGGATTGAGAGC
Tlr7	GGACTTCTTCAAGAATCTGC	GGCTAAGGAGAGAGTCGTTAG

Table 1. Primer sequences of genes of interest.

In addition to host gene expression analyses, viral transcription was quantified using primer sets designed for immediate-early, early, and late α-herpesvirus genes. Primers were obtained from Integrated DNA Technologies (IDT, Coralville, IA, USA) and optimized for amplification of HSV-1 ICP27 (immediate-early), HSV-1 ICP8 (early), and HSV-1 gC (late), as well as PRV IE180 (immediate-early), PRV UL54 (early), and PRV UL5 (late). SCG neuronal cell bodies were collected from cultures pre-treated with rat IFN-λ2 (200 ng/mL, 24 h) and subsequently infected with HSV-1 (OK14, Δ34.5, or 34.5R) or PRV (PRV-180). RNA isolation, cDNA synthesis, and qPCR amplification were performed as described above, and viral transcript abundance was calculated using the comparative Ct method ($2^{-\Delta\Delta Ct}$) normalized to GAPDH. These primer sets enabled precise quantification of stage-specific viral gene expression in IFN-λ-primed neurons, as shown below in Table 2.

Gene	Forward Primer	Reverse Primer
Gapdh	GCAACAATGTCCACTTTGTC	GCCTGGTTACCAGGGCTGC
gC	AAGACGTTCACCAAGCTGCT	CAGATCCACGCCCTTGATGA
ICP27	GCATCTTCGTGTTTGTCATTCTG	GCATCTTCTCTCCGACCCCG
ICP8	GTCGTTACCGAGGGCTTCAA	GTTACCTTGTCCGAGCCTCC
IE180	CATCGTGCTGGACACCATCGAG	ACGTAGACGTGGTAGTCCCCCA
Ifit1	CGCTACGCAGCCAAGTATTTCC	CTGTTGCTTGTAACAGAGCCC
Oas1a	CGAATGTATCTCCCTGGGG	GCATAGACCGTGAGCAGC
RSAD2	CCCTTGGCCACGACCAATG	CCGAGAGAGATGGTTCAAGG
UL5	TGGACATGGCCACCTACGT	ACCGCGCGATGGTCAT
UL54	TGCAGCTACACCCTCGTCC	TCAAAACAGGTGGTTGCAGTAAA

Table 2. Primer sequences for genes expressed during viral infection in SCGs.

RNA Isolation for RNA-Sequencing

Total RNA for RNA-sequencing was isolated from primary SCG neurons and Rat2 fibroblasts using the RNeasy Mini Kit (Qiagen, Hilden, Germany), following the manufacturer's column-based protocol to ensure high-purity RNA suitable for downstream library preparation. For neuronal samples, cell bodies from 2 wells of a 12-well plate were lysed directly in RLT buffer supplemented with β-mercaptoethanol. Rat2 cells were harvested from culture dishes and similarly lysed in RLT buffer. Lysates were homogenized using spin columns (Qiagen) prior to column binding. Genomic DNA contamination was removed using on-column RNase-free DNase I digestion (Qiagen) according to the manufacturer's guidelines. Samples were washed and eluted in nuclease-free water, snap-frozen, and stored at -20°C until quality assessment. Only samples with RNA integrity numbers (RIN) suitable for library preparation were submitted for sequencing. All RNA isolations were performed in RNase-free conditions, and all neuronal samples were processed in parallel to minimize batch effects during downstream transcriptomic analyses.

siRNA Knockdown of RSAD2 in SCG Neurons

RSAD2 knockdown was performed using rat RSAD2-specific siRNA delivered via siMagnetofection, optimized for primary neuron transfection (OzBiosciences, San Diego, CA, USA). Neurons were treated with either RSAD2 siRNA or a non-targeting (NT) control siRNA according to the manufacturer's instructions at 1uM (Horizon Discovery, Cambridge, UK). After 48 hours, knockdown efficiency was validated via immunoblotting. Protein lysates were collected in RIPA buffer supplemented with protease and phosphatase inhibitors, quantified using a BCA assay, and resolved by SDS-PAGE. Membranes were probed with antibodies against anti-RSAD2 (1:5000) (Invitrogen, Waltham, MA, USA) and SNAP25 (1:2000) (loading control) (Cell Signaling Technology, Danvers, MA, USA). Band intensities were quantified in

ImageJ and normalized to SNAP25. SCGs were infected with HSV-1 Δ34.5 or 34.5R at a multiplicity of infection (MOI) of 10 for 24 hours prior to harvest.

Statistical Analysis

All graphical analyses were conducted in *GraphPad Prism*. An unpaired Student's *t* test was used as indicated. Additionally, one-way analysis of variance (ANOVA) was applied, where variance homogeneity could not be assumed; Brown-Forsythe and Welch ANOVA tests were used. Upon significance, Games-Howell post hoc tests were applied for multiple comparisons. Data are presented as mean ± SEM. Statistical significance thresholds were defined as follows: ns, not significant; *, $p < 0.05$; **, $p < 0.005$, ***, $p < 0.0005$; ****, $p < 0.00005$.

Western Blot Analysis

Cell lysates were prepared using RIPA-light buffer including 1 mM Dithiothreitol (DTT) and a protease inhibitor cocktail (Roche Holding AG, Basel, Switzerland). Following 30 min incubation on ice and sonication, cells were pelleted, and the supernatant was placed in a new tube with 5X Laemmli buffer before boiling at 95 °C. Immunoblotting was performed using anti-Beta-actin (1:10,000) (Millipore Sigma, Burlington, MA, USA), anti-pSTAT1 (1:2000) (Cell Signaling Technology, Danvers, MA, USA), anti-pSTAT2 (1:2000) (Millipore Sigma, Burlington, MA, USA), anti-Oas1 (1:2000) (Proteintech, Rosemont, IL, USA), anti-IFIT1 (1:2000) (Life Technologies Carlsbad, CA, USA), and anti-IRF9 (1:2000) (Proteintech, Rosemont, IL, USA). Immunoblotting was also performed using anti-p-eIF2α (1:2000) (Cell Signaling Technology, Danvers, MA, USA), anti-SNAP25 (1:2000) (Cell Signaling Technology, Danvers, MA, USA), anti-RSAD2 (Invitrogen, Waltham, MA, USA), anti-ICP4 (Abcam, Cambridge, UK), anti-ICP8 (Abcam, Cambridge, UK), and anti-gC (Abcam, Cambridge, UK).

Secondary mouse or rabbit antibodies (Millipore Sigma, Burlington, MA, USA, 1:5000) were used following primary antibody incubation.

Viruses

All HSV-1 or PRV strains were propagated and titered by plaque assay on Vero or PK15 cells, respectively, in DMEM supplemented with 2% FBS and 1% penicillin-streptomycin. PRV-Becker is a wild-type laboratory strain [177]. PRV-180 expresses mRFP1-VP26 in a PRV-Becker background [108]. OK14 was sourced from the Lynn Enquist Laboratory at Princeton University and confirmed through whole-genome analysis. HSV-1 OK14, which expresses an mRFP-VP26 capsid tag, was previously described [79]. HSV-1 Δ34.5 and 34.5R were obtained from the Nir Drayman Laboratory (University of California, Irvine). Δ34.5, originally known as *17terma*, has been previously described along with its revertant, 34.5R, respectively [134, 136]. Viral titers were measured in PK15 cells (after PRV infection) or Vero cells (after HSV-1 infection) after infecting epithelial or neuronal cells with the mentioned viral strains, respectively.

Acknowledgments and Author Contributions

The work in Chapter 1 was contributed to by individuals in the Orkide Koyuncu Laboratory at UCI. Khanh T. Y. Luong and Dr. Orkide O. Koyuncu helped with conceptualization, writing, review, and editing during the preparation of this chapter. Portions of the text and Figure 1.2 were taken from Salazar, S., Luong, K.T.Y., Koyuncu, O.O. (2023). Cell Intrinsic Determinants of Alpha Herpesvirus Latency and Pathogenesis in the Nervous System, *Viruses*. Figures 1.1 and 1.3 were adapted from Aryal, S. (2022). Herpes Simplex Virus 1 (HSV-1). Microbe Notes. Retrieved from https://microbenotes.com/herpes-simplex-virus-1-hsv-1/ and [110], K.J., et al. (2015), respectively.

The work in Chapter 2 was contributed to by multiple individuals across laboratories and facilities at UCI. From UCI, Dr. Orkide O. Koyuncu helped with conceptualization, investigation, data acquisition and analysis, supervision, writing, review, and editing. Khanh T. Y. Luong and Audrey D. Loaiza contributed to investigation and data acquisition during the preparation of this chapter. Additional contributions were provided by Dr. Nir Drayman, who helped with conceptualization, investigation, and data interpretation. Dillon Cheng, the Drayman laboratory manager, assisted in the preparation of RNA sequencing libraries, and Melanie Oakes, head of the UCI Genomics Core, supervised and performed the RNA sequencing of the samples. Portions of this chapter were taken from Salazar, S., Luong, K. T. Y., Nua, T., & Koyuncu, O. O. (2023). Interferon-λ Activates a Differential Response in Peripheral Neurons That Is Effective against Alpha Herpesvirus Infections, *Pathogens*.

The work in Chapter 3 was contributed to by multiple individuals across laboratories. Dr. Orkide O. Koyuncu helped with conceptualization, supervision, writing, review, and editing. Dr. Nir Drayman provided additional support through the contribution of the HDF cell line and the

HSV-1 Δ34.5 and 34.5R viruses used in this chapter. The Bert Semler laboratory provided the SK-N-SH cell line used in the experimental work. Further contributions were made by Khanh T. Y. Luong and Audrey D. Loaiza, who assisted with investigation and data acquisition during the preparation of this chapter. Relevant figures and text were taken from Salazar, S., Luong, K. T. Y., Nua, T., & Koyuncu, O. O. (2023). Interferon-λ Activates a Differential Response in Peripheral Neurons That Is Effective against Alpha Herpesvirus Infections, *Pathogen.*

The work in Chapters 4 and 5 was contributed to by multiple individuals across laboratories at UCI. Dr. Orkide O. Koyuncu contributed extensively to the conceptualization of these studies and to the writing, review, and editing of these chapters. Khanh T. Y. Luong and Audrey D. Loaiza supported the investigation and data collection, ensuring comprehensive and accurate results. Dr. Nir Drayman also contributed valuable materials to the study, including the gC antibody used for the western blot assays and immunofluorescence staining described in these chapters.

The work in Chapter 6 was contributed to by multiple individuals at UCI. Dr. Orkide O. Koyuncu played a key role in conceptualizing the study and in writing, reviewing, and editing the chapter. Audrey D. Loaiza and Khanh T. Y. Luong assisted with investigation and data acquisition during the preparation of this chapter.

This work was primarily funded by the National Institutes of Health (NIH): NIH-IMSD GM055246, NIAID R21 AI144492, and NIAID R01 A1185349. Additional funding and support came from the UCI Virology training grant T32 A1007319 and the Neuroimmunology training grant T32 AG081185.

References

1. Koyuncu, O.O., I.B. Hogue, and L.W. Enquist, *Virus infections in the nervous system.* Cell Host Microbe, 2013. **13**(4): p. 379-93.
2. Kramer, T. and L.W. Enquist, *Directional spread of alphaherpesviruses in the nervous system.* Viruses, 2013. **5**(2): p. 678-707.
3. Rosato, P.C. and D.A. Leib, *Neurons versus herpes simplex virus: the innate immune interactions that contribute to a host-pathogen standoff.* Future Virol, 2015. **10**(6): p. 699-714.
4. Szpara, M.L., O. Kobiler, and L.W. Enquist, *A common neuronal response to alphaherpesvirus infection.* J Neuroimmune Pharmacol, 2010. **5**(3): p. 418-27.
5. Card, J.P., et al., *Pseudorabies virus infection of the rat central nervous system: ultrastructural characterization of viral replication, transport, and pathogenesis.* J Neurosci, 1993. **13**(6): p. 2515-39.
6. Zerboni, L., et al., *Molecular mechanisms of varicella zoster virus pathogenesis.* Nat Rev Microbiol, 2014. **12**(3): p. 197-210.
7. Dempsher, J., et al., *Physiological changes in sympathetic ganglia infected with pseudorabies virus.* Am J Physiol, 1955. **182**(1): p. 203-16.
8. Ugolini, G., *Rabies virus as a transneuronal tracer of neuronal connections.* Adv Virus Res, 2011. **79**: p. 165-202.
9. Agelidis, A.M. and D. Shukla, *Cell entry mechanisms of HSV: what we have learned in recent years.* Future Virol, 2015. **10**(10): p. 1145-1154.
10. Lomonte, P., *Herpesvirus Latency: On the Importance of Positioning Oneself.* Adv Anat Embryol Cell Biol, 2017. **223**: p. 95-117.
11. Cliffe, A.R. and A.C. Wilson, *Restarting Lytic Gene Transcription at the Onset of Herpes Simplex Virus Reactivation.* J Virol, 2017. **91**(2).
12. Maroui, M.A., et al., *Latency Entry of Herpes Simplex Virus 1 Is Determined by the Interaction of Its Genome with the Nuclear Environment.* PLoS Pathog, 2016. **12**(9): p. e1005834.
13. Wilson, A.C. and I. Mohr, *A cultured affair: HSV latency and reactivation in neurons.* Trends Microbiol, 2012. **20**(12): p. 604-11.
14. Decman, V., et al., *Immune control of HSV-1 latency.* Viral Immunol, 2005. **18**(3): p. 466-73.
15. Chew, T., K.E. Taylor, and K.L. Mossman, *Innate and adaptive immune responses to herpes simplex virus.* Viruses, 2009. **1**(3): p. 979-1002.
16. Delhaye, S., et al., *Neurons produce type I interferon during viral encephalitis.* Proc Natl Acad Sci U S A, 2006. **103**(20): p. 7835-40.
17. De Regge, N., et al., *Interferon alpha induces establishment of alphaherpesvirus latency in sensory neurons in vitro.* PLoS One, 2010. **5**(9).
18. Danastas, K., et al., *Interferon inhibits the release of herpes simplex virus-1 from the axons of sensory neurons.* mBio, 2023: p. e0181823.
19. Hu, Q., et al., *JAK/STAT pathway: Extracellular signals, diseases, immunity, and therapeutic regimens.* Front Bioeng Biotechnol, 2023. **11**: p. 1110765.
20. Walker, F.C., P.R. Sridhar, and M.T. Baldridge, *Differential roles of interferons in innate responses to mucosal viral infections.* Trends Immunol, 2021. **42**(11): p. 1009-1023.

21. Lazear, H.M., J.W. Schoggins, and M.S. Diamond, *Shared and Distinct Functions of Type I and Type III Interferons.* Immunity, 2019. **50**(4): p. 907-923.
22. Philip, D.T., et al., *Interferon lambda restricts herpes simplex virus skin disease by suppressing neutrophil-mediated pathology.* mBio, 2024: p. e0262323.
23. Arnold, K.A., et al., *JAK Signaling Is Critically Important in Cytokine-Induced Viral Susceptibility of Keratinocytes.* Int J Mol Sci, 2023. **24**(11).
24. Pino-Belmar, C., et al., *An Intrinsic Host Defense against HSV-1 Relies on the Activation of Xenophagy with the Active Clearance of Autophagic Receptors.* Cells, 2024. **13**(15).
25. Bolen, C.R., et al., *Dynamic expression profiling of type I and type III interferon-stimulated hepatocytes reveals a stable hierarchy of gene expression.* Hepatology, 2014. **59**(4): p. 1262-72.
26. Dickensheets, H., et al., *Interferon-lambda (IFN-lambda) induces signal transduction and gene expression in human hepatocytes, but not in lymphocytes or monocytes.* J Leukoc Biol, 2013. **93**(3): p. 377-85.
27. Erttmann, S.F., et al., *The gut microbiota prime systemic antiviral immunity via the cGAS-STING-IFN-I axis.* Immunity, 2022. **55**(5): p. 847-861 e10.
28. Broggi, A., et al., *Type III interferons disrupt the lung epithelial barrier upon viral recognition.* Science, 2020. **369**(6504): p. 706-712.
29. Salazar, S., et al., *Interferon-lambda Activates a Differential Response in Peripheral Neurons That Is Effective against Alpha Herpesvirus Infections.* Pathogens, 2023. **12**(9).
30. Hinson, E.R. and P. Cresswell, *The N-terminal amphipathic alpha-helix of viperin mediates localization to the cytosolic face of the endoplasmic reticulum and inhibits protein secretion.* J Biol Chem, 2009. **284**(7): p. 4705-12.
31. Honarmand Ebrahimi, K., et al., *ddhCTP produced by the radical-SAM activity of RSAD2 (viperin) inhibits the NAD(+) -dependent activity of enzymes to modulate metabolism.* FEBS Lett, 2020. **594**(10): p. 1631-1644.
32. Grunkemeyer, T.J., et al., *The antiviral enzyme viperin inhibits cholesterol biosynthesis.* J Biol Chem, 2021. **297**(1): p. 100824.
33. Jones, C., *Herpes simplex virus type 1 and bovine herpesvirus 1 latency.* Clin Microbiol Rev, 2003. **16**(1): p. 79-95.
34. Kuny, C.V. and M.L. Szpara, *Alphaherpesvirus Genomics: Past, Present and Future.* Curr Issues Mol Biol, 2021. **42**: p. 41-80.
35. Kinchington, P.R., et al., *Herpes simplex virus and varicella zoster virus, the house guests who never leave.* Herpesviridae, 2012. **3**(1): p. 5.
36. Roizman, B. and G. Campadelli-Fiume, *Alphaherpes viral genes and their functions*, in *Human Herpesviruses: Biology, Therapy, and Immunoprophylaxis*, A. Arvin, et al., Editors. 2007: Cambridge.
37. Pomeranz, L.E., A.E. Reynolds, and C.J. Hengartner, *Molecular biology of pseudorabies virus: impact on neurovirology and veterinary medicine.* Microbiol Mol Biol Rev, 2005. **69**(3): p. 462-500.
38. Norberg, P., et al., *A genome-wide comparative evolutionary analysis of herpes simplex virus type 1 and varicella zoster virus.* PLoS One, 2011. **6**(7): p. e22527.
39. Stempel, M., B. Chan, and M.M. Brinkmann, *Coevolution pays off: Herpesviruses have the license to escape the DNA sensing pathway.* Med Microbiol Immunol, 2019. **208**(3-4): p. 495-512.

40. Gray, W.L., *Comparative Analysis of the Simian Varicella Virus and Varicella Zoster Virus Genomes.* Viruses, 2022. **14**(5).
41. Grinde, B., *Herpesviruses: latency and reactivation - viral strategies and host response.* J Oral Microbiol, 2013. **5**.
42. Honess, R.W. and B. Roizman, *Regulation of herpesvirus macromolecular synthesis. I. Cascade regulation of the synthesis of three groups of viral proteins.* J Virol, 1974. **14**(1): p. 8-19.
43. Simpson, S.A., et al., *Nectin-1/HveC Mediates herpes simplex virus type 1 entry into primary human sensory neurons and fibroblasts.* J Neurovirol, 2005. **11**(2): p. 208-18.
44. Richart, S.M., et al., *Entry of herpes simplex virus type 1 into primary sensory neurons in vitro is mediated by Nectin-1/HveC.* J Virol, 2003. **77**(5): p. 3307-11.
45. Spear, P.G. and R. Longnecker, *Herpesvirus entry: an update.* J Virol, 2003. **77**(19): p. 10179-85.
46. Hafezi, W., et al., *Entry of herpes simplex virus type 1 (HSV-1) into the distal axons of trigeminal neurons favors the onset of nonproductive, silent infection.* PLoS Pathog, 2012. **8**(5): p. e1002679.
47. Hilterbrand, A.T., R.E. Daly, and E.E. Heldwein, *Contributions of the Four Essential Entry Glycoproteins to HSV-1 Tropism and the Selection of Entry Routes.* mBio, 2021. **12**(2).
48. Manoj, S., et al., *Mutations in herpes simplex virus glycoprotein D that prevent cell entry via nectins and alter cell tropism.* Proc Natl Acad Sci U S A, 2004. **101**(34): p. 12414-21.
49. Lathe, R. and J.G. Haas, *Distribution of cellular HSV-1 receptor expression in human brain.* J Neurovirol, 2017. **23**(3): p. 376-384.
50. Cooper, R.S. and E.E. Heldwein, *Herpesvirus gB: A Finely Tuned Fusion Machine.* Viruses, 2015. **7**(12): p. 6552-69.
51. Smith, G., *Herpesvirus transport to the nervous system and back again.* Annu Rev Microbiol, 2012. **66**: p. 153-76.
52. Musarrat, F., V. Chouljenko, and K.G. Kousoulas, *Cellular and Viral Determinants of HSV-1 Entry and Intracellular Transport towards Nucleus of Infected Cells.* J Virol, 2021. **95**(7).
53. Wysocka, J. and W. Herr, *The herpes simplex virus VP16-induced complex: the makings of a regulatory switch.* Trends Biochem Sci, 2003. **28**(6): p. 294-304.
54. Harkness, J.M., M. Kader, and N.A. DeLuca, *Transcription of the herpes simplex virus 1 genome during productive and quiescent infection of neuronal and nonneuronal cells.* J Virol, 2014. **88**(12): p. 6847-61.
55. Roizman, B., *The checkpoints of viral gene expression in productive and latent infection: the role of the HDAC/CoREST/LSD1/REST repressor complex.* J Virol, 2011. **85**(15): p. 7474-82.
56. Cliffe, A.R. and D.M. Knipe, *Herpes simplex virus ICP0 promotes both histone removal and acetylation on viral DNA during lytic infection.* J Virol, 2008. **82**(24): p. 12030-8.
57. Lilley, C.E., et al., *Multiple immediate-early gene-deficient herpes simplex virus vectors allowing efficient gene delivery to neurons in culture and widespread gene delivery to the central nervous system in vivo.* J Virol, 2001. **75**(9): p. 4343-56.
58. Pesola, J.M., et al., *Herpes simplex virus 1 immediate-early and early gene expression during reactivation from latency under conditions that prevent infectious virus production.* J Virol, 2005. **79**(23): p. 14516-25.

59. Zhu, S. and A. Viejo-Borbolla, *Pathogenesis and virulence of herpes simplex virus.* Virulence, 2021. **12**(1): p. 2670-2702.
60. Roizman, B. and R.J. Whitley, *An inquiry into the molecular basis of HSV latency and reactivation.* Annu Rev Microbiol, 2013. **67**: p. 355-74.
61. Smith, S., et al., *Structure of the herpes simplex virus 1 genome: manipulation of nicks and gaps can abrogate infectivity and alter the cellular DNA damage response.* J Virol, 2014. **88**(17): p. 10146-56.
62. Hogue, I.B., et al., *Cellular mechanisms of alpha herpesvirus egress: live cell fluorescence microscopy of pseudorabies virus exocytosis.* PLoS Pathog, 2014. **10**(12): p. e1004535.
63. Mateo, J., et al., *DNA-Repair Defects and Olaparib in Metastatic Prostate Cancer.* N Engl J Med, 2015. **373**(18): p. 1697-708.
64. Scanlan, H., et al., *Herpes simplex virus 1 as an oncolytic viral therapy for refractory cancers.* Front Oncol, 2022. **12**: p. 940019.
65. Alandijany, T., *Host Intrinsic and Innate Intracellular Immunity During Herpes Simplex Virus Type 1 (HSV-1) Infection.* Front Microbiol, 2019. **10**: p. 2611.
66. Verzosa, A.L., et al., *Herpes Simplex Virus 1 Infection of Neuronal and Non-Neuronal Cells Elicits Specific Innate Immune Responses and Immune Evasion Mechanisms.* Front Immunol, 2021. **12**: p. 644664.
67. Goldstein, M.E. and M.A. Scull, *Modeling Innate Antiviral Immunity in Physiological Context.* J Mol Biol, 2022. **434**(6): p. 167374.
68. Boo, K.H. and J.S. Yang, *Intrinsic cellular defenses against virus infection by antiviral type I interferon.* Yonsei Med J, 2010. **51**(1): p. 9-17.
69. Duggal, N.K. and M. Emerman, *Evolutionary conflicts between viruses and restriction factors shape immunity.* Nat Rev Immunol, 2012. **12**(10): p. 687-95.
70. Bieniasz, P.D., *Intrinsic immunity: a front-line defense against viral attack.* Nat Immunol, 2004. **5**(11): p. 1109-15.
71. Verhelst, J., P. Hulpiau, and X. Saelens, *Mx proteins: antiviral gatekeepers that restrain the uninvited.* Microbiol Mol Biol Rev, 2013. **77**(4): p. 551-66.
72. Calderon, B.M. and G.L. Conn, *A human cellular noncoding RNA activates the antiviral protein 2'-5'-oligoadenylate synthetase 1.* J Biol Chem, 2018. **293**(41): p. 16115-16124.
73. Olagnier, D. and J. Hiscott, *Type I and type III interferon-induced immune response: it's a matter of kinetics and magnitude.* Hepatology, 2014. **59**(4): p. 1225-8.
74. Barragan-Iglesias, P., et al., *Type I Interferons Act Directly on Nociceptors to Produce Pain Sensitization: Implications for Viral Infection-Induced Pain.* J Neurosci, 2020. **40**(18): p. 3517-3532.
75. Yordy, B., et al., *A neuron-specific role for autophagy in antiviral defense against herpes simplex virus.* Cell Host Microbe, 2012. **12**(3): p. 334-45.
76. Low-Calle, A.M., J. Prada-Arismendy, and J.E. Castellanos, *Study of interferon-beta antiviral activity against Herpes simplex virus type 1 in neuron-enriched trigeminal ganglia cultures.* Virus Res, 2014. **180**: p. 49-58.
77. Al-khatib, K., et al., *The murine double-stranded RNA-dependent protein kinase PKR and the murine 2',5'-oligoadenylate synthetase-dependent RNase L are required for IFN-beta-mediated resistance against herpes simplex virus type 1 in primary trigeminal ganglion culture.* Virology, 2003. **313**(1): p. 126-35.

78. Carr, D.J., et al., *Astrocyte-targeted expression of IFN-alpha1 protects mice from acute ocular herpes simplex virus type 1 infection.* J Immunol, 1998. **161**(9): p. 4859-65.
79. Song, R., et al., *Two Modes of the Axonal Interferon Response Limit Alphaherpesvirus Neuroinvasion.* mBio, 2016. **7**(1): p. e02145-15.
80. Koyuncu, O.O., et al., *Compartmented neuronal cultures reveal two distinct mechanisms for alpha herpesvirus escape from genome silencing.* PLoS Pathog, 2017. **13**(10): p. e1006608.
81. Koyuncu, O.O., et al., *The number of alphaherpesvirus particles infecting axons and the axonal protein repertoire determines the outcome of neuronal infection.* mBio, 2015. **6**(2).
82. Guo, F., et al., *Autophagy in neurodegenerative diseases: pathogenesis and therapy.* Brain Pathol, 2018. **28**(1): p. 3-13.
83. Chun, Y. and J. Kim, *Autophagy: An Essential Degradation Program for Cellular Homeostasis and Life.* Cells, 2018. **7**(12).
84. Maday, S. and E.L. Holzbaur, *Compartment-Specific Regulation of Autophagy in Primary Neurons.* J Neurosci, 2016. **36**(22): p. 5933-45.
85. Young, J.E., R.A. Martinez, and A.R. La Spada, *Nutrient deprivation induces neuronal autophagy and implicates reduced insulin signaling in neuroprotective autophagy activation.* J Biol Chem, 2009. **284**(4): p. 2363-73.
86. Alexander, D.E. and D.A. Leib, *Xenophagy in herpes simplex virus replication and pathogenesis.* Autophagy, 2008. **4**(1): p. 101-3.
87. Orvedahl, A., et al., *HSV-1 ICP34.5 confers neurovirulence by targeting the Beclin 1 autophagy protein.* Cell Host Microbe, 2007. **1**(1): p. 23-35.
88. Tran, S., W.D. Fairlie, and E.F. Lee, *BECLIN1: Protein Structure, Function and Regulation.* Cells, 2021. **10**(6).
89. Leib, D.A., et al., *Interaction of ICP34.5 with Beclin 1 modulates herpes simplex virus type 1 pathogenesis through control of CD4+ T-cell responses.* J Virol, 2009. **83**(23): p. 12164-71.
90. Alexander, D.E., et al., *Analysis of the role of autophagy in replication of herpes simplex virus in cell culture.* J Virol, 2007. **81**(22): p. 12128-34.
91. Liu, X., et al., *Disassembly of the TRIM23-TBK1 Complex by the Us11 Protein of Herpes Simplex Virus 1 Impairs Autophagy.* J Virol, 2019. **93**(17).
92. Lussignol, M., et al., *The herpes simplex virus 1 Us11 protein inhibits autophagy through its interaction with the protein kinase PKR.* J Virol, 2013. **87**(2): p. 859-71.
93. Lewis, H.C., et al., *HSV-1 exploits host heterochromatin for nuclear egress.* J Cell Biol, 2023. **222**(9).
94. Halford, W.P. and P.A. Schaffer, *ICP0 is required for efficient reactivation of herpes simplex virus type 1 from neuronal latency.* J Virol, 2001. **75**(7): p. 3240-9.
95. Thompson, R.L. and N.M. Sawtell, *Evidence that the herpes simplex virus type 1 ICP0 protein does not initiate reactivation from latency in vivo.* J Virol, 2006. **80**(22): p. 10919-30.
96. Sinani, D., et al., *Stress-induced cellular transcription factors expressed in trigeminal ganglionic neurons stimulate the herpes simplex virus 1 ICP0 promoter.* J Virol, 2013. **87**(23): p. 13042-7.
97. Abraham, R.T., *PI 3-kinase related kinases: 'big' players in stress-induced signaling pathways.* DNA Repair (Amst), 2004. **3**(8-9): p. 883-7.

98. Catez, F., et al., *HSV-1 genome subnuclear positioning and associations with host-cell PML-NBs and centromeres regulate LAT locus transcription during latency in neurons.* PLoS Pathog, 2012. **8**(8): p. e1002852.
99. Nicoll, M.P., et al., *The HSV-1 Latency-Associated Transcript Functions to Repress Latent Phase Lytic Gene Expression and Suppress Virus Reactivation from Latently Infected Neurons.* PLoS Pathog, 2016. **12**(4): p. e1005539.
100. Rosato, P.C., et al., *Neuronal IFN signaling is dispensable for the establishment of HSV-1 latency.* Virology, 2016. **497**: p. 323-327.
101. St Leger, A.J., et al., *Local Immune Control of Latent Herpes Simplex Virus Type 1 in Ganglia of Mice and Man.* Front Immunol, 2021. **12**: p. 723809.
102. Salazar, S., K.T.Y. Luong, and O.O. Koyuncu, *Cell Intrinsic Determinants of Alpha Herpesvirus Latency and Pathogenesis in the Nervous System.* Viruses, 2023. **15**(12).
103. Looker, K.J., et al., *Global and Regional Estimates of Prevalent and Incident Herpes Simplex Virus Type 1 Infections in 2012.* PLoS One, 2015. **10**(10): p. e0140765.
104. Curanovic, D., et al., *Compartmented neuron cultures for directional infection by alpha herpesviruses.* Curr Protoc Cell Biol, 2009. **Chapter 26**: p. Unit 26 4.
105. Amendola, J., et al., *Optimization of neuronal cultures from rat superior cervical ganglia for dual patch recording.* Sci Rep, 2015. **5**: p. 14455.
106. Nascimento, A.I., F.M. Mar, and M.M. Sousa, *The intriguing nature of dorsal root ganglion neurons: Linking structure with polarity and function.* Prog Neurobiol, 2018. **168**: p. 86-103.
107. Tierney, W.M., et al., *Methods and Applications of Campenot Trichamber Neuronal Cultures for the Study of Neuroinvasive Viruses.* Methods Mol Biol, 2022. **2431**: p. 181-206.
108. del Rio, T., et al., *Heterogeneity of a fluorescent tegument component in single pseudorabies virus virions and enveloped axonal assemblies.* J Virol, 2005. **79**(7): p. 3903-19.
109. Pervolaraki, K., et al., *Differential induction of interferon stimulated genes between type I and type III interferons is independent of interferon receptor abundance.* PLoS Pathog, 2018. **14**(11): p. e1007420.
110. Bhushal, S., et al., *Cell Polarization and Epigenetic Status Shape the Heterogeneous Response to Type III Interferons in Intestinal Epithelial Cells.* Front Immunol, 2017. **8**: p. 671.
111. Stanifer, M.L., et al., *Importance of Type I and III Interferons at Respiratory and Intestinal Barrier Surfaces.* Front Immunol, 2020. **11**: p. 608645.
112. Jacobs, S., et al., *Species Specificity of Type III Interferon Activity and Development of a Sensitive Luciferase-Based Bioassay for Quantitation of Mouse Interferon-lambda.* J Interferon Cytokine Res, 2018. **38**(11): p. 469-479.
113. Miner, J.J., et al., *HSV-1 and Zika Virus but Not SARS-CoV-2 Replicate in the Human Cornea and Are Restricted by Corneal Type III Interferon.* Cell Rep, 2020. **33**(5): p. 108339.
114. Ye, L., D. Schnepf, and P. Staeheli, *Interferon-lambda orchestrates innate and adaptive mucosal immune responses.* Nat Rev Immunol, 2019. **19**(10): p. 614-625.
115. Ank, N., et al., *Lambda interferon (IFN-lambda), a type III IFN, is induced by viruses and IFNs and displays potent antiviral activity against select virus infections in vivo.* J Virol, 2006. **80**(9): p. 4501-9.

116. Li, J., et al., *Interferon lambda inhibits herpes simplex virus type I infection of human astrocytes and neurons.* Glia, 2011. **59**(1): p. 58-67.
117. Ch'ng, T.H., E.A. Flood, and L.W. Enquist, *Culturing primary and transformed neuronal cells for studying pseudorabies virus infection.* Methods Mol Biol, 2005. **292**: p. 299-316.
118. Cheung, A.K., *Detection of pseudorabies virus transcripts in trigeminal ganglia of latently infected swine.* J Virol, 1989. **63**(7): p. 2908-13.
119. Edmans, J.G., et al., *Mucoadhesive Electrospun Fibre-Based Technologies for Oral Medicine.* Pharmaceutics, 2020. **12**(6).
120. Schneider, W.M., M.D. Chevillotte, and C.M. Rice, *Interferon-stimulated genes: a complex web of host defenses.* Annu Rev Immunol, 2014. **32**: p. 513-45.
121. Solanki, K., et al., *The expanding roles of neuronal nitric oxide synthase (NOS1).* PeerJ, 2022. **10**: p. e13651.
122. Abramson, S.B., et al., *The role of nitric oxide in tissue destruction.* Best Pract Res Clin Rheumatol, 2001. **15**(5): p. 831-45.
123. Ayanlaja, A.A., et al., *Distinct Features of Doublecortin as a Marker of Neuronal Migration and Its Implications in Cancer Cell Mobility.* Front Mol Neurosci, 2017. **10**: p. 199.
124. Davis, T.A., B. Loos, and A.M. Engelbrecht, *AHNAK: the giant jack of all trades.* Cell Signal, 2014. **26**(12): p. 2683-93.
125. Sundararaj, S., A. Ravindran, and M.G. Casarotto, *AHNAK: The quiet giant in calcium homeostasis.* Cell Calcium, 2021. **96**: p. 102403.
126. Clark, D.N., L.R. Begg, and A.J. Filiano, *Unique aspects of IFN-gamma/STAT1 signaling in neurons.* Immunol Rev, 2022. **311**(1): p. 187-204.
127. Mettenleiter, T.C., *Pathogenesis of neurotropic herpesviruses: role of viral glycoproteins in neuroinvasion and transneuronal spread.* Virus Res, 2003. **92**(2): p. 197-206.
128. Ripa, I., et al., *Interplay between Autophagy and Herpes Simplex Virus Type 1: ICP34.5, One of the Main Actors.* Int J Mol Sci, 2022. **23**(21).
129. Tang, S., et al., *An acutely and latently expressed herpes simplex virus 2 viral microRNA inhibits expression of ICP34.5, a viral neurovirulence factor.* Proc Natl Acad Sci U S A, 2008. **105**(31): p. 10931-6.
130. Platt, K.B., C.J. Mare, and P.N. Hinz, *Differentiation of vaccine strains and field isolates of pseudorabies (Aujeszky's disease) virus: trypsin sensitivity and mouse virulence markers.* Arch Virol, 1980. **63**(2): p. 107-14.
131. Engel, E.A., J.P. Card, and L.W. Enquist, *Transneuronal Circuit Analysis with Pseudorabies Viruses.* Curr Protoc, 2023. **3**(7): p. e841.
132. Gimenez-Cassina, A., F. Lim, and J. Diaz-Nido, *Differentiation of a human neuroblastoma into neuron-like cells increases their susceptibility to transduction by herpesviral vectors.* J Neurosci Res, 2006. **84**(4): p. 755-67.
133. Chou, J. and B. Roizman, *The terminal a sequence of the herpes simplex virus genome contains the promoter of a gene located in the repeat sequences of the L component.* J Virol, 1986. **57**(2): p. 629-37.
134. Manivanh, R., et al., *Herpes Simplex Virus 1 ICP34.5 Alters Mitochondrial Dynamics in Neurons.* J Virol, 2020. **94**(14).
135. Klupp, B.G., et al., *Complete, annotated sequence of the pseudorabies virus genome.* J Virol, 2004. **78**(1): p. 424-40.

136. Bolovan, C.A., N.M. Sawtell, and R.L. Thompson, *ICP34.5 mutants of herpes simplex virus type 1 strain 17syn+ are attenuated for neurovirulence in mice and for replication in confluent primary mouse embryo cell cultures.* J Virol, 1994. **68**(1): p. 48-55.
137. Li, Y., et al., *ICP34.5 protein of herpes simplex virus facilitates the initiation of protein translation by bridging eukaryotic initiation factor 2alpha (eIF2alpha) and protein phosphatase 1.* J Biol Chem, 2011. **286**(28): p. 24785-92.
138. Liu, Y., et al., *The role of host eIF2alpha in viral infection.* Virol J, 2020. **17**(1): p. 112.
139. Manivanh, R., et al., *Role of Herpes Simplex Virus 1 gamma34.5 in the Regulation of IRF3 Signaling.* J Virol, 2017. **91**(23).
140. Wang, C., et al., *Evasion of the Antiviral Innate Immunity by PRV.* Int J Mol Sci, 2024. **25**(23).
141. Cui, Q., et al., *Viperin: A Multifunctional Protein in Antiviral Immunity and Disease Pathogenesis.* Pathogens, 2025. **14**(5).
142. Fitzgerald, K.A., *The interferon inducible gene: Viperin.* J Interferon Cytokine Res, 2011. **31**(1): p. 131-5.
143. Chen, S., et al., *Crucial Roles of RSAD2/viperin in Immunomodulation, Mitochondrial Metabolism and Autoimmune Diseases.* Inflammation, 2025. **48**(2): p. 520-540.
144. Ghosh, S. and E.N.G. Marsh, *Viperin: An ancient radical SAM enzyme finds its place in modern cellular metabolism and innate immunity.* J Biol Chem, 2020. **295**(33): p. 11513-11528.
145. Gizzi, A.S., et al., *A naturally occurring antiviral ribonucleotide encoded by the human genome.* Nature, 2018. **558**(7711): p. 610-614.
146. Mohr, K., *[Acyclovir].* Dtsch Med Wochenschr, 1993. **118**(49): p. 1817-8.
147. Honarmand Ebrahimi, K., *A unifying view of the broad-spectrum antiviral activity of RSAD2 (viperin) based on its radical-SAM chemistry.* Metallomics, 2018. **10**(4): p. 539-552.
148. Chin, K.C. and P. Cresswell, *Viperin (cig5), an IFN-inducible antiviral protein directly induced by human cytomegalovirus.* Proc Natl Acad Sci U S A, 2001. **98**(26): p. 15125-30.
149. Rivera-Serrano, E.E., et al., *Viperin Reveals Its True Function.* Annu Rev Virol, 2020. **7**(1): p. 421-446.
150. Chen, S., et al., *Crucial Roles of RSAD2/viperin in Immunomodulation, Mitochondrial Metabolism and Autoimmune Diseases.* Inflammation, 2024.
151. Tseng, Y.Y., et al., *Viperin has species-specific roles in response to herpes simplex virus infection.* J Gen Virol, 2021. **102**(8).
152. Shen, G., et al., *Herpes simplex virus 1 counteracts viperin via its virion host shutoff protein UL41.* J Virol, 2014. **88**(20): p. 12163-6.
153. Hou, L., et al., *RSAD2 suppresses viral replication by interacting with the Senecavirus A 2 C protein.* Vet Res, 2024. **55**(1): p. 115.
154. Ye, L., et al., *Functional Profile of Human Cytomegalovirus Genes and Their Associated Diseases: A Review.* Front Microbiol, 2020. **11**: p. 2104.
155. Tommasi, C. and J. Breuer, *The Biology of Varicella-Zoster Virus Replication in the Skin.* Viruses, 2022. **14**(5).
156. Cohen, J.I., *The varicella-zoster virus genome.* Curr Top Microbiol Immunol, 2010. **342**: p. 1-14.

157. Cho, H., et al., *Differential innate immune response programs in neuronal subtypes determine susceptibility to infection in the brain by positive-stranded RNA viruses.* Nat Med, 2013. **19**(4): p. 458-64.
158. Kamada, R., et al., *Interferon stimulation creates chromatin marks and establishes transcriptional memory.* Proc Natl Acad Sci U S A, 2018. **115**(39): p. E9162-E9171.
159. Kambara, H., et al., *Negative regulation of the interferon response by an interferon-induced long non-coding RNA.* Nucleic Acids Res, 2014. **42**(16): p. 10668-80.
160. Cheng, G., Z. Feng, and B. He, *Herpes simplex virus 1 infection activates the endoplasmic reticulum resident kinase PERK and mediates eIF-2alpha dephosphorylation by the gamma(1)34.5 protein.* J Virol, 2005. **79**(3): p. 1379-88.
161. Cavanaugh, S.E., A.M. Holmgren, and G.F. Rall, *Homeostatic interferon expression in neurons is sufficient for early control of viral infection.* J Neuroimmunol, 2015. **279**: p. 11-9.
162. Brice, D.C., et al., *Type I interferon and interferon-stimulated gene expression in oral epithelial cells.* Mol Oral Microbiol, 2019. **34**(6): p. 245-253.
163. Lee, A.J. and A.A. Ashkar, *Herpes simplex virus-2 in the genital mucosa: insights into the mucosal host response and vaccine development.* Curr Opin Infect Dis, 2012. **25**(1): p. 92-9.
164. Altayb, H.N., *Fludarabine, a Potential DNA-Dependent RNA Polymerase Inhibitor, as a Prospective Drug against Monkeypox Virus: A Computational Approach.* Pharmaceuticals (Basel), 2022. **15**(9).
165. Frank, D.A., S. Mahajan, and J. Ritz, *Fludarabine-induced immunosuppression is associated with inhibition of STAT1 signaling.* Nat Med, 1999. **5**(4): p. 444-7.
166. Maday, S., et al., *Axonal transport: cargo-specific mechanisms of motility and regulation.* Neuron, 2014. **84**(2): p. 292-309.
167. Wilson, D.W., *Motor Skills: Recruitment of Kinesins, Myosins and Dynein during Assembly and Egress of Alphaherpesviruses.* Viruses, 2021. **13**(8).
168. Rosato, P.C. and D.A. Leib, *Neuronal Interferon Signaling Is Required for Protection against Herpes Simplex Virus Replication and Pathogenesis.* PLoS Pathog, 2015. **11**(7): p. e1005028.
169. Seo, D. and D.B. Gammon, *Manipulation of Host Microtubule Networks by Viral Microtubule-Associated Proteins.* Viruses, 2022. **14**(5).
170. Kaminska, P., et al., *Cytokines on the way to secretion.* Cytokine Growth Factor Rev, 2024. **79**: p. 52-65.
171. Nagano, S. and T. Araki, *Axonal Transport and Local Translation of mRNA in Amyotrophic Lateral Sclerosis*, in *Amyotrophic Lateral Sclerosis*, T. Araki, Editor. 2021: Brisbane (AU).
172. Li, L., J. Yu, and S.J. Ji, *Axonal mRNA localization and translation: local events with broad roles.* Cell Mol Life Sci, 2021. **78**(23): p. 7379-7395.
173. Sahoo, P.K., et al., *Axonal mRNA transport and translation at a glance.* J Cell Sci, 2018. **131**(8).
174. Romanova, E.V., et al., *Small-volume analysis of cell-cell signaling molecules in the brain.* Neuropsychopharmacology, 2014. **39**(1): p. 50-64.
175. Hsu, J.C., et al., *Viperin triggers ribosome collision-dependent translation inhibition to restrict viral replication.* Mol Cell, 2022. **82**(9): p. 1631-1642 e6.

176. Dalla Costa, I., et al., *The functional organization of axonal mRNA transport and translation.* Nat Rev Neurosci, 2021. **22**(2): p. 77-91.
177. Platt, K.B., C.J. Mare, and P.N. Hinz, *Differentiation of vaccine strains and field isolates of pseudorabies (Aujeszky's disease) virus: thermal sensitivity and rabbit virulence markers.* Arch Virol, 1979. **60**(1): p. 13-23.